BHLH Transcription Factor Manipulation in Human Glioma

Dissertation

zur

Erlangung der naturwissenschaftlichen Doktorwürde

(Dr. sc. nat.)

vorgelegt der

Mathematisch-naturwissenschaftlichen Fakultät

der

Universität Zürich

von

Sarah Beyeler

von

Avry FR

Promotionskomitee

Prof. Dr. Esther Stöckli (Vorsitz)

Prof. Dr. Martin E. Schwab

Dr. Olivier Raineteau (Leitung der Dissertation)

Zürich, 2014

"*Success consists of going from failure to failure without loss of enthusiasm*."

Winston Churchill

A mes parents, pour leur amour et soutient inconditionnels

Table of Contents

Summary

Glioblastoma multiforme (GBM) are the most aggressive type of gliomas and lead to poor prognosis. Despite modern multimodal therapy, relapse recurs in up to 90% of all cases and the survival of patients is around one year in average. GBM are highly heterogenous at the genomic, histopathological and disease progression level, which represents a great challenge for developing treatments. The aggressiveness and relapsing behavior of GBM partly relies on the presence of a population of cells with stem cell properties that are resistant to therapies and have the capacity to replenish the tumor bulk. These cancer stem cells (CSCs) share features with neural stem cells (NSCs) such as similar transcriptional regulatory pathways. In this study, we focused on the helix-loop-helix (i.e. ID proteins) and basic helix-loop-helix transcription factor network (i.e. E proteins and Olig2) to investigate its potential as target for therapeutic approaches. This transcriptional network regulates proliferation and differentiation of stem cells and is also involved in maintenance of tumor homeostasis. In this thesis, the aim was to disrupt the (b)HLH network in its ensemble with endogenous E proteins in order to induce anti-glioma effects.

The first chapter describes how overexpression of a dominant-negative E protein (dnE47) lacking its nuclear localization signal in human glioblastoma-derived cells led to sequestration of HLH and bHLH proteins in the cytoplasm. DnE47 overexpression induced apoptosis in adherent immortalized tumor cell lines and down-regulation of pro-proliferative as well as anti-apoptotic genes. Similar effects were detected in tumor-initiating cells derived from human GBM biopsies. In these later cells, overexpression of dnE47 impaired the sphere formation capacities of tumor-initiating cells and delayed the onset of clinical symptoms in a murine xenograft model.

Chapter two describes the development and establishment of tools and methods necessary for the study presented in Chapter one. We engineered an inducible lentiviral vector and established the optimal conditions for its application in patient-derived tumor-initiating cells. We also present a more detailed histology of tumors induced in immunosuppressed mice as well as possible novel analytical approaches for characterizing the number and distribution of grafted cells within the mouse brain.
In chapter three, we finally tested a novel xenograft model for assessing the ability of glioma-initiating cells to form tumors. We transplanted tumor-initiating cells in *Drosophila melanogaster* flies and monitored the survival, migration and tumor-formation of the xenografts.

To conclude, in this thesis I demonstrate the feasibility of using properties of endogenous proteins in order to disrupt a transcriptional network globally in the context of human glioblastoma and to achieve anti-glioma effects.

Zusammenfassung

Glioblastoma multiforme (GBM) ist die aggressivste Art eines Glioms und ist mit einer geringen Überlebenschance assoziiert. Trotz multimodaler Therapie haben GBM Patienten eine Rückfallquote von bis zu 90% und überleben nach Diagnose durchschnittlich ein Jahr. GBM sind auf der genomischen, molekularen und histopathologischen Ebene sowie im Krankheitsverlauf extrem heterogen, was die Anpassung der Behandlung nötig, aber auch diffizil macht. Die Aggressivität und die hohe Rückfallquote von GBM sind teilweise auf die Präsenz einer Zellpopulation mit Stammzelleigenschaften zurückzuführen. Diese Zellen sind auf gewöhnliche Therapien resistent, da die überlebenden Stammzellen den Tumor wieder aufbauen können. Die physiologischen Eigenschaften von Krebsstammzellen und neuralen Stammzellen werden von gleichen molekularen Mechanismen reguliert, unter anderem vom Helix-loop-helix- (HLH) und Basic-Helix-loop-helix- (bHLH) Transkriptionsnetzwerk. In dieser Dissertation liegt der Focus sowohl auf HLH (i.e. ID Proteine) als auch auf bHLH (i.e. E Proteine und Olig2) Proteinen, um ihr Potential als neue therapeutische Zielmoleküle zu erforschen. Dieses Netzwerk von Transkriptionsfaktoren reguliert die Proliferation und Differenzierung von Stammzellen und ist auch bekannt dafür, die physiologischen Eigenschaften eines Tumors, wie zum Beispiel starke Proliferationsrate, Bildung neuer Blutgefässe und Invasion zu unterstützen. Das Ziel dieser Dissertation ist es, das gesamte HLH und bHLH Netzwerk mittels endogenen E Proteinen zum Erliegen zu bringen, um das Tumorwachstum zu unterbinden.

Im ersten Kapitel wird gezeigt, wie die Überexpression eines dominant-negativen E Proteins (dnE47), das kein Kernlokalisationssignal hat, in von GBM abstammenden Zelllinien zu HLH und bHLH Sequestrierung im Zytoplasma fuhr. DnE47-Überexpression verursachte den Zelltod von immortalisierten Gliomazelllinien und verringerte die Expression von pro-proliferativen als auch von anti-apoptotischen Genen. Ähnliche Effekte wurden in Tumorstammzellen erzielt, die aus menschlichem GBM Gewebe isoliert wurden. DnE47-Überexpression in diesen Zellen

beeinträchtigte ihre Fähigkeit, Sphären zu bilden, und verzögerte das Auftreten von Krankheitssymptomen in einem Maus Xenotransplantationsmodell.

Das zweite Kapitel beschreibt, wie die für die Studie vom ersten Kapitel nötigen Werkzeuge und Methoden etabliert wurden. Wir entwickelten induzierbare lentiviralen Vektoren und stellten den optimalen Rahmen her, um sie in Tumorstammzellen von Patienten anzuwenden. Wir stellen auch eine ausführlichere Histologie von Tumoren vor, die in immunsupprimierten Mäusen induziert wurden, sowie mögliche neue analytische Methoden für die Charakterisierung von Anzahl und Verteilung transplantierter Zellen innerhalb des Mausgehirns.

Im dritten Kapitel testeten wir ein neues Xenotransplantatmodell für Tumorbildung. In diesem Experiment wurden menschliche Krebsstammzellen in *Drosophila melanogaster* Fliegen transplantiert und das Verhalten des Transplantats und das Tumorwachstum beobachtet.

In dieser Dissertation beweise ich, dass Eigenschaften von endogenen Proteinen benutzt werden können, um ein Transkriptionsnetzwerk im Kontext von Glioblastomen global zum Erliegen zu bringen und dadurch gegen den Tumor zu wirken.

Chapter I

Introduction

Introduction

1. Glioblastoma multiforme

1.1 Clinical prognosis and standard therapy

Gliomas are the most aggressive and common primary brain tumors. Approximately 3-4 cases per 100'000 people are diagnosed each year worldwide and the median survival rate is of 3 months without treatment (Ohgaki & Kleihues 2005; Parkin & Muir 1992; Chaudhry et al. 2013). These aggressive tumors generally occur in elderly patients over 60 and actual standard treatments are adapted to the age of the patient (Chaudhry et al. 2013). Treating brain tumors typically involves surgical resection, followed by radiotherapy, which already significantly improves the median survival of patients (Walker et al. 1980; Laperriere et al. 2002). Adjuvant chemotherapy with nitrosourea-based drugs or oral administration of Temozolomide (TMZ), an atypical alkylating agent, increases the median survival of patients (Stewart 2002; Stupp et al. 2005; Stupp et al. 2009). More specifically, the combination of radiations and TMZ treatment was shown to significantly improve survival (Stupp et al. 2005). However, despite combining radiotherapy and chemotherapy, tumors recur in 90% of the cases with a more aggressive phenotype and to this day, no existing cure can offer survival on the long-term (Brada et al. 2001; Stupp et al. 2009).

1.2 Classifications

Primary brain tumors were originally named gliomas according to the neural cell type they share features mostly with: glial cells. Based on histopathology, immunohistochemistry and ultrastructural analyses, gliomas are classified as astrocytomas and oligendrogliomas or oligoastrocytomas if showing a mixed astrocytic and oligodendrocytic signature (Furnari et al. 2007; Westphal & Lamszus 2011). Primary brain tumors are further distinguished depending on their aggressiveness according to a scale developed by the World Health Organization (WHO), grouping tumors into four grades: I to IV (Louis et al. 2007). Oligodendroglioma and oligoastrocytoma can range from grade II to III, astrocytomas from grade I to IV and the most aggressive types of tumor are astrocytomas grade IV,

also known as glioblastoma multiforme (Louis 2006). Glioblastoma multiforme (GBM) are malignant tumors with poor prognosis and a median survival of about 14 months (Stupp et al. 2005). High-grade tumors (grade III-IV) are characterized by rapidly proliferating cells, a dense vasculature and are highly anaplastic whereas low-grade tumors (grade I-II) divide slowly and show a high cell density with a more differentiated histology (Miller & Perry 2007; Riemenschneider & Reifenberger 2009). Low-grade tumors generally occur in patients younger than 45 years old whereas high-grade glioblastoma are predominantly diagnosed in elder patients (Furnari et al. 2007). Interestingly, lower-grade tumors grow diffusely throughout the brain without affecting normal functions whereas high-grade tumors are more rapidly fatal (Furnari et al. 2007; Westphal & Lamszus 2011). GBM can either appear *de novo* (therefore called primary tumors) or evolve from lower grade astrocytomas and form secondary tumors. This progression from low to high grade occurs through oncogenic molecular events, thereby generating genetic alterations leading to a more aggressive and metastatic phenotype (Westphal & Lamszus 2011). Although primary and secondary tumors share similar histopathological features, their genomic profiles show striking differences. This heterogeneity challenges therapeutic approaches even more as tumors will not react in the same manner to different therapies (Maher et al. 2006; Furnari et al. 2007).

1.3 Histological and molecular heterogeneity

Each GBM is unique in its histopathology, genomic profile and time course, which accounts for a high inter- and intra-tumor heterogeneity. This makes it difficult for clinicians to adapt therapies for each individual for optimization of survival and life quality (Chaudhry et al. 2013). Hopes to develop more personalized treatments rely on a more accurate classification and correlation between phenotype and prognosis in order to discover markers that predict the survival of patients. Hence, scientists have been aiming at developing new classifications based on genomic analyses in order to better understand GBM and improve health care (Phillips et al. 2006; Maher et al. 2006; Verhaak et al. 2010). In these studies, transcriptome analyses combined with cohort patient history and histology revealed recurrent mutations present in GBM tumors showing phenotypic similarities. For example, amplifications of *epidermal*

growth factor receptor (*EGFR*) and loss of *phosphatase and tensin homolog* (*PTEN*) loci leading to a highly proliferative behavior of tumor cells correlate with poor prognosis whereas tumors showing neuronal features respond better to therapy (Phillips et al. 2006; Maher et al. 2006; Verhaak et al. 2010). In 2010, a study based on The Cancer Genome Atlas (TCGA) database introduced a new classification model with four molecular subclasses of GBM. Proneural, neural, classical and mesenchymal subtypes were distinguished along alterations in *EGFR*, *neurofibromin 1* (*NF1*), *platelet-derived growth factor receptor alpha/isocitrate dehydrogenase 1* (*PDGFRα/IDH1)* and neuronal markers such as *neurofilament light chain (NFL)* or *gamma-aminobutyric acid (GABA) A receptor alpha subunit 1 (GABRA1)*, respectively. Here as well, responses to therapy correlated with the different subtypes, proneural tumors showing poor and classical tumors good responses (Verhaak et al. 2010). Individualization of therapy is not only challenged by the heterogeneity between tumors but also by heterogeneity within the tumor itself (Swanton 2012). In fact, genomic profiles of biopsies obtained from different areas of a single tumor showed diverse fingerprints, underlining the presence of different subtypes of cell populations (Liang et al. 2005; Sottoriva et al. 2013). Furthermore, this intra-tumor heterogeneity evolves over time, which might partially explain the variability in response to therapy (Sottoriva et al. 2013). In conclusion, the correlation between tumor heterogeneity and the clinical outcome still needs to be further investigated in order to better understand the pathology of brain tumors and optimize therapeutic approaches accordingly.

2. The origin of glioblastoma multiforme

More precise knowledge of tumor characteristics relies on unraveling where and how tumors arise. One of the biggest controversies in this field of research concerns the origin of primary brain tumors. In the last decade, three possibilities for cell-of-origin were suggested. First, tumors might occur through dedifferentiation of non-dividing mature neural cells. Second, slowly dividing neural progenitor cells might give rise to tumors. Finally, the existing pool of neural stem cells in the adult brain offers a plausible explanation for the origin of gliomas. In the following paragraphs, I will describe these three different hypotheses and discuss data supporting them in more details.

2.1 Dedifferentiating post-mitotic neural cells

The adult human brain is made of approximately a 100 billion of neurons and ten to fifty times more glial cells, the vast majority of which are in a post-mitotic state. The possibility that tumors arise from these cell populations implies their dedifferentiation into a less mature state (Bachoo et al. 2002; Moon et al. 2011; Friedmann-Morvinski et al. 2012). In the healthy postnatal brain, astrocytes have been shown to dedifferentiate into neurons after overexpression of pro-neural genes such as *Pax6*, *Neurogenin2 (Ngn2)* or *murine acyl-CoA synthetase long-chain family member 1 (Mash1)*, revealing a more plastic potential than previously thought (Heins et al. 2002; Berninger et al. 2007). Similarly, by silencing both tumor suppressor genes *NF1* and *p53* in either *glial fibrillary acidic protein (GFAP)*-expressing glial or *Synapsin I*-expressing neuronal cells, formation of tumors was induced in mice (Friedmann-Morvinski et al. 2012). Also, the embryonic marker *Nanog* was shown to induce dedifferentiation of astrocytes in the absence of *p53*, leading to the formation of cancer stem-like cells (Moon et al. 2011). Finally, it was demonstrated that in the absence of both tumor suppressor genes $p16^{Ink4a}$ and $p19^{Arf}$, astrocytes dedifferentiate upon *EGFR* activation and form high-grade gliomas (Bachoo et al. 2002). However, despite the possibility that post-mitotic neural cells show the potential to dedifferentiate, this process still remains unlikely as it implies two steps: first, a de-differentiation of the mature cell and second, the transformation of the de-differentiated cell. Thus, although the experiments discussed above represent proof-of-principle that post-mitotic neural cells can generate tumors, these cells are not

favored as the cells of origin of tumors (Westphal & Lamszus 2011). The existence of neural progenitor cells which show a proliferative behavior represents a more plausible source of origin for tumors.

2.2 Gliomas from neural progenitor cells

Neural progenitors such as oligodendrocytes progenitor cells (OPCs) or neural stem cells are present in the adult mammalian brain, have the ability to proliferate and were shown to induce tumors after the occurrence of oncogenic events such as mutations or copy-number alterations (Levine et al. 2001; Alvarez-Buylla & Lim 2004; Persson et al. 2010; Liu et al. 2011). OPCs are present throughout the central nervous system (CNS), proliferate constantly and respond to injury by increasing their proliferation (Levine et al. 1993; Dawson et al. 2000; Horner et al. 2000; Levine et al. 2001; Barnabé-Heider et al. 2010). Similar to astrocytes, the potential of OPCs in the adult brain is not fully restricted to an oligodendrocytic fate since they are able to dedifferentiate into multipotent progenitors and re-differentiate into neurons *in vitro* and *in vivo* (Kondo 2000; Belachew et al. 2003; Nunes et al. 2003). Using a mosaic analysis with double markers (MADM) approach, OPCs were shown to grow aberrantly and to form tumors when *NF1* and *p53* were mutated. The contribution of OPCs to tumor formation was also observed when the mutations were introduced in neural stem cells, indicating that the oligodendroglial lineage is the most permissive to transformation (Liu et al. 2011). Based on a transgenic murine glioma model in which *p53* was deleted concomitantly with *EGFR* activation under the control of the *S100beta* promoter, OPCs were suggested to be at the origin of oligodendrogliomas. These tumors showed an enrichment of OPC markers such as *Sox10*, *PDGFRα* or *NG2* both in mouse and human oligodendroglioma (Weiss et al. 2003; Persson et al. 2010). These findings imply that progenitor cells, in particular those from the oligodendroglial lineage, retain the potential to proliferate and are highly sensitive to oncogenic molecular events. Besides lineage specific progenitors, neural stem cells are believed to be present in particular regions of the adult CNS and may participate to tumor formation as well.

2.3 Adult neural stem cells as the origin of tumors

In the adult human brain neural stem cells proliferate constantly, self-renew their pool and are able to give rise to both glial cells and neurons (Eriksson et al. 1998). They are present in the two neurogenic niches of the adult mammalian brain: the dentate gyrus of the hippocampus and the subventricular zone (Alvarez-Buylla & Lim 2004). In the context of cancer, a subpopulation of GFAP positive neural stem cells expressing PDGFRα and located within the walls lining ventricles were shown to overproliferate and to form glioma-like hyperplasias upon PDGF infusion (Jackson et al. 2006). Similarly, overexpression of *Akt* and *Ras*, two genes known to be highly active in GBM, in Nestin^{+} stem cells induced gliomas in a murine tumor model (Holland et al. 2000; Cheng et al. 2009; Feldkamp et al. 1997). On the other hand, heterozygous deletion of tumor suppressor genes *Nf1*, *p53* and *Pten* in Nestin^{+} stem/progenitor cells lead to the formation of malignant astrocytomas (Alcantara Llaguno et al. 2009). These findings suggest that germinal zones of the adult CNS constitute environments potentially favorable for oncogenic events and that these initial transformation steps preferentially occur in non-committed cells such as NSCs rather than in their progeny: i.e. astrocytes or oligodendrocyte precursor cells. Unraveling the true origin of brain tumors will contribute to better understand their physiology and develop cell-specific therapies.

3. The cancer stem cell theory

Although the identity of the cell-of-origin for brain tumors remains to be fully determined, tumors themselves are known to contain populations of stem cells that build up and replenish the bulk of the tumor (Stiles & Rowitch 2008). The terminology is still under debate with a lack of clear definitions. For this reason, it is important to make the difference between a cancer stem cell (CSC) as the cell in which the original oncogenic events occurred and a CSC as a cell able to give rise to the different type of cells constituting the tumor (Valent et al. 2012).

3.1 Cancer stem cells

In 2003, a new area of research arose when Singh and colleagues isolated a cell population able to proliferate, self-renew and differentiate *in vitro* from human pediatric brain tumors (Singh et al. 2003). The purification was based on the cell surface marker CD133 (also known as Prominin-1, a transmembrane glycoprotein) which is also expressed on the surface of adult neural stem cells (Obermair et al. 2010; Beckervordersandforth et al. 2010). *In vivo* xenografts of these CD133 positive cells (but not CD133 negative cells) led to the formation of tumors that could be serially transplanted and which phenocopied the histopathology of the patient's tumor (Singh et al. 2004). The presence of this cancer stem-like cell population was confirmed in GBM (Yuan et al. 2004). CD133 positive cells are characterized by the expression of other neural stem cell markers such as Nestin and Sox2 (Lendahl et al. 1990; Komitova & Eriksson 2004). However, the relevance of this marker for CSC identification was questioned when CD133 negative cancer cells were shown to be able to form tumors as well (Nishide et al. 2009). The folding of the CD133 surface marker is glycosylation-dependent and might influence its detection as it is present on both CSCs and differentiated tumor cells (Kemper et al. 2010). These controversial findings might also be due to technical issues, different isolation methods showing diverse CD133 purification levels (Clément et al. 2009). Therefore, additional surface markers such as transmembrane glycoprotein CD44, or the adhesion molecule CD15 (also called LewisX or stage-specific embryonic antigen 1 (SSEA-1)) are needed for a more stringent detection and isolation of CSCs (T.-A. Read et al. 2009; Son et al. 2009; Anido et al. 2010). Another alternative would be to isolate CSCs without relying on markers based on autofluorescence properties and morphology (Clément et al. 2010). All in all, there is a need for more specific markers for CSC detection, as it will help revealing the cell-of-origin of the tumor and ultimately lead to the development of more specific therapeutic approaches.

Adaptation of therapies has to be considered as CSCs have the ability to resist to current treatments such as radiations and chemotherapy. Their resistance to radiotherapy is due to their increased DNA repair capacity and to chemotherapeutic agents such as Temozolomide (TMZ) thanks to the detoxifying protein O^6-methylguanine-DNA-methyltransferase (MGMT) (Bao et al. 2006; Eramo et al. 2006; Beier et al. 2008). Highlighting this resistant phenotype, a small sub-population of CSCs within tumors was shown to be the cause for tumor reappearance after temozolomide (TMZ) treatment in a genetic glioma mouse model (Chen et al. 2012). Additionally, resistance to therapy might be influenced by other extrinsic factors such as tumor niche factors, the hypoxic environment or the reacquisition of stem cells features by non-stem cells (Beier et al. 2011). Since more $CD133^+$ cells appear under hypoxic conditions, CSCs or non-CSCs seem to be able to adapt to the environment (Griguer et al. 2008; Soeda et al. 2009). Thus, CD133 might be more representative for a transient state of stem cells within a tumor than an absolute detecting marker, further highlighting the necessity to better characterize the expression markers and physiology of CSCs (Griguer et al. 2008).

3.2 Cancer stem cells and neural stem cells

Since brain cancer stem cells and neural stem cells share common properties such as self-renewal, proliferation and differentiation into neural lineages, it has been suggested that common regulatory pathways control the physiology of both cell types. Confirming this hypothesis, evidences show that canonical developmental signaling pathways such as NOTCH and Wnt are implicated in glioblastoma as well (Pierfelice et al. 2008; Gong & Huang 2012). In addition to common regulatory pathways, these cells also share the ability to migrate throughout the brain: neural stem cells (NSCs) migrate during development through cortical layers to reach their final location and CSCs spread along white matter tracts to invade all brain regions (Cayre et al. 2009; Westphal & Lamszus 2011). This migratory phenotype is seen as well when NSCs are attracted to the site of tumor, where both populations can interact (Aboody et al. 2000; Mapara et al. 2007). Additionally, CSCs and NSCs were suggested to be related at the molecular level and to share similar transcriptional profiles (Taylor et al. 2005; Sharma et al. 2007). However, although they share common stem- and lineage characteristic markers, genome-wide studies revealed a greater heterogeneity in the transcriptome of CSCs showing a deregulated Wnt pathway when compared with

NSCs (Sandberg et al. 2013). Nevertheless, knowledge acquired from NSCs can be transposed to CSCs in order to better understand the neurobiology of gliomas since similar pathways are involved in the physiology and behavior of both cell populations.

4. (basic) helix-loop-helix transcription factors

4.1 (basic) helix-loop-helix transcription factors in the healthy brain

Helix-loop-helix (HLH) and basic helix-loop-helix (bHLH) proteins are transcription factors involved in stem cell homeostasis during development as well as later on in the postnatal brain (Massari & Murre 2000; Jones 2004). According to Murre's classification system, the four E proteins (E47, E12, E2-2- and HEB) constitute Class I; whereas Class II regroups tissue-specific bHLH proteins responsible for differentiation such as Olig proteins. Class I proteins form homo- or heterodimers with Class II proteins in order to transactivate transcription of target genes through E-box sequence recognition in many tissues (Murre, McCaw & Baltimore 1989; Massari & Murre 2000). Class IV encloses the four ID proteins (1-4) which lack a DNA binding domain, can dimerize with Class I and II and therefore negatively regulate transcription (Murre et al. 1994; Massari & Murre 2000). ID proteins show no preferential binding affinity with E proteins, suggesting interchangeable dimerization properties (Massari & Murre 2000; Teachenor et al. 2012). BHLH and HLH proteins are involved in the development, proliferation, differentiation and maintenance of neural stem cell during development and in the adult neurogenic niches (Lee 1997; Ruzinova & Benezra 2003; Niola et al. 2012).

4.2 (basic) helix-loop-helix transcription factors in cancer

Both bHLH and HLH are implicated in tumor homeostasis. BHLH proteins such as Olig1, Olig2 and Ascl1 are expressed in different types of glioma and have been shown to be involved in the maintenance of a proliferative state as well as in the formation of tumors (Aguirre-Cruz et al. 2004; Ligon et al. 2004; Somasundaram et al. 2005; Ligon et al. 2007). Especially Olig2 has been investigated in the context of cancer. Olig2 antagonizes the action of the tumor suppressor p53 by interfering with its post-translational modification and therefore rendering cells resistant to toxic damage (Mehta et al. 2011). Olig2 has a differential action depending on its phosphorylation state since it supports a proliferative behavior only when phosphorylated (Ligon et al. 2007; Li et al. 2011; Sun et al. 2011). This phosphorylated state appears to be a characteristic of high-grade tumors whereas low-grade tumors rather express unphosphorylated Olig2 (Mehta et al. 2011).

Besides bHLH proteins, ID proteins are also involved in tumor homeostasis by playing diverse and important roles in angiogenesis, proliferation and migration of cancer cells (Lyden et al. 1999; Coma et al. 2010; Paolella et al. 2011; O'Brien et al. 2012). In absence of ID proteins, angiogenis is impaired during development as well as the neovascularization of tumors (Lyden et al. 1999). HLH proteins were suggested to sustain a highly proliferative state by interacting with the $p16^{Ink4a}$/Rb pathway (Lasorella et al. 2000; Ouyang et al. 2002). Finally, repression of Semaphorin 3F through ID2 implicates that these proteins support of migratory behavior as well (Coma et al. 2010). Because of all their roles in sustaining tumor homeostasis, ID proteins became attractive targets for designing novel therapeutic approaches (Ciarapica et al. 2009; Demissew S Mern et al. 2010; Mellick et al. 2010; Trabosh et al. 2009).

Finally, E proteins seem to be involved in the regulation of proliferation, cell death and cell adhesion as well. Overexpression of E12 or E47 in the absence of E2A induced cell death in murine lymphoma cell lines, suggesting a tumor suppressive role for E2A proteins (Engel & Murre 1999b). In fibroblasts, E47 overexpression and ID neutralization suppresses proliferation (Peverali et al. 1994). Confirming the anti-proliferative action of E proteins, E12 and E47 were shown to induce the transcription of cyclin-dependent kinase inhibitors $p27^{KIP1}$ in the absence of ID2 (Trabosh et al. 2009). Cell-cycle progression was reported to be impaired after E47 overexpression in the context of pancreatic ductal adenocarcinoma (Lee et al. 2011). Lastly, E47 was also shown to be involved in the epithelial-mesenchymal transition (EMT) of epithelial cells by repressing *E-cadherin* expression (Perez-Moreno et al. 2001). It is still unclear whether these effects are mediated directly by E proteins or by their dimerization with ID and/or other bHLH proteins. Therefore, further investigation is needed before considering these transcription factors as potential anti-glioma targets, as described in this thesis.

Since both HLH and bHLH sustain hallmarks of tumor homeostasis such as proliferation, neovascularization and migration, they appear as potential targets for the development of novel therapeutic approaches. Furthermore, the ability of E proteins to interact with the entire ensemble of HLH and bHLH proteins highlight their potential as tool for global targeting of this transcriptional network.

5. Therapeutic approaches

5.1 Individualized therapies

It has been known for a long time already that drug sensitivity correlates with pathway alterations in human glioma cell lines (Weller 1998). Hence, large-cohort clinical studies have been aiming at solving the question of correlation between the molecular expression profiles of tumors and the patients' response to therapy. A recent finding showed that promoter methylation of the *MGMT* gene correlates with a longer survival and a better response to TMZ treatment than radiotherapy (Wick et al. 2012). On the other hand, *TP53* mutations and *CDKN2A* deletions were found to correlate with resistance to radiotherapy and poor survival prognosis (Shih et al. 2005). These findings underline the fact that patients with different tumor profiles will respond differentially to various treatment modes and that there is a need for individualized therapies.

5.2 Disruption of transcription factor networks as a therapeutic goal

Since tumor formation and maintenance rely on mutations and alterations of different signaling and transcriptional pathways, scientists have been aiming at modulating or interfering with them with the hope to disrupt tumor cell homeostasis. A lot of efforts have been put into finding out ways to interfere at the level of transcription or at the level of protein-interaction (Zhou et al. 2009; Yan & Higgins 2013; Ivanov et al. 2013). Developmental regulatory pathways such as the Sonic Hedgehog (Shh), NOTCH or Wnt pathways are such prominent targets for glioblastoma therapy and small inhibitor molecules or antibodies have already been identified (Zhou et al. 2009). NOTCH signaling blockade provoked cancer stem cell depletion and apoptosis in embryonal brain tumors (Fan et al. 2006). Alternatively, differentiation was obtained by activation of the Wnt pathway in GBM-derived cells in a hypoxic environment, leading to a less oncogenic phenotype (Rampazzo et al. 2013). The HLH/bHLH transcription factor family accounts for attractive therapeutic targets as well, especially ID proteins (Iavarone & Lasorella 2006). One successful approach was to induce cell death and differentiation in glioma stem-like cells by overexpressing neurogenic transcription factors such as Ngn2 or NeuroD1 (Guichet et al. 2012). Using peptides specifically interfering with ID protein interactions,

differentiation, cell death and cell cycle arrest were induced *in vitro* (Ciarapica et al. 2009; Demissew S Mern et al. 2010; D S Mern et al. 2010a). These findings highlight the potential of transcription factors as both targets and means for therapeutic approaches (Yan & Higgins 2013). Nevertheless, developing new therapeutic tools also implies the development of efficient and specific delivery.

5.3 Delivery tools: from nanoparticles to cellular vehicles

Treating brain tumors is challenging since the central nervous system is protected by the blood-brain-barrier, thereby preventing the entry of most drugs and chemotherapeutic agents (Pardridge 2005; de Vries et al. 2006). Furthermore, the brain is an organ in which cells are mostly differentiated or have a very slow turnover, which has implications for recovery after surgical resections (Westphal & Lamszus 2011). The challenge is therefore to combine knowledge from oncology and neurobiology in order to deliver an individualized treatment specifically and efficiently to the site of the tumor or even to a subpopulation of cells whilst minimizing any toxic events that would lead to dramatic consequences in the healthy neighboring tissue.

The emergence of nanomedicine led to the discovery of new ways to deliver small compounds to tumor sites. Both organic and inorganic nanoparticles have the potential of a better blood-brain-barrier penetration and can be engineered to selectively target the cell of interest based on their affinity for specific antibodies or ligands (Liu et al. 2007). Additionally, they could be used not only for therapeutic purposes but also as imaging tools for diagnosis, for example with fluorescently labeled particles (Liu et al. 2007; del Burgo et al. 2013). A successful application of nanovesicles as therapeutic tools was achieved by efficiently disrupting angiogenesis in glioblastoma (Wojton et al. 2013). Coupled to nanoparticles, small peptides offer the possibility to target tumor cells based on receptor affinity, internalization and cleavage of the peptide (Teesalu et al. 2009; Alberici et al. 2012). Alternatively, based on recent progress in viral therapy, targeting tumor cells is also possible with viruses. For example, using a modified oncolytic measle virus to target human $CD133^{+}$ glioblastoma cells selectively killed this subpopulation of cells both *in vitro* and *in vivo* (Bach et al. 2013). Finally, since endogenous and transplanted stem cells were shown to migrate to the site of tumor, their potential as drug delivery units has been

investigated as well (Aboody et al. 2000; Benedetti et al. 2000; Uhl et al. 2005; Aboody et al. 2008). Unfortunately, these innovative approaches are not clinically applicable yet, and new findings should therefore be considered cautiously. In conclusion, further investigations of the potential of nanoparticles, peptides, therapeutic viruses and stem cells as carriage tools will lead to optimization of targeted treatment delivery.

5.4 Single vs. combined vs. global approaches

Considering the large inter- and intra-heterogeneity in tumors and the number of molecular pathways involved in oncogenic events, therapeutic approaches targeting a single component or aspect do not offer a cure for tumors on the long term. Currently, radiotherapy or chemotherapy which attack the tumor sites broadly still are the standard and most efficient treatments for brain cancer (Stupp et al. 2009). Yet, the numerous side effects including damaging the healthy tissue, resistance and mutation of cancer cells as well as a poor quality of life highlight the lack of optimal therapeutic approaches. There is a need for wide-range approaches but in a specific context, meaning the targeting of cancer cells without provoking any collateral damages. The answer might lie in predictive identification of key nodes in cancer pathways by metabolomics for example (Tang et al. 2013; Aboud & Weiss 2013; Gupta & Chawla 2013). Following this larger approach, polypharmacology is a new field for drug discovery, for example aiming at finding broad tropism kinase inhibitors (Knight et al. 2010; Rehemtulla 2012; Tang & Aittokallio 2013). The same logic might apply to transcription factor networks. The identification of transcriptional hubs or nodes critical for tumor physiology have the potential to reveal targets that are essential for supporting multiple aspects of tumorigenesis.

To conclude, combining knowledge from transcriptional networks sustaining tumor homeostasis, with delivery tool engineering is necessary to develop more efficient and personalized cancer therapies in the future.

6. Aims of the thesis

Based on the central role of HLH/bHLH proteins in controlling the physiology of neural stem cells and cancer stem cells, the aims of my thesis were as follows:

1) Manipulate E proteins in order to interfere with the natural activity of HLH/bHLH networks in GBM cells and investigate the consequences of these manipulations
2) Test a mutated form of E proteins that could disrupt more efficiently HLH/bHLH networks in GBM cells
3) Explore the potential of this approach in GBM-initiating stem cells

Globally, the aim of the thesis was to use properties of endogenous proteins in order to achieve anti-glioma effects by targeting a transcriptional network in its ensemble.

Chapter 2

Targeting the bHLH transcriptional networks by mutated E proteins in experimental glioma

(under review)

Targeting the bHLH transcriptional networks by mutated E proteins in experimental glioma

Beyeler Sarah [1], Joly Sandrine [1], Fries Michel[1], Obermair Franz-Josef [3], Burn Felice[2], Mehmood Rashid [4], Tabatabai Ghazaleh[2], Raineteau Olivier [1,5]

1 Brain Research Institute, University of Zurich/ Swiss Federal Institute of Technology Zurich, Switzerland

2 Department of Neurology, University Hospital Zurich, Switzerland

3 Institute of Integrative Biology, Swiss Federal Institute of Technology Zurich, Switzerland

4 Children's Health Research Institute, Department of Paediatrics, University of Western Ontario, London, ON, Canada

5 Stem Cell and Brain Research Institute, Inserm U846, Bron, France

Running title: bHLH networks disruption results in glioma apoptosis

Keywords: cytoplasmic sequestration, patient-derived tumor initiating cells, glioma cell lines, Olig2, Ascl1, Id proteins, xenograft

Financial support: This project was supported by the Swiss National Fund (NF 31-144127). SB was supported by the University of Zurich (Forschungskredit) and the Krebsliga Zurich: "E proteins as transcriptional targets in experimental gliomas".

Corresponding author: Dr. Olivier Raineteau, Brain Research Institute, University of Zurich/ETH, Winterthurerstrasse 190, 8057 Zurich, Switzerland. Tel.: +41 44 635 3228. Fax: Fax +41 44 635 3303.

Disclosure of potential conflicts of interest: No potential conflicts of interest were disclosed.

Author's contribution:

Sarah Beyeler: conception and design, collection and/or assembly of data, data analysis and interpretation, manuscript writing
Sandrine Joly: collection and/or assembly of data
Michel Fries: collection and/or assembly of data
Franz-Josef Obermair: collection and/or assembly of data
Felice Burn: collection and/or assembly of data
Rashid Mehmood: technical and/or material support
Ghazaleh Tabatabai: conception and design, provision of study material or patients, data analysis and interpretation, manuscript writing, final approval of manuscript
Olivier Raineteau: conception and design, financial support, administrative support , data analysis and interpretation, manuscript writing, final approval of manuscript, study supervision

Abstract

Glioblastomas (GB) are aggressive primary brain tumors. Helix-loop-helix (HLH, ID proteins) and basic HLH (bHLH, e.g. Olig2) proteins are transcription factors that regulate stem cell proliferation and differentiation throughout development and into adulthood. Their convergence on many oncogenic signaling pathways combined with the observation that their overexpression in GB correlates with poor clinical outcome identifies these transcription factors as promising therapeutic targets. Important dimerization partners of HLH/bHLH proteins are E proteins that are necessary for nuclear translocation and DNA binding. Here, we overexpressed a wildtype or a dominant negative form of E47 (dnE47) that lacks its nuclear localization signal thus preventing nuclear translocation of bHLH proteins in long-term glioma cell lines and in patient-derived glioma-initiating cell lines and analyzed the effects *in vitro* and *in vivo*. Whilst overexpression of E47 was sufficient to induce apoptosis in absence of bHLH proteins, dnE47 was necessary to prevent nuclear translocation of Olig2 and to achieve similar pro-apoptotic responses. Transcriptional analyses revealed down-regulation of the anti-apoptotic gene *BCL2L1* and the pro-proliferative gene *CDC25A* as underlying mechanisms. Overexpression of dnE47 in patient-derived glioma-initiating cell lines with high HLH and bHLH protein levels reduced sphere formation capacities and expression levels of *Nestin, BCL2L1 and CDC25A*. Finally, the *in vivo* induction of dnE47 expression in established xenografts prolonged survival. In conclusion, our data introduce a novel approach to jointly neutralize HLH and bHLH transcriptional networks activities, and identify these transcription factors as potential targets in glioma.

Introduction

Glioblastoma (GB) are aggressive primary brain tumours. Despite therapeutic interventions including surgical resection, radiation therapy and temozolomide chemotherapy, the median overall survival is only in the range of 15-16 months even in selected clinical trial populations (Stupp et al. 2009; Gilbert et al. 2011).

Recently, a link between neural stem/glial progenitor cells and tumour cells in the central nervous system has been suggested (Jackson et al. 2006; Tabatabai & Weller 2011). Indeed, brain tumours comprise a population of stem cells that are resistant to therapy and may thus contribute to relapsing cancer following treatment (Germano et al. 2010; Tabatabai & Weller 2011). This phylogeny suggests similarities in the molecular control of neural stem and glioma cells and provides opportunities to identify key transcriptional networks involved in GB pathogenesis.

The regulatory networks controlling stem cell behaviour in the vertebrate brain are well characterized. Helix-loop-helix (HLH) and basic helix-loop-helix (bHLH) transcription factors play a central role in both normal and pathologic cell proliferation. These transcription factors (TFs) can be categorized in subclasses based on their structure and transcriptional activity (Murre's classification; (Massari & Murre 2000)). Class I bHLH proteins, i.e. E proteins consisting of E2-2, E2A and its two splicing variants E12 and E47, as well as HEB, are ubiquitously present in embryonic as well as adult stem cells. These TFs act by homo or hetero-dimerizing with tissue-specific bHLH proteins (Class II), in order to facilitate their nuclear translocation and binding to E-box elements in promoter regions of target genes (Massari & Murre 2000). Inhibitors of DNA-binding or differentiation proteins (ID1-4) belong to Class V. ID1-4 lack the basic DNA binding domain and form inactive heterodimers with Class I and Class II proteins, thereby acting as negative regulators of bHLH transcription factors activity by actively preventing their DNA binding (Benezra et al. 1990).

Interestingly, Class V proteins are over-expressed in a wide range of human tumors, including GB (Hasskarl & Munger 2002). Four essential hallmarks of malignancy are conferred by dysregulated expression of ID proteins during tumourigenesis: anaplasia, uncontrolled proliferation, sustained neo-angiogenesis and invasion of neighbouring tissues (Lasorella et al. 2001). ID proteins may act in cancer cells by: i) sequestering

E proteins, ii) interaction with non-bHLH proteins such as pocket proteins of the retinoblastoma family, E-twenty six (ETS) or Paired-Box (Pax) proteins (Ruzinova & Benezra 2003). In addition to ID proteins, malignant gliomas of WHO grades II-IV express the class II bHLH protein Olig2 (Ligon et al. 2004) which is required for glioma formation in a genetically relevant murine model (Ligon et al. 2007). Notably, Olig2 expression is correlated with poor outcome in human gliomas (Ligon et al. 2004; Lu et al. 2001).

Although HLH and bHLH proteins (thereafter jointly defined as (b)HLH proteins) have been proposed as potential therapeutic targets (Fong et al. 2004; Ciarapica et al. 2009; Demissew S Mern et al. 2010), single gene approaches are prone to lead to acquired escape mechanisms. This is particularly true for bHLH proteins that show heterogeneous expression levels among tumour classes and highly dynamic regulation among tumour cell types. Moreover, the transcriptional nature and nuclear location of these proteins hampers their efficient targeting for therapeutic intervention (Yan & Higgins 2013; Henke et al. 2008). The dynamic interactions and inter-dependence of (b)HLH protein classes to fine tune transcriptional activity however give rise to a unique opportunity to develop such a strategy. In particular, E protein might represent a prime target to neutralize (b)HLH transcriptional networks activity as a whole. E proteins bind Class II and V proteins with high affinity (Massari & Murre 2000; Teachenor et al. 2012; Samanta & Kessler 2004; Geoffroy et al. 2009) to regulate their sub-cellular localization and DNA binding. Moreover, subtle changes in their expression levels critically impact their function in regulating gene expression and cellular function (Dorshkind 1994).

Here, we used overexpression of wild-type or mutated E proteins to induce cell cycle arrest and death in glioma cells. We demonstrate that overexpression of a dominant-negative form of E47 lacking its nuclear localization signal, allows co-targeting of class II and V (b)HLH proteins and represents a novel potent anti-glioma strategy.

Material and Methods

Cell lines and Culture

The human glioma cell lines LN-308 and LNT-229 (Wischhusen et al. 2003) were cultured in Dulbecco's Modified Eagle's Medium (DMEM, Gibco, Life Technologies, Carlsbad, CA, USA), supplemented with 10% fetal bovine serum (Invitrogen, Life Technologies, Carlsbad, CA, USA) and 1% antibiotic-antimycotic 100x (Gibco). Cells were split every 3-4 days using 0.25% Trypsin-EDTA (Gibco). Glioma-initiating cell lines (S24, T269 and T325) (Rieger et al., 2008) were cultured in DMEM:F12 (Gibco) supplemented with 2% B-27 minus Vitamin A (Gibco), 1% antibiotic-antimycotic 100x (Gibco), human leukemia inhibitory factor 20ng/ml (Millipore, Merck, Billerica, MA, USA), Heparin 5ug/ml (STEMCELL Technologies, Vancouver, BC, Canada), recombinant human fibroblast growth factor 20ng/ml (Peprotech, Hamburg, Germany) and epidermal growth factor 20ng/ml. Cells were maintained at clonal densities (10 cells/µl) in T75 culture flasks (TPP, Trasadingen, Switzerland) and passaged weekly using Accutase (Chemie Brunschwig AG, Basel, Switzerland) for dissociation.

Cell transfection

The generation of E47-RFP and dnE47-RFP constructs has been described elsewhere (Mehmood et al. 2009). As a control plasmid we used a pCAGGS_IRES_NLS_GFP vector. Cells were transfected by using both nucleofection and lipofectamin, as described below.

LNT-229 and LN-308 cells were nucleofected using the Amaxa Nucleofector™ 4D kit for cell lines (Lonza, Basel, Switzerland) following manufacturer's instructions using the C-20 program. For flow cytometry experiments 300,000 cells were plated on P100 plastic culture dishes while 10,000 cells were plated on four-well dishes (Greiner Bio-one, Frickenhausen, Germany) for immunocytochemistry. Three to four hours later (i.e. once the cell adhered) the medium was changed to remove dead cells and debris.

For short term immunocytochemical experiments onto adherent cultures, we used lipofection as a transfection method. The day before, 10,000 cells per well were plated in 24-well plates on 20µg/ml Poly-L-lysin-coated coverslips (Sigma-Aldrich, St. Louis, MO, United States). The next day, cells were transfected with 50µl of Optimem, 0.8µg of DNA and 2µl of Lipofectamine (Invitrogen) per well. Four hours later, medium was replaced.

Flow cytometry

Cells were passaged, fixed with ethanol, incubated with RNAse A (50µg/ml, Sigma-Aldrich) and filtered through a 70µm cell strainer (BD Biosciences, San Jose, CA, USA) to remove cell aggregates. Samples were then stained with propidium iodide (125µg/ml, Sigma-Aldrich) or Hoechst (1.25µl/ml, Sigma-Aldrich) depending on the reporter protein of the construct used, and analyzed on a Beckman Coulter FC500 (Beckman Coulter, Indianapolis, IN, USA). Doublets were eliminated by forward scatter (FSC), side scatter (SSC) area, width and height function dot plots. For cell cycle analyses, data

were plotted on gated linear histograms using the WinMDI 2.9 software (free software, http://facs.scripps.edu/software.html).

Immunocytochemistry

Cells were first blocked in TBS/10% horse serum/0.4% Triton-X-100 (TBS^{++}) and then incubated with primary antibodies, washed and incubated with fluorescent conjugated secondary antibodies. Finally cells were counterstained with 4′, 6-diamidino-2-phenylindole (DAPI; Invitrogen) and mounted with Mowiol. The following primary antibodies and dilutions were used: rabbit α-hOlig2 (1:200, LifeSpan Biosciences, Seattle, WA, USA), mouse α-APC (1:500, Calbiochem, Merck KGaA, Darmstadt, Germany), chicken α-GFP (1: 1000, Abcam, Cambridge, ENG, United Kingdom), rabbit α-RFP (1: 500, MBL International Corporation, Woburn, MA, USA), Rabbit α-Casp3A (1: 500, R&D Systems, Minneapolis, MN, USA), mouse α-Ki67 (1: 400, BD Bioscences). Species-matched, cross-absorbed AlexaFluor-488/555/647 secondary antibodies were used at 1:1000 (Invitrogen).

Semi-quantitative Real Time PCR (qPCR)

All RNA extractions were performed using the Qiagen RNAeasy kit, including a DNAse treatment (Qiagen, Valencia, CA, USA). Similar amounts of RNA were converted to cDNA using oligo (dTs) and the M-MLV reverse transcriptase (Promega, Madison, WI, USA).

For each reaction 10ng of cDNA were amplified with specifically designed primers (see Table 1 in Supplementary Data) and SybrGreen mix (Roche, Basel, Switzerland) using the Roche LightCycler 480 technology. Relative gene expression was determined using the ΔΔ-CT method versus the housekeeping genes HPRT1 and PPIA.

For the qPCR array data, RNA extraction was performed as described above and reverse transcription as specified by the manufacturer with the RT^2 first strand kit (SABiosciences, Roche). The Human Cancer Pathway Finder PCR Array (PAHS-033 3.0) was used and the data analyzed with the provided Microsoft Excel template using B2M and RPL13A as housekeeping genes. The heat map plot was generated using the online analysis tool from SABiosciences and presented as "log2 fold change of expression".

Lentiviral vectors production and titration

The production of both lentiviruses was performed as previously described (Barde et al. 2010). The inducible pSIN_RFP_hPGK_rtTA2SM21 and pSIN_dnE47RFP_hPGK_rtTA2SM21 lentiviral constructs were generated by inserting amplified PCR fragments of RFP and dnE47RFP into MluI restriction sites of the pSIN-TRE-mSEAP-hPGK-rtTA2SM21 vector (Barde et al. 2006). Correct insertion was verified by sequencing of the fragments of interest. These lentiviral vectors allow tight, dose-dependent, inducible control of transgene expression upon doxycyclin (Sigma) exposure.

For lentiviral production, 293T cells were transfected with three plamids encoding for the VSV G envelope protein, HIV-1 Gag, Pol, Tat and Rev proteins as well as the recombinant vector. All three constructs were transfected with Calcium Phosphate and the supernatant collected three times before ultracentrifugation (120min, 50'000 x g, 16°C, Beckman Coulter). The titers ranged from $5x10^8$ to $5x10^9$ IU/ml and were determined by both flow cytometry and qPCR on HCT116 cells. Flow cytometry measured the numbers of fluorescent transfected cells and qPCR, the number of copies of the lentivirus integrated in the genome of infected cells.

Sphere Formation Assay

Glioma-initiating cell lines were infected with 100 IU of lentiviral constructs per cell and seeded at a clonal density of 10 cells/µl in 24-well-plates, four wells per condition. The medium containing doxycycline (2µl/ml) was replenished every 2nd or 3rd day and the number of spheres and the diameter were determined 7 days later. Both bright-field and fluorescence pictures of each well were taken on an inverted microscope (Carl Zeiss, Oberkochen, Germany) and overlaid for quantifications on the ImageJ software (Rasband WS, ImageJ, Bethesda, MD, USA). Only transfected spheres were considered for quantification. The spheres were passaged four times and replated at clonal densities each time. Results are the mean of four independent experiments. For qPCR measurements, infected glioma-initiating cells were seeded in T75 culture flasks. After 7 days spheres were collected at 300 x g and dissociated. Single cells were replated in doxycycline containing growth medium and the RNA extracted 48 hours following induction. For RFP/GFP competition experiments, cells were transduced with a constitutive GFP lentivirus (pRRLSIN.cPPT.PGK-GFP.WPRE) and mixed 1:1 with cells transduced with either the RFP or the dnE47RFP lentivirus. The formation of GFP and RFP positive spheres was monitored over three passages.

Animal studies and tissue processing

All animal procedures were approved by the Ethics Committee of the Veterinary Department of the Canton of Zurich and performed in accordance with Swiss law. T269 cells, previously transduced with either the RFP or dnE47RFP lentivirus were transduced with a constitutive GFP lentivirus (pRRLSIN.cPPT.PGK-GFP.WPRE) and FACS-sorted to reach a 100% GFP positive population. 100,000 cells in 3µl were stereotaxically grafted in the right striatum of 7-9 week old female athymic mice (CD1*nu/nu* mice, Charles River, Wilmington, MA, USA). 4.5 weeks post-transplantation, mice were divided into 4 groups (n=10): those who received T269 transfected with GFP/RFP (group 1) or with GFP/dnE47::RFP (group 2) were treated with doxycycline (2mg/ml, 1% sucrose) in the drinking water to induce expression of the construct. Groups 3 and 4 (transfected with GFP/RFP or GFP/dnE47::RFP) received 1% sucrose solution as their respective control. Two weeks following doxycycline induction, 3 animals per group were sacrificed for histological analyses and the remaining animals (n=7) left to survive until onset of clinical symptoms. Animals were perfused with 4% PFA and brains, postfixed for 24 hours in the same fixative and cryoprotected in 30% Sucrose. 50um thick brain sections were cut on a sliding microtome and serially collected. To study transduction and induction efficiency, free floating sections were washed and, blocked in PB with 1% Triton X-100 (Sigma-Aldrich, Switzerland) and 10% horse serum (Gibco) for 1h at RT. and incubated with the

following primary antibodies: mouse anti-human nuclear antigen (1:500; Millipore, Billerica, MA, USA) or rabbit anti-RFP (1:500; MBL International Corporation). Sections were then revealed with the corresponding fluorescent conjugated secondary antibodies (1:1000; Life Technologies), counterstained with DAPI, mounted and coverslipped with Mowiol.

Image acquisition and analysis

Images were acquired using a Leica DM5500 B upright microscope (Leica Microsystems, Mannheim, Germany) or a Zeiss Axiovert 10 inverted microscope (Carl Zeiss), for *in vivo* and *in vitro* analysis, respectively. For all long-term glioma cell lines *in vitro* immuno-experiments, 4 wells per condition were analyzed in 3 independent experiments (n>3). A total of 5 random fields per well were acquired and the average over wells was calculated. For all patient-derived glioma-initiating cell *in vitro* experiments, 4 wells per condition were analyzed in 4 independent experiments (n=4). For histological analyses, 200 cells per region in three animals (n=3) were randomly selected and analyzed using the Leica Software (Leica Microsystems) at 10x (hNA analyses) and 20x (induction efficiency)-fold magnification.

For single cell densitometry, in each experiment (n=3) and condition a total of 20 randomly chosen cells per well were imaged using a Leica TCS SPE II confocal microscope (Leica Microsystems). Confocal stacks consisting of 10 images (step size 2µm) were acquired using a 40X objective (N.A. 1.15) and were analyzed using the Leica Software (Leica Microsystems). The compared conditions were exposed with the exact same settings and 3 regions of interest were drawn in each cell (nucleus and cytoplasm) in order to measure the mean grey value.

Statistical analyses

All statistical analyses were performed with Prism 5 (GraphPad Software, La Jolla, CA, USA). Analyses are presented as mean + SEM, and samples were compared for significance using unpaired t-test or ANOVA followed by Tukey's post-hoc tes, as appropriate.

Results

Human glioma cell lines show heterogeneous patterns and levels of expression of class II and V (b)HLH proteins

We selected two human glioma cell lines (i.e. LN-308 and LNT-229) based on their level and pattern of expression of transcripts coding for Class I, II and V bHLH proteins. Both cell lines expressed high levels of inhibitors of differentiation transcripts (ID1-4), when compared to whole-brain RNA extracts, although with marked differences. While both cell lines expressed higher levels of *ID1*, *ID3* was shown to be specifically up-regulated in LN-308 cells and *ID4* in LNT-229 cells (**Fig. 1A**). Class I E47 was enriched only marginally in both cell lines (**Suppl. Fig. 2A**). Measurement of transcript levels for selected Class II bHLH proteins revealed a clear difference between the LN-308 cells that express low levels of *Olig2*, *hAscl1* and *Ngn2* and LNT-229 cells in which these genes were highly transcribed (**Fig. 1B,** e.g. > 1000 fold change for *Olig2* compared to whole-brain or LN308 cells RNA). Immunodetection and optical density measurements of Olig2 confirmed its overexpression in LNT229 cells at the protein level, while the early pan-glial marker *adenomatous polyposis coli* (APC) was expressed at similar levels in both glioma cell lines (**Fig. 1C-D**).

Altogether, these results reveal that human glioma cell lines express heterogeneous levels of (b)HLH transcription factors, which allows comparing the consequences of E protein overexpression in the relative presence or absence of Class II bHLH dimerization partners.

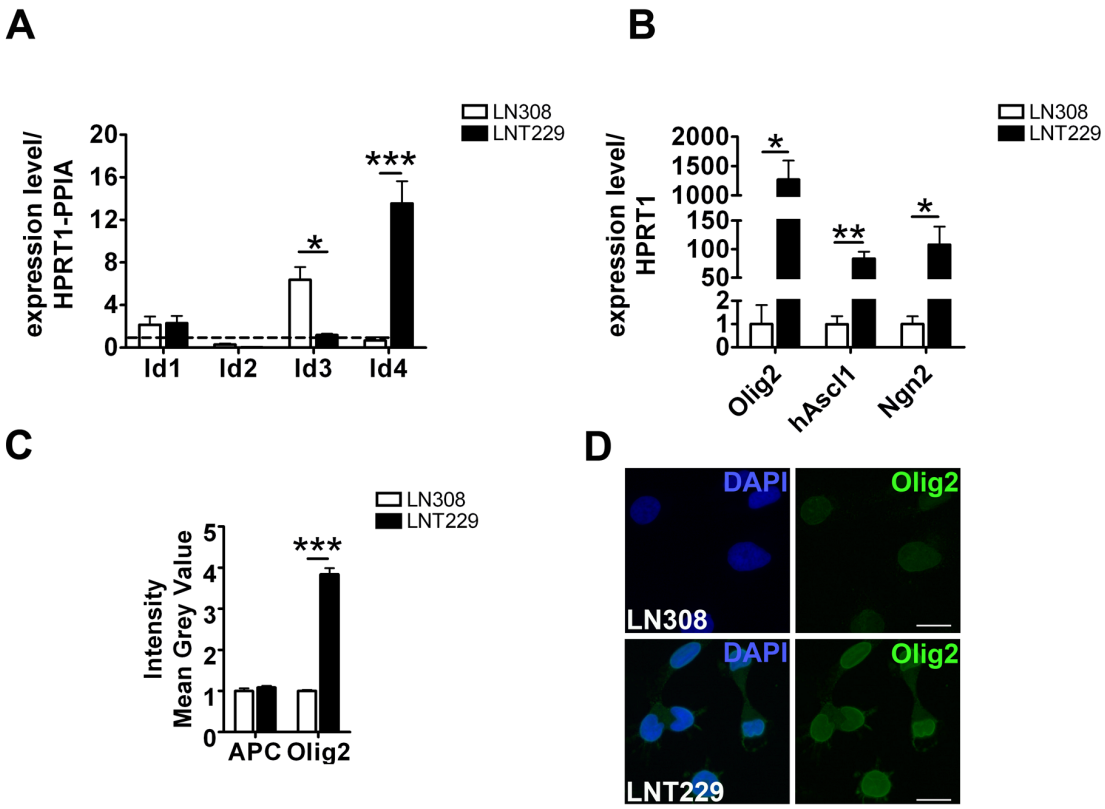

Figure 1 Human glioblastoma cell lines show heterogeneous expression levels of HLH and bHLH proteins. A**,** mRNA expression levels of all four ID proteins compared to whole-brain extract revealed enrichment of distinct ID proteins in the LN308 and LNT229 cell lines. B, mRNA expression levels of the bHLH transcription factors Olig2, Ascl1 and Ngn2, revealed overexpression of proneural proteins in the LNT229 cell line only. C**,** normalized single cell densitometry for the glial marker APC and Olig2, confirmed Olig2 protein enrichment in LNT229 cells. D**,** confocal microscopy of hOlig2 protein expression in LN308 and LNT229 cells. * $p < 0.05$; *** $p < 0.001$. Scale bar = 100µm.

E47 overexpression differentially induces cell death in LN-308 and LNT-229 glioma cells

We next tested the consequences of E protein overexpression on glioma cell proliferation and death. As E proteins have been previously shown to be interchangeable, we arbitrarily selected E47 to perform these experiments. We overexpressed E47 fused with RFP (E47::RFP) in LN-308 and LNT-229 and analyzed the effects onto cell proliferation and cell death 48 hours post-nucleofection by flow cytometry and immunostaining. The effects of E47::RFP overexpression on proliferation were minimal in both cell lines, with neither changes in the G2/G1 (**Fig. 2A**) nor in the percentage of electroporated cells expressing the proliferation marker Ki67 (**Fig. 2B-C**). Surprisingly however, E protein overexpression resulted in a 4-fold induction of cell death in LN-308 cells (**Fig. 2D**) as revealed by the percentage of cells detected in the subG1 region (i.e. 5.7 ± 0.1 in controls *vs*. 20.3 ± 3.8 in E47 overexpressing cells). Similarly, while only 7.7 ± 2.1% of the LN308 cells transfected with a control plasmid expressed the apoptosis marker Caspase3A, this percentage was raised to 20.5 ± 1.9% following E47 overexpression (**Fig. 2E-F**). Interestingly, survival of LNT-229 cells was not affected by E47 overexpression (**Fig. 2D-F**). Taken together, E protein overexpression differentially induced cell death in LN-308 but not in LNT-229 cells, possibly due to their contrasted expression levels of Class II bHLH proteins.

Overexpression of the Class II bHLH proteins Olig2 blocks E47-induced cell death in LN-308 glioma cells

We reasoned that the presence of Class II bHLH proteins (i.e. Olig2) might have counteracted E47-mediated apoptosis in LNT229 glioma cells. To test this hypothesis, we overexpressed Olig2 alone or together with E47 in LN-308 cells and monitored proliferation and cell death after 48 hours. Overexpression of Olig2 proteins increased significantly the proliferation of LN308 cells as revealed by flow cytometry (i.e. G2/G1 ratio, **Suppl. Fig. 3A**) and Ki67 immunodetection (**Suppl. Fig. 3B**). Interestingly these changes were not potentiated by co-nucleofection of class II bHLH proteins with E47, suggesting they may depend on homodimer formation. In contrast to cell proliferation, Olig2 overexpression did not significantly influence cell death in LN308 cells, but fully blocked E47-induced apoptosis in LN-308 (**Fig. 2G-H**).

Altogether, these results indicate that Class II bHLH proteins are critically involved in glioma cell proliferation and survival, and suggest that their activity must be counteracted together with ID proteins in order to achieve anti-glioma effects.

Figure 2 (next page) E47-induced cell death in glioma cells depends on low Olig2 expression levels. A, proliferation was unaffected in either cell line at 48h after nucleofection as seen by the G2/G1 ratio. B, the number of RFP/Ki67 positive cells showed similar trends. C, Arrowheads indicate transduced LN308 cells positive for Ki67. Higher magnifications show a representative RFP/Ki67^{+} cell. D, the subG1 population percentage was significantly higher in the low-bHLH cell line LN308. E, Immunodetection of the apoptotic marker activated-Caspase3 confirmed the flow cytometry data. F, Arrowheads show transfected LN308 cells positive for Casp3A. Higher magnifications show a representative RFP/Casp3a^{+} cell. G-H, co-overexpression of E47 and Olig2 blocked E47-induced cell death E47 in the LN308 line, as revealed by flow cytometry (G) and Cassp3A immunodetection (H). All significances were compared to control; * $p<0.05$; ** $p<0.01$; *** $p<0.001$. Scale bars = 20μm (higher magnification scale bar = 10μm)

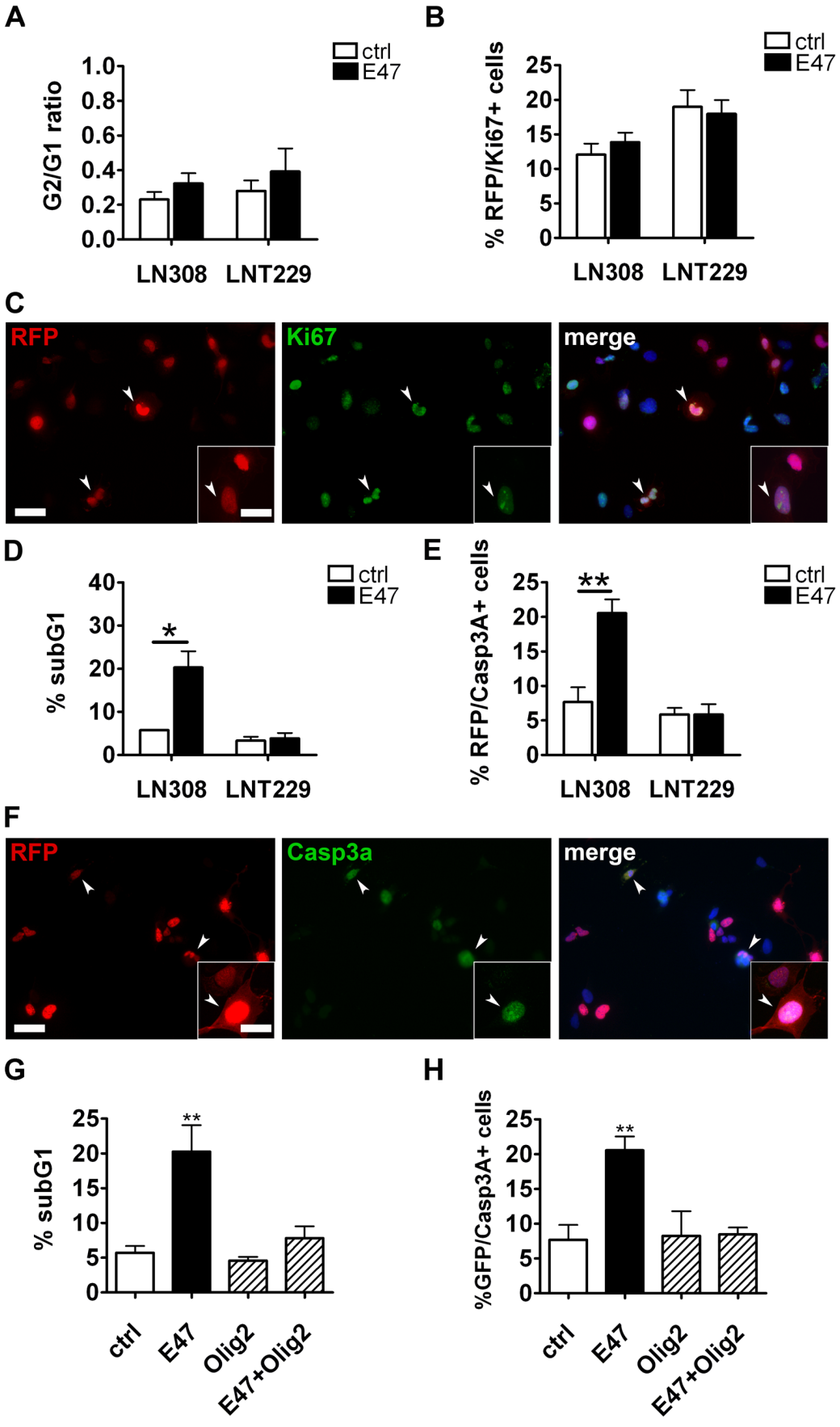
A
G2/G1 ratio
1.0
0.8
0.6
0.4
0.2
0.0
ctrl
E47
LN308
LNT229
B
% RFP/Ki67+ cells
25
20
15
10
5
0
ctrl
E47
LN308
LNT229
C
RFP
Ki67
merge
D
% subG1
40
30
20
10
0
*
ctrl
E47
LN308
LNT229
E
% RFP/Casp3A+ cells
25
20
15
10
5
0
**
ctrl
E47
LN308
LNT229
F
RFP
Casp3a
merge
G
% subG1
25
20
15
10
5
0
**
ctrl
E47
Olig2
E47+Olig2
H
%GFP/Casp3A+ cells
25
20
15
10
5
0
**
ctrl
E47
Olig2
E47+Olig2

E47 lacking its nuclear localization signal sequesters Olig2 in the cytoplasm and induces cell death in both low and high-bHLH expressing gliomas

The E47 protein forms homodimers or heterodimers with Class II bHLH proteins and translocate to the cell nucleus where it is transcriptionally active. As a consequence, single-cell densitometry analysis revealed an exclusive nuclear location of the E47::RFP fusion protein (**Fig. 3A-C**). In order to sequester both E47 and its binding partners in the cytoplasm, and therefore block their transcriptional activity, we used a dominant-negative mutant form of E47 (dnE47) lacking its nuclear localization signal (NLS). Single densitometry analysis for RFP confirmed the cytoplasmic localization of the dnE47::RFP fusion protein (**Fig. 3D-F**), as well as the rapid and efficient cytoplasmic sequestration of its dimerization partner Olig2 (**Fig. 3G**). Thus, E47 proteins can be successfully engineered to prevent their translocation as homo or heterodimers to the cellular nucleus and to modulate transcription (see below).

We next tested the consequences of dnE47::RFP overexpression in LNT229 and LN308 cells, 48 hours post- transfection. Similarly to E47::RFP, dnE47::RFP overexpression had only marginal effects onto glioma cell proliferation (**Fig. 3H-J**). In contrast, the effect of dnE47 overexpression onto glioma cell death was pronounced, and observed in both glioma cell lines (**Fig. 3K-M**). Flow cytometry analyses revealed a significant increase in the percentage of cells in subG1 in LN308 and LNT229 cells, with LNT229 cells showing a stronger response (**Fig. 3K**). These observations were confirmed by analyzing the number of RFP^{+}/$Casp3a^{+}$ cells (**Fig. 3L-M**). The LN-308 glioma cell line exhibited a similar response to dnE47::RFP overexpression compared with wtE47::RFP (compare **Fig. 2D & 3K**) whereas LNT-229 cells remarkably revealed higher levels of apoptosis. These findings emphasize the need to neutralize Class II (b)HLH proteins transcriptional activity to achieve anti-glioma effects.

Figure 3 (next page) Overexpression of E47 lacking its nuclear localization signaling sequesters Olig2 in the cytoplasm and induces cell death in both glioma cell lines. A-C, the E47 wild-type protein fused to a RFP reporter showed an exclusively nuclear location following electroporation, as quantified by single-cell densitometry in LN308 (B) and LNT229 (C) cells. D-F, the mutant form of E47 lacking its NLS was retained in the cytoplasm in both cell lines. G, hOlig2 is located in the nucleus or in the cytoplasm in LNT229 cells, following overexpression of E47 or dnE47, respectively. H, Flow cytometry measurements of the G2/G1 ratios, revealed a reduced proliferation in LNT229 cells following dnE47 overexpression. I, No changes in the percentage of RFP/Ki67^{+} cells was detected. J, Arrowheads show transduced LNT229 cells positive for Ki67. Inserts show higher magnifications of a representative RFP/Ki67^{+} cell. K-L, overexpression of dnE47 induced cell death in both glioma lines as shown by flow cytometry subG1 measurements (K) and immunodetection of Casp3A (L). M, Arrowheads show transduced LNT229 cells positive for Casp3A. Inserts show higher magnifications of a representative RFP/Casp3A^{+} cell. * $p<0.05$; ** $p<0.01$; *** $p<0.001$; Scale bars = 20μm (higher magnification scale bar = 10μm)

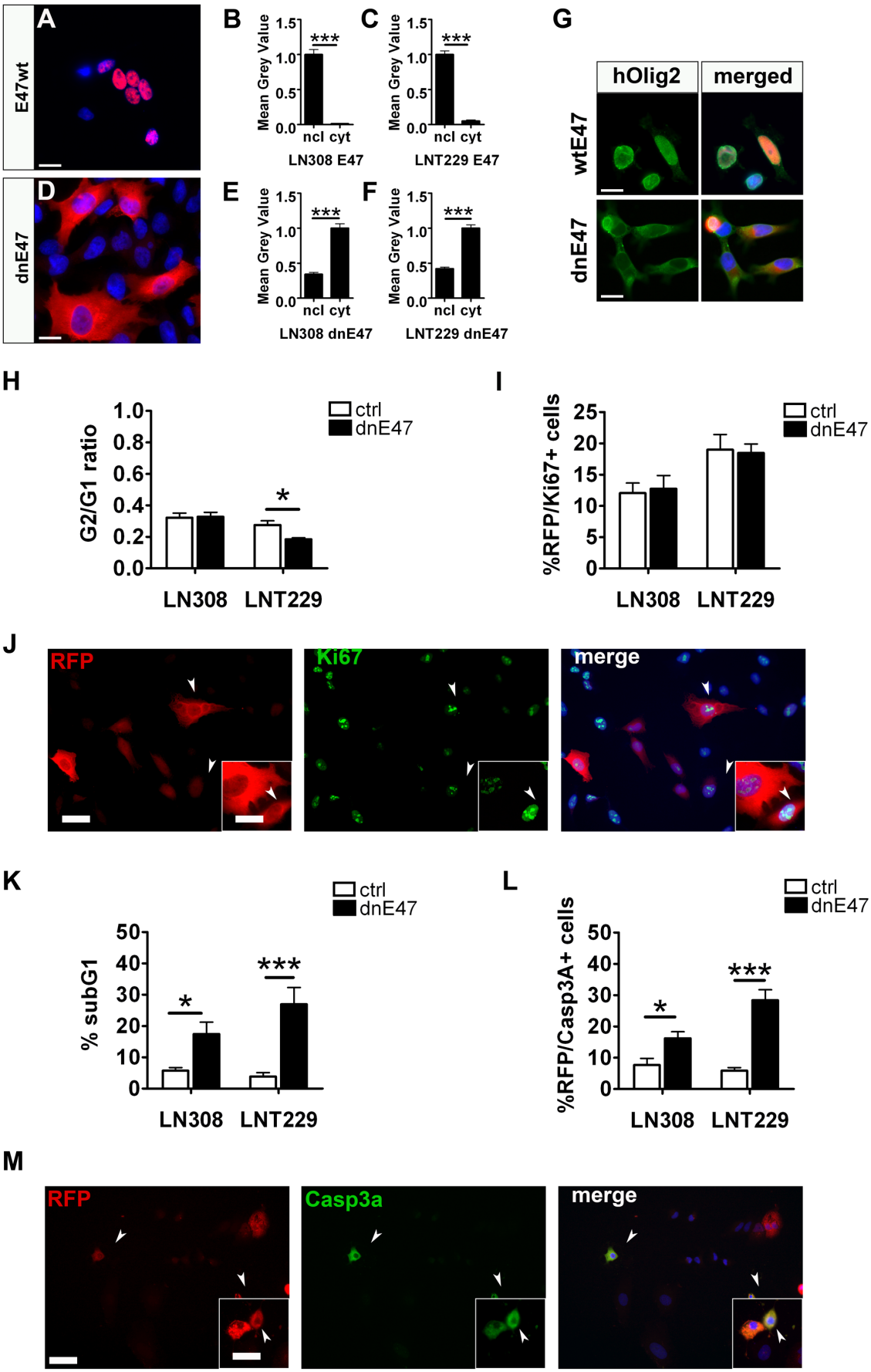
A
E47wt
D
dnE47
B
C
Mean Grey Value
1.5
1.0
0.5
0.0
***
ncl cyt
LN308 E47
LNT229 E47
E
F
LN308 dnE47
LNT229 dnE47
G
hOlig2
merged
wtE47
dnE47
H
G2/G1 ratio
ctrl
dnE47
*
LN308
LNT229
I
%RFP/Ki67+ cells
J
RFP
Ki67
merge
K
% subG1
L
%RFP/Casp3A+ cells
M
Casp3a

DnE47 overexpression induces dramatic changes at the gene expression level

Gene expression modifications following dnE47::RFP overexpression in LNT-229 gliomas was assayed by qPCR at 48 hours following transfection using an array of genes representative of six biological pathways involved in transformation and tumorigenesis (see Material and Methods and **Suppl. Table S4**). Overexpression of E47::RFP induced minimal transcriptional changes in LNT-229 (**Fig. 4A**), in agreement with the minor phenotypic changes described above. In contrast, overexpression of dnE47::RFP induced marked gene expression modifications throughout (**Fig. 4B**). In particular, genes involved in cell cycle and apoptosis were only significantly induced following dnE47::RFP overexpression (**Fig. 4C**). These include, *CDC25A* and *BCL2L1* that were significantly down-regulated following dnE47::RFP overexpression, consistent with reduced proliferation and increased cell death observed in LNT-229 glioma cells, respectively. These data were confirmed by qPCR using self-designed primers (**Fig. 4D-E**).

Taken together, these results highlight superiority of dnE47::RFP over E47::RFP in disrupting gene expression in glioma cells, in particular the expression of pro-proliferative and anti-apoptotic genes.

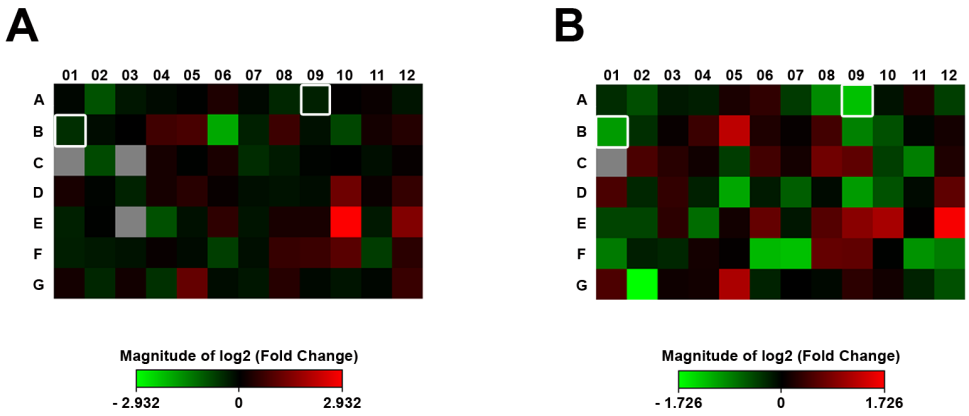

C

Table 1

	E47		dnE47	
	fold change	p value	fold change	p value
Cell Cycle				
CCNE1	-1.17	0.12	**-1.34**	**0.01****
CDC25A	-1.44	0.16	**-2.08**	**0.01****
CDK2	-1.10	0.28	**-1.24**	**0.05***
Apoptosis				
BCL2	-1.36	0.18	**-1.93**	**0.01****
BCL2L1	-1.30	0.52	**-2.48**	**0.05***

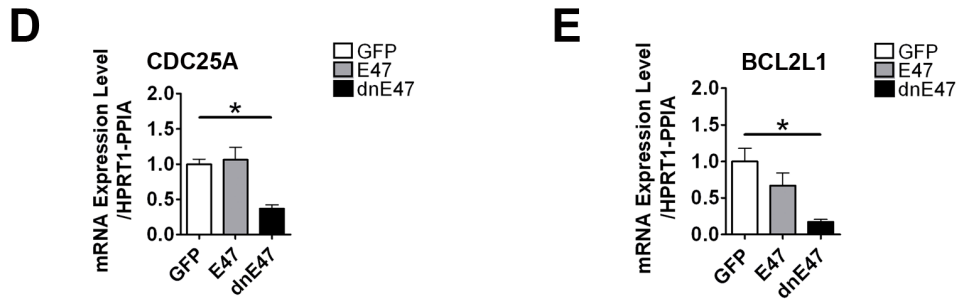

Figure 4 Overexpression of dnE47 in LNT229 glioma cells induces down-regulation of pro-proliferative and anti-apoptotic genes. A, changes in gene expression representative of six biological pathways involved in transformation and tumorigenesis were minor after E47 overexpression in LNT229 cells. B, dnE47 overexpression induced more pronounced changes in gene expression levels. C, E47 overexpression did not influence the expression of genes involved in proliferation and apoptosis whereas dnE47 significantly altered their expression levels. D-E, 48h after transfection, qPCR confirmed that mRNA levels of CDC25a (D, B01 in A and B) and BCL2L1 (E, A09 in A and B) were significantly reduced. Heatmap: log2 fold change. * $p<0.05$; ** $p<0.01$

DnE47 efficiently reduces the sphere-forming capacity of glioma-initiating cells

We next expanded our studies with 2 patient-derived glioma-initiating cells (T269 and S24). qRT-PCR analysis revealed an enrichment for the common stem-cell marker Nestin in both T269 and S24 cells, when compared with whole brain RNA (**Fig. 5A**). Similarly to glioma cell lines, high levels of Class II bHLH transcripts expression, in particular of *Olig2* (**Fig. 5A**), as well as specific ID proteins transcripts were detected (**Fig. 5B**), while E protein transcripts were only marginally enriched (**Suppl. Fig. 2B**). A clonogenic sphere assay was next performed to examine dnE47 overexpression on self-renewal and survival in glioma-initiating cells. Cells were transduced with a doxycycline-inducible lentivirus coding for dnE47::RFP or RFP as a control. T269 and S24 cells were plated at clonal densities (10 cells/µl) and the number of spheres and their diameter were analyzed every 7 days, prior and over four subsequent passages following transgene induction (i.e. 2ug/ml of doxycyclin). Induction of dnE47::RFP expression in T269 cells resulted in a decreased number of large (>90 µm) as well as medium-sized (70-90µm) spheres, that could already be observed at the 1st passage (i.e. 1 week post-induction. **Fig. 5C**). At the 4th passage, dnE47::RFP dramatically decreased the number of spheres in all size categories, to values <25% to controls, (**Fig. 5D & E**). Similarly to glioma cell lines, quantification of gene expression 48 hours post-induction revealed that *Cdc25A* and *Bcl2-L1* were significantly down-regulated in dnE47::RFP transduced cells (**Fig. 5F**), suggesting that changes in proliferation and survival could contribute to sphere loss. In addition, a 60% reduction of Nestin expression was observed following dnE47::RFP induction (**Fig. 5F**), supporting loss of stemness. To more directly assess the anti-glioma effects of dnE47::RFP over-expression, T269 cells transduced with a constitutive control GFP lentivirus or an inducible dnE47::RFP lentivirus were mixed (1:1) and the number of GFP+ and RFP+ neurospheres quantified prior or following doxycycline-treatment. Induction in both cell lines showed a rapid and strong decrease of RFP expressing spheres (~40%) already at the 1st passage (P1). Strikingly, RFP-expressing spheres were almost extinguished at the 2nd and 3rd passages, illustrating their marked disadvantage compared to control GFP-expressing spheres (**Fig. 5G-H**). Similar results were obtained with S24 cells, demonstrating the robustness and consistency of dnE47 overexpression as an anti-glioma strategy (**Suppl. Fig. 5**).

Figure 5 (next page). Patient-derived glioma-intiating cells express high levels of (b)HLH transcripts and show reduced sphere formation capacities upon dnE47 overexpression. A, both S24 and T269 glioma-intiating cells showed enrichment for the stem cell *Nestin* transcript as well as for *Olig2* and *hAscl1* transcripts. B, their expression profile of ID proteins transcripts is more heterogeneous. C, following dnE47 overexpression in T269 glioma-initiating cells, medium and large sphere numbers were reduced at the first passage compared to RFP overexpression. D, sphere numbers of all sizes were reduced within four passages. E, the total number of spheres dropped significantly after dnE47 overexpression over passages. F, the reduction in sphere formation capacities correlates with a lower expression of genes coding for the pro-proliferative marker CDC25A, the anti-apoptotic protein BCL2L1 and the stem-cell marker Nestin. G, when mixed with GFP-expressing spheres at a ratio of 1:1, the number of dnE47::RFP-overexpressing spheres rapidly declined. H, representative picture of GFP and dnE47::RFP mixed sphere cultures. * $p<0.05$; ** $p<0.01$; *** $p<0.001$. Scale bar = 100µm

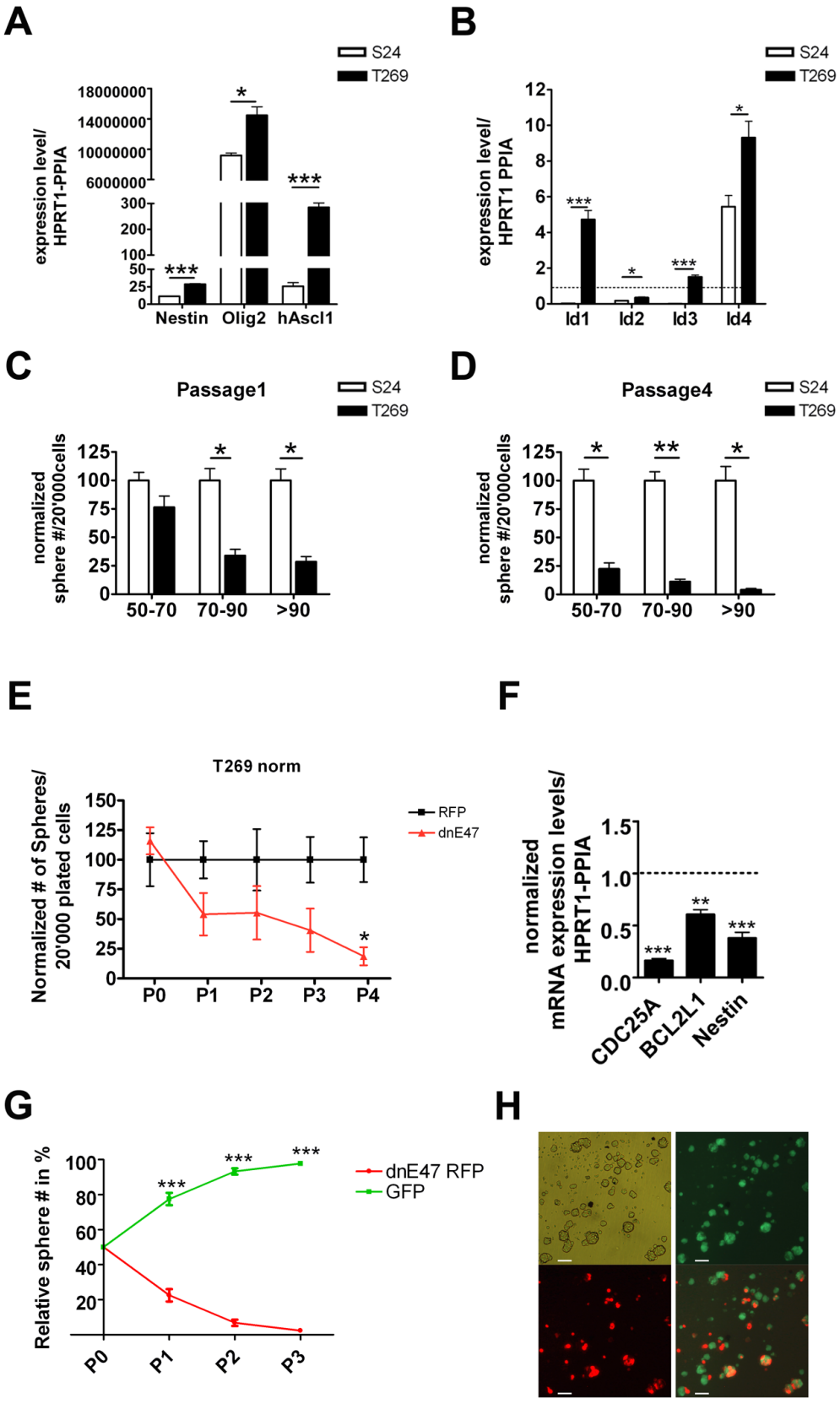
A
S24
T269
expression level/ HPRT1-PPIA
18000000
14000000
10000000
6000000
300
200
100
50
25
0
*
***
***
Nestin
Olig2
hAscl1
B
S24
T269
expression level/ HPRT1 PPIA
12
10
8
6
4
2
0
***
*
***
*
Id1
Id2
Id3
Id4
C
Passage1
S24
T269
normalized sphere #/20'000cells
125
100
75
50
25
0
*
*
50-70
70-90
>90
D
Passage4
S24
T269
normalized sphere #/20'000cells
125
100
75
50
25
0
*
**
*
50-70
70-90
>90
E
T269 norm
Normalized # of Spheres/ 20'000 plated cells
150
125
100
75
50
25
0
RFP
dnE47
*
P0
P1
P2
P3
P4
F
normalized mRNA expression levels/ HPRT1-PPIA
1.5
1.0
0.5
0.0
***
**
***
CDC25A
BCL2L1
Nestin
G
Relative sphere # in %
100
80
60
40
20
***
***
***
dnE47 RFP
GFP
P0
P1
P2
P3
H

Overexpression of dnE47 delays the onset of clinical symptoms following T269 glioma xenografts

Finally, we investigated the effects of dnE47 overexpression *in vivo* by using a doxycylin-inducible gene expression approach in established T269 glioma xenografts. First, T269 cells were co-transduced with a constitutive GFP and an inducible RFP or dnE47-RFP lentiviral construct. Then, these *ex vivo* transduced T269 cells were grafted into the right striatum of athymic mice. Histological analysis on day 30 (i.e. before doxycycline administration) showed that all transplanted T269 glioma cells, identified by their expression of the human nuclear antigen, were GFP-positive in the corpus callosum, the subventricular zone and the fimbriae hippocampi (**Fig. 6A**). Forty-five days post-transplantation, doxycycline was administered in the drinking water to induce dnE47-RFP or RFP expression in the established T269 experimental glioma. Because both constructs contained an RFP reporter protein, we monitored the subcellular localization of the induced target protein by RFP fluorescence. The efficiency of doxycyline-mediated induction *in vivo* was high for both constructs with grafted GFP cells being 97.6 ± 0.2% RFP positive in the control group; whereas 90.7 ± 0.4% of the cells expressed the dnE47 construct (**Fig.6B**). As before, the RFP signal was localized only in the cytoplasm upon induction of dnE47 expression but the RFP signal in control-transfected glioma cells was distributed ubiquitously in cellular compartments (**Fig. 6C** left and right, respectively). In parallel, we monitored all glioma-bearing mice daily and sacrificed them at onset of clinical symptoms. Upon doxycycline administration, the median survival for the RFP control group was of 75 days whereas >60% of dnE47-glioma-bearing mice remained symptom-free beyond 90 days (**Fig.6D**).

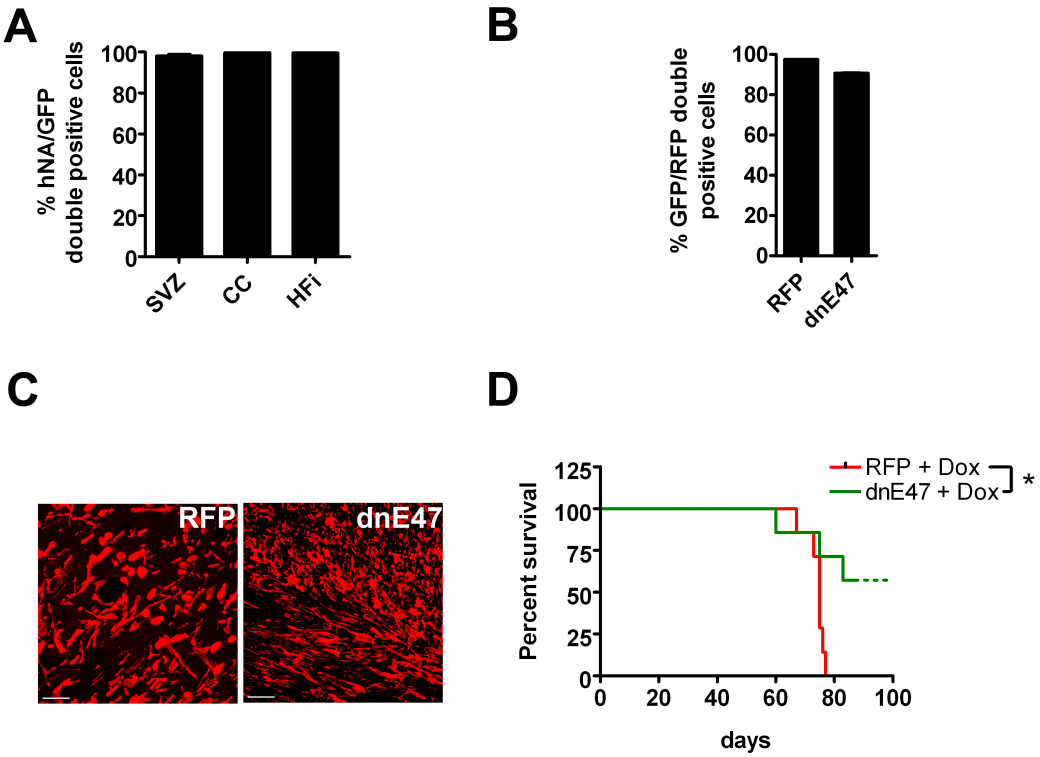

Figure 6. The induction of dnE47 expression in experimental gliomas delays the onset of clinical symptoms. A, all human nuclear antigen (hNA) transplanted glioma cells were positive for GFP. B, detection of RFP expression revealed that doxycycline-mediated induction of transgene expression *in vivo* was efficient with both the RFP and dnE47::RFP lentiviral vectors. C, the RFP reporter signal was localized in the whole cell body when the control RFP lentivirus was induced (left) whereas the RFP signal was only localized in the cytoplasm upon doxycyline-mediated induction of dnE47-RFP (right). D, dnE47 overexpression prolonged the survival of tumor bearing mice. SVZ: subventricular zone ; CC: corpus callosum ; HFi: Fimbria Hippocampi. * $p<0.05$. Scale bar = 20µm

Discussion

The pro-tumorigenic features of Class II and V proteins in glioma cells call for the establishment of a feasible therapeutic anti-cancer strategy by disrupting (b)HLH transcriptional networks. Here we used E proteins in order to target (b)HLH transcriptional networks in glioma cells because of their ability to bind all ID proteins with identical affinity (Massari & Murre 2000; Teachenor et al. 2012) as well as the proneural proteins Olig2 and Ascl1 (Samanta & Kessler 2004; Geoffroy et al. 2009).

By investigating the consequences of E proteins overexpression in glioma cell lines expressing low or high levels of Class II (b)HLH proteins, our results show that the nuclear translocation/transactivation of proneural proteins by E proteins should be prevented in order to achieve anti-glioma responses. Thus, although E47 overexpression was sufficient to induce cell death in the low Olig2-expressing cell line LN-308, it failed to show the same effect in the LNT-229 cell line, which expresses high levels of Olig2. Furthermore, these pro-apoptotic effects were blocked in LN-308 cells by co-transfection of E47 with Olig2, confirming its rescuing role on the observed phenotype. We used a dominant-negative approach in which E proteins were engineered to prevent their nuclear translocation without affecting their dimerization pattern (Mehmood et al. 2009; Murre, McCaw, Vaessin, et al. 1989), resulting in cytoplasmic sequestration of Class II and V (b)HLH proteins (our results; (Murre, McCaw, Vaessin, et al. 1989; Deed et al. 1996). Accordingly, the anti-glioma effects of dnE47 overexpression were consistently superior to wtE47 in all glioma cell lines tested despite important differences in proneural protein expression pattern.

Our results revealed significant changes in expression levels of several cell cycle protein transcripts (i.e. CCNE1, CDC25A and CDK2). However, direct measurements of cycling cells by flow cytometry and immunostaining was not possible as their detection was obscured from the strongly induced apoptosis (see below). These anti-proliferative properties are likely to be mediated by sequestration of ID proteins whose overexpression has been associated with increased proliferation in several cell types (Christy & Nathans 1989; Murphy & Norton 1990; Ruzinova & Benezra 2003), by directly interacting and inhibiting proteins of the small retinoblastoma family (Rb, p107, p130; (Sherr 1996; Iavarone et al. 1994; Lasorella et al. 1996). In addition, ID

proteins are known to inhibit Ets-mediated transcription of P16lnk4a, a tumor suppressor gene operating in a common pathway as Rb (Ohtani et al. 2001; Ouyang et al. 2002). In parallel, our results demonstrate an enhanced proliferation in glioma cell lines following Olig2 or Ascl1 overexpression. These results support a role for proneural proteins in promoting glioma cell proliferation, in agreement with previous studies showing regulation of neural progenitors and glioma cells by proneural gene overexpression and/or phosphorylation (Ligon et al. 2004; Ligon et al. 2007; Sun et al. 2011; Castro et al. 2011).

A pronounced apoptosis response was observed following E proteins overexpression in glioma cell lines. Such a pro-apoptotic effect of E proteins has been previously described in other cell types. Overexpression of E2A lead to apoptosis in 293T cells whereas ectopic expression of E47 or E12 proteins promoted cell death in E2A-deficient lymphomas (Engel & Murre 1999a; Pagliuca et al. 2000). Restoration of E2A activity in Jurkat leukemic T cells resulted in an inhibition of cell growth and induction of cell death associated with an increase in apoptotic cells (Park et al. 1999), suggesting that bHLH proteins and in particular ID proteins might be promoting cell growth by inhibiting apoptosis in specific settings (Norton & Atherton 1998). Our results revealed superior and consistent effects following dnE47 overexpression compared to wtE47, highlighting the need to concomitantly neutralize ID and proneural proteins activity to achieve pro-apoptotic responses. Interestingly, although our data phenocopied these previous observations, they revealed that these effects were only visible in cells expressing low levels of proneural proteins such as Olig2. These observations highlight a role for Olig2 in tumor cell survival, possibly through its interaction with p53 (Mehta et al. 2011). In addition, our gene expression analyses revealed Bcl2 and Bcl2l1 are downstream target genes through which E proteins mediate apoptosis. It is known that the expression of anti-apoptotic Bcl2 proteins increases over time during tumor evolution and support an invasive phenotype in glioma cells (Weiler et al. 2006). Furthermore, overexpression of Bcl2 familly proteins in glioma prevents cell death both *in vitro* and *in vivo* (Roth et al. 2000; Weiler et al. 2006).

Patient-derived glioma-initiating cells can be grown in the presence of LIF, FGF2 and EGF, and mirror more closely the phenotype and genotype of primary tumors than serum-cultured cell lines (Lee et al. 2006). As a consequence, contrasting results have

for example been obtained for the role of proneural proteins in promoting human glioma cell lines and patient-derived glioma-initiating cells differentiation (Tabu et al. 2006; Ligon et al. 2007). Importantly, our results in T269 and S26 lines confirmed the anti-glioma effects observed following dnE47 overexpression. The sphere formation capacity of glioma-initiating cells was rapidly and sustainably reduced following induction of dnE47 expression when compared with control-transduced cells. Modifications to proliferation and apoptosis are likely to jointly participate to these effects. Indeed, our qPCR data confirmed in glioma-initiating cells the down-regulation of CDC25A and BCL2-L1 upon dnE47 overexpression, as observed in LN-308 and LNT-229 cells. In addition, Nestin transcripts were down-regulated suggesting changes in patient-derived tumor-initiating cell stemness (Singh et al. 2003; Singh et al. 2004). Finally, we confirmed these *in vitro* observations in a xenograft model. Intrastriatal transplantation of T269 glioma-initiating cells led to the formation of diffusely infiltrating glioma, similar to the GB phenotype in patients. Following doxycycling application, the induction of dnE47 could be readily obtained *in vivo* (Siolas & Hannon 2013). Induction of dnE47 expression was however markedly prominent around the ventricular zone, possibly reflecting better drug diffusion in this region. Here, induction of dnE47 confirmed our *in vitro* results by showing cytoplasmic distribution and by significantly prolonging the survival of tumor bearing animals.

Altogether, our results highlight that neutralization of bHLH transcriptional networks by cytoplasmic sequestration is feasible. Thus, although transcription factors have often been considered to be “undruggable” owing to the nuclear location, dynamic expression and functional redundancy, simultaneous cytoplasmic sequestration of multiple transcription factors by mutating their dimerization partners might represent a novel path for designing anti-glioma intervention strategies.

Acknowledgements

We are grateful to Dr. Isabelle Barde from the Core facility at EFPL Lausanne for here help with the production of the doxycycline-inducible lentiviruses. We thank Dr. Anahi Hurtado and Dr. Kasum Azim for reading the manuscript. We also thank Laetitia Tudeau for technical help with this project. This project was supported by the Swiss National Fund (NF 31-144127). SB was supported by the University of Zurich (Forschungskredit) and the Krebsliga Zurich: "E proteins as transcriptional targets in experimental gliomas".

Disclosure of potential conflicts of interest:

No potential conflicts of interest were disclosed.

Supplementary Data

Supplementary Table S1. List of primers used for quantitative real time PCR experiments.

Supplementary Table S1			
Gene	Sequence	Amplicon lenght	T° and Elongation time
HPRT1 fw	CTGGCGTCGTGATTAGTGAT	134 bp	62°, 6sec
HPRT1 rev	AGCAAGACGTTCAGTCCTGT		
PPIA fw	TTCATCTGCACTGCCAAGAC	39 bp	62°, 7sec
PPIA rev	CTTGCCATCCAACCACTCA		
Id1 fw	CACCCTCAACGGCGAGAT	146 bp	62°, 6sec
Id1 rev	CCACAGAGCACGTAATTCCTC		
Id2 fw	AGCCTGCATCACCAGAGAC	99 bp	62°, 4sec
Id2 rev	TTCAGAAGCCTGCAAGGAC		
Id3 fw	AAATCCTACAGCGCGTCATCG	129 bp	6 sec
Id3 rev	AGATGACAAGTTCCGGAGTGAG		
Id4	QuantiTect Primer Assay QT00234920, Qiagen	149 bp	62°, 6sec
CDC25a fw	CTTCACACAGAGGCAGAACT	139 bp	62°, 6sec
CDC25a rev	GCCATCATCCTCATCAGAC		
Bcl-xl fw	CCACTTACCTGAATGACCACC	96 bp	62°, 4sec
Bcl-xl rev	TCTCGGCTGCTGCATTGTT		
Olig2 fw	TAGATCGACGCGACACCAG	133 bp	62°, 6sec
Olig2 rev	GGAAGATAGTCGTCGCAGC		
hAscl1 fw	CGACTTCACCAACTGGTTCTG	118 bp	62°, 5sec
hAscl1 rev	CCAACGCCACTGACAAGAA		
Nestin fw	AGACTTCCCTCAGCTTTCAGGAC	93 bp	64°, 4sec
Nestin rev	TCAGGACTGGGAGCAAAGATCC		

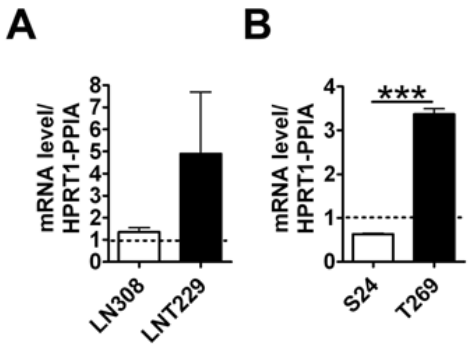

Supplementary Figure S2. E47 is ubiquitously expressed in cancer cells although at various levels. A, qPCR revealed similar or enriched *E47* transcript levels in LN308 and LNT229 cells, respectively, when compared with whole brain extracts. B, S24 cells showed lower levels and T269 higher E47 transcripts levels when compared with whole brain extracts. *** p<0.001

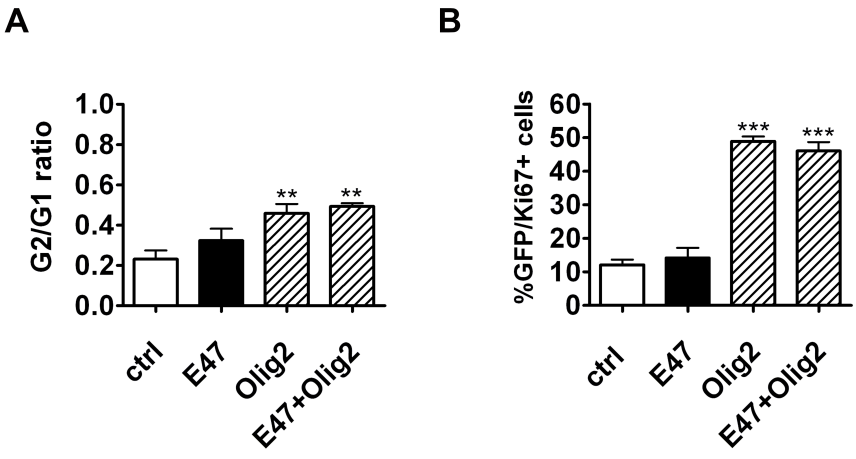

Supplementary Figure S3. Co-overexpression of E47 and Olig2 enhanced proliferation in the LN308 line. A, an increased proliferation was detected in the LN308 cell line following transfection of Olig2 or E47 + Olig2, as revealed by flow cytometry measurements of the G2/G1 ratio. B, Similar results were obtained by immunodetection of Ki67 in the transfected (i.e. GFP-positive) cells. All significances were compared to control; **p<0.01; ***p<0.001

Supplementary Table S4. List of up- or down-regulated genes from the Human Cancer Pathway Finder PCR Array following wtE47 and dnE47 overexpression.

Supplementary Table S4						
			wtE47		dnE47	
Gene name	**Ref Seq**	**Gene description**	**up/down regulation**	**p value**	**up/down regulation**	**p value**
Cell Cycle Control and DNA Damage Repair						
ATM	NM_000051	Ataxia telangiectasia mutated	-1.01	0.87	1.13	0.51
BRCA1	NM_007294	Breast cancer 1, early onset	1.01	0.95	-1.09	0.47
CCNE1	NM_001238	Cyclin E1	-1.17	0.12	-1.34	**0.01****
CDC25A	NM_001789	Cell division cycle 25 homolog A (S. pombe)	-1.44	0.16	-2.08	**0.01****
CDK2	NM_001798	Cyclin-dependent kinase 2	-1.10	0.28	-1.24	**0.05***
CDK4	NM_000075	Cyclin-dependent kinase 4	1.01	0.89	1.03	0.89
CDKN1A	NM_000389	Cyclin-dependent kinase inhibitor 1A (p21, Cip1)	1.67	0.13	1.32	0.30
CDKN2A	NM_000077	Cyclin-dependent kinase inhibitor 2A (melanoma, p16, inhibits CDK4)	1.77	0.32	2.44	0.31
CHEK2	NM_007194	CHK2 checkpoint homolog (S. pombe)	-1.29	0.22	1.03	0.77
E2F1	NM_005225	E2F transcription factor 1	-1.14	0.57	-1.84	0.10
MDM2	NM_002392	Mdm2 p53 binding protein homolog (mouse)	-1.16	0.55	-1.05	0.83
RB1	NM_000321	Retinoblastoma 1	1.07	0.46	1.10	0.39
S100A4	NM_002961	S100 calcium binding protein A4	-1.08	0.59	1.02	0.92
TP53	NM_000546	Tumor protein p53	-1.06	0.60	1.22	0.14
Apoptosis and Cell Senescence						
APAF1	NM_001160	Apoptotic peptidase	-1.09	0.69	-1.15	0.60

		activating factor 1				
BAD	NM_004322	BCL2-associated agonist of cell death	1.27	0.57	1.25	0.58
BAX	NM_004324	BCL2-associated X protein	-1.07	0.82	-1.32	0.19
BCL2	NM_000633	B-cell CLL/lymphoma 2	-1.36	0.18	-1.93	**0.01****
BCL2L1	NM_138578	BCL2-like 1	-1.30	0.52	-2.48	**0.05***
CASP8	NM_001228	Caspase 8, apoptosis-related cysteine peptidase	1.08	0.56	1.17	0.39
CFLAR	NM_003879	CASP8 and FADD-like apoptosis regulator	-3.90	0.85	1.15	0.45
FAS	NM_000043	Fas (TNF receptor superfamily, member 6)	1.33	0.19	1.10	0.62
GZMA	NM_006144	Granzyme A (granzyme 1, cytotoxic T-lymphocyte-associated serine esterase 3)	1.27	0.34	1.20	0.31
HTATIP2	NM_006410	HIV-1 Tat interactive protein 2, 30kDa	1.20	0.41	1.07	0.59
TERT	NM_198253	Telomerase reverse transcriptase	-1.61	0.21	-2.01	0.40
Signal Transduction Molecules and Transcription Factors						
AKT1	NM_005163	V-akt murine thymoma viral oncogene homolog 1	-1.05	0.86	-1.23	0.62
ERBB2	NM_004448	V-erb-b2 erythroblastic leukemia viral oncogene homolog 2	-1.74	0.10	-1.45	0.53
ETS2	NM_005239	V-Ets erythroblastosis virus E26 oncogene homolog 2 (avian)	1.17	0.48	-1.03	0.94

FOS	NM_005252	V-fos FBJ murine osteosarcoma viral oncogene homolog	-1.81	0.24	1.42	0.27
JUN	NM_002228	Jun oncogene	1.39	0.46	-2.20	0.12
MAP2K1	NM_002755	Mitogen-activated protein kinase kinase 1	1.07	0.09	-1.13	0.30
MYC	NM_002467	V-myc myelocytomatosis viral oncogene homolog (avian)	-1.88	**0.05***	-1.66	0.15
NFKB1	NM_003998	Nuclear factor of kappa light polypeptide gene enhancer in B-cells 1	-1.13	0.72	1.09	0.49
NFKBIA	NM_020529	Nuclear factor of kappa light polypeptide gene enhancer in B-cells inhibitor, alpha	1.45	0.33	1.59	0.25
PIK3R1	NM_181504	Phosphoinositide-3-kinase, regulatory subunit 1 (alpha)	-1.20	0.13	1.01	0.88
RAF1	NM_002880	V-raf-1 murine leukemia viral oncogene homolog 1	-1.15	0.07	-1.20	**0.01****
SNCG	NM_003087	Synuclein, gamma (breast cancer-specific protein 1)	1.54	0.28	1.60	0.35
TNFRSF10B	NM_003842	Tumor necrosis factor receptor superfamily, member 10b	-1.09	0.55	-1.17	0.43
TNFRSF1A	NM_001065	Tumor necrosis factor receptor superfamily, member 1A	-1.19	0.44	1.00	0.91
TNFRSF25	NM_003790	Tumor necrosis factor receptor superfamily, member 25	1.35	0.54	-1.04	0.92
Adhesion						
ITGA1	NM_181501	Integrin, alpha 1	-1.03	0.94	1.55	**0.05***

ITGA2	NM_002203	Integrin, alpha 2 (CD49B, alpha 2 subunit of VLA-2 receptor)	1.00	0.69	-1.34	0.26
ITGA3	NM_002204	Integrin, alpha 3 (antigen CD49C, alpha 3 subunit of VLA-3 receptor)	-1.12	0.96	-1.80	0.23
ITGA4	NM_000885	Integrin, alpha 4 (antigen CD49D, alpha 4 subunit of VLA-4 receptor)	1.05	0.63	1.15	0.19
ITGAV	NM_002210	Integrin, alpha V (vitronectin receptor, alpha polypeptide, antigen CD51)	1.20	0.21	1.41	**0.05***
ITGB1	NM_002211	Integrin, beta 1 (fibronectin receptor, beta polypeptide, antigen CD29 includes MDF2, MSK12)	-1.04	0.89	-1.20	0.39
ITGB3	NM_000212	Integrin, beta 3 (platelet glycoprotein IIIa, antigen CD61)	-1.31	0.80	1.26	0.45
ITGB5	NM_002213	Integrin, beta 5	1.20	0.49	-1.16	0.51
MCAM	NM_006500	Melanoma cell adhesion molecule	-1.12	0.56	-1.55	0.15
MTSS1	NM_014751	Metastasis suppressor 1	1.27	0.34	1.23	0.29
PNN	NM_002687	Pinin, desmosome associated protein	-1.21	0.08	-1.15	0.28
SYK	NM_003177	Spleen tyrosine kinase	1.59	0.31	1.57	0.08
Angiogenesis						
ANGPT1	NM_001146	Angiopoietin 1	-1.91	0.30	-1.44	0.12
ANGPT2	NM_001147	Angiopoietin 2	-1.19	0.75	-1.12	0.68
COL18A1	NM_030582	Collagen, type XVIII, alpha 1	1.62	**0.05***	1.37	0.07
FGFR2	NM_000141	Fibroblast growth	1.27	0.34	1.14	0.45

		factor receptor 2				
IFNA1	NM_024013	Interferon, alpha 1	-1.01	0.70	-1.32	0.11
IFNB1	NM_002176	Interferon, beta 1, fibroblast	1.23	0.40	1.37	0.33
IGF1	NM_000618	Insulin-like growth factor 1 (somatomedin C)	-1.42	0.57	1.10	0.99
IL8	NM_000584	Interleukin 8	-1.22	1.00	1.70	0.56
PDGFA	NM_002607	Platelet-derived growth factor alpha polypeptide	1.22	0.29	1.91	**0.05***
PDGFB	NM_002608	Platelet-derived growth factor beta polypeptide (simian sarcoma viral (v-sis) oncogene homolog)	7.63	0.11	2.19	0.13
TEK	NM_000459	TEK tyrosine kinase, endothelial	2.03	0.10	-1.01	0.86
TGFB1	NM_000660	Transforming growth factor, beta 1	1.41	0.26	-1.78	**0.05***
TGFBR1	NM_004612	Transforming growth factor, beta receptor 1	1.18	0.27	1.43	0.05
THBS1	NM_003246	Thrombospondin 1	-1.35	0.35	-3.31	**0.001*** **
TNF	NM_000594	Tumor necrosis factor (TNF superfamily, member 2)	2.23	0.33	2.24	0.19
EPDR1	NM_017549	Ependymin related protein 1 (zebrafish)	-1.05	0.62	-1.17	0.18
VEGFA	NM_003376	Vascular endothelial growth factor A	1.57	**0.05***	-1.46	0.38
Invasion and Metastasis						
MET	NM_000245	Met proto-oncogene (hepatocyte growth factor receptor)	-1.09	0.60	-2.07	**0.05***
MMP1	NM_002421	Matrix metallopeptidase 1 (interstitial collagenase)	2.40	0.43	-1.47	0.30

MMP2	NM_004530	Matrix metallopeptidase 2 (gelatinase A, 72kDa gelatinase, 72kDa type IV collagenase)	1.08	0.54	-1.04	0.85
MMP9	NM_004994	Matrix metallopeptidase 9 (gelatinase B, 92kDa gelatinase, 92kDa type IV collagenase)	1.51	0.33	1.55	0.38
MTA1	NM_004689	Metastasis associated 1	-1.30	0.21	-1.37	**0.05***
MTA2	NM_004739	Metastasis associated 1 family, member 2	-1.01	0.94	-1.37	0.51
NME1	NM_000269	Non-metastatic cells 1, protein (NM23A) expressed in	-1.16	0.20	-1.11	0.08
NME4	NM_005009	Non-metastatic cells 4, protein expressed in	1.21	0.46	1.49	0.15
PLAU	NM_002658	Plasminogen activator, urokinase	2.83	0.24	3.21	0.26
PLAUR	NM_002659	Plasminogen activator, urokinase receptor	-1.27	0.33	-1.77	**0.05***
SERPINB5	NM_002639	Serpin peptidase inhibitor, clade B (ovalbumin), member 5	-1.64	**0.05***	-2.40	**0.01****
SERPINE1	NM_000602	Serpin peptidase inhibitor, clade E (nexin, plasminogen activator inhibitor type 1), member 1	-1.12	0.69	-2.49	**0.01****
TIMP1	NM_003254	TIMP metallopeptidase inhibitor 1	1.16	0.55	1.07	0.49
TIMP3	NM_000362	TIMP metallopeptidase inhibitor 3	-1.47	0.50	1.09	0.72
TWIST1	NM_000474	Twist homolog 1 (Drosophila)	-1.18	0.35	1.09	0.65

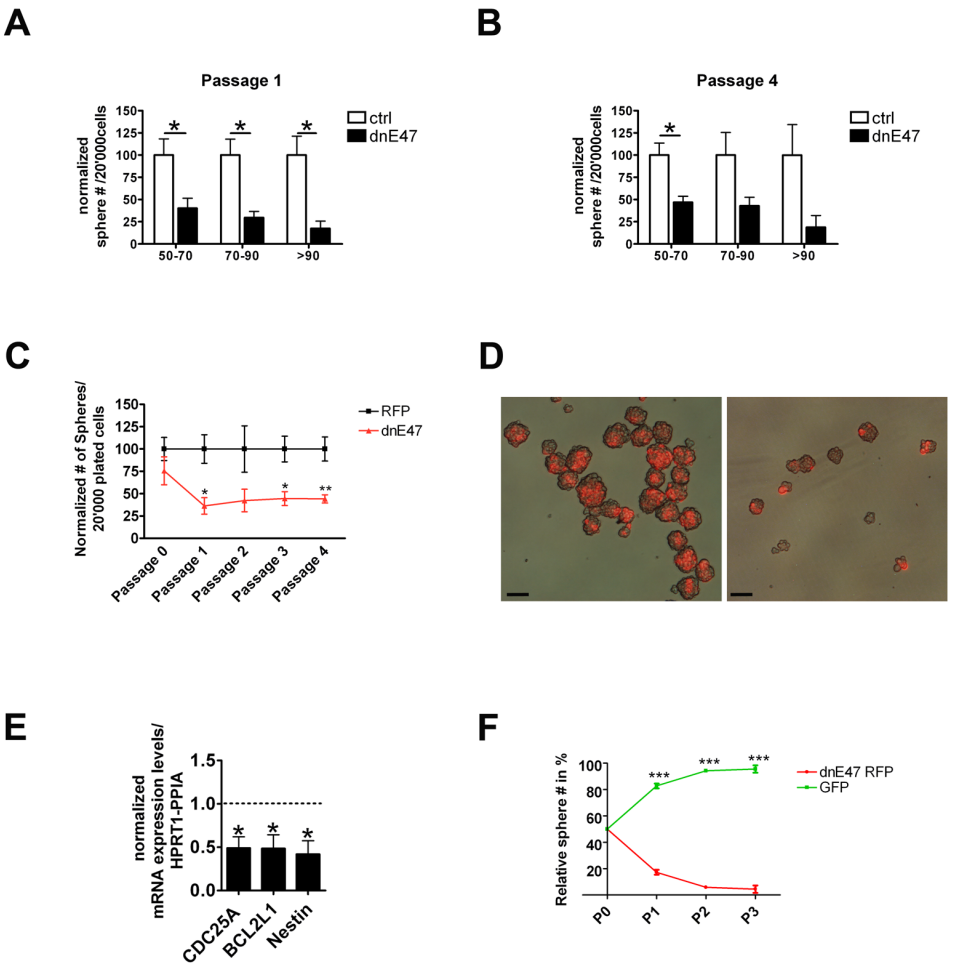

Supplementary Figure S5. Patient-derived glioma-intiating cells show reduced sphere formation capacities upon dnE47 overexpression. A-B, following dnE47 overexpression in S24 glioma-intiating cells, spheres numbers of all size categories were rapidly reduced. C, the total number of spheres dropped significantly after dnE47 overexpression over passages. D, representative pictures of control RFP spheres (left) and dnE47::RFP expressing spheres (right) at passage 4 following doxycycline induction. E, the reduction in sphere formation capacities correlates with a lower expression of the pro-proliferative gene CDC25A, the anti-apoptotic gene BCL2L1 and the stem-cell gene Nestin. F, when mixed with GFP-expressing spheres at a ratio of 1:1, the number of dnE47::RFP-overexpressing S24 spheres declined rapidly. * $p<0.05$; ** $p<0.01$; *** $p<0.001$; Scale bars = 100µm

Chapter III

"Targeting the bHLH transcriptional networks by mutated E proteins in experimental glioma": behind the scenes

“Targeting the bHLH transcriptional networks by mutated E proteins in experimental glioma”: *behind the scenes*

Abstract

In this chapter, I describe the establishment and design of tools and methods to investigate the impact of (b)HLH transcriptional network disruption onto human tumor-initiating cells. First, we cloned a mutated form of E47RFP and a control RFP into a Doxycycline inducible lentiviral vector. Then, high titer lentivirus batches were produced and finally, the optimal conditions for transduction and induction of the lentivirus in tumor-initiating cells were established. Having the tools at hand, we next tested the best culturing conditions for sphere formation analyses for both T269 and S24 tumor-initiating cells. As a last step, we tested the influence of dnE47 on tumor formation in a murine xenograft model. For this, we chose the T269 tumor-initiating cell line, as its invading capacity was higher than that of the S24 cell line mirroring more closely the behavior of human glioblastoma tumors. The key results obtained in this series of experiments have been presented in chapter II and here, a more detailed description of tumor morphology will be presented. Finally, examples of possible histological interpretations and an outlook for further analyses will be discussed.

Introduction

In vivo cell labeling and transgenesis took a new turn in 1996 when Naldini and colleagues demonstrated the efficient and stable transduction of neurons *in vivo* with a human immunodeficiency virus (HIV)-derived retrovirus (Naldini et al. 1996). Compared with other virus types commonly used in research such as retroviruses, adenoviruses or adeno-associated viruses (AAV), lentiviruses present the advantage to infect both dividing and non-dividing cells (O'Connor & Crystal 2006). Lentiviruses are a subclass of HIV-derived retroviruses, are replication-defective and have been adapted for highly efficient gene delivery *in vitro* and *in vivo*. Over time, engineering of the packaging vectors was improved and HIV safety issues were resolved by keeping only three out of nine viral genes: gag, pol and rev in the viral backbone (Zufferey et al. 1997). The gene delivery vectors were modified over time to bring three major improvements that led to the emergence of second-generation constructs. First, the Woodchuck Hepatitis Virus Post-transcriptional Regulatory Element (WPRE) was added in order to improve transcription (Zufferey et al. 1999). Second, the transgene RNA retains the central polypurine tract of HIV for high titer productions (Follenzi et al. 2000; Zennou et al. 2000). Third, removal the U3 3' LTR (long terminal repeat) region containing the viral promoter in its RNA genome rendered the vectors unable to replicate themselves, i.e. self-inactivating (SIN) (Zufferey et al. 1998). These second-generation vectors provide sufficient transduction efficiency and biosafety for *in vitro* and *in vivo* research. In the case of clinical research and gene delivery therapies, third-generation vectors with an engineered chimeric 5' LTR enabling promoter recruitment in the absence of the Tat gene provide a safer lentiviral system (Dull et al. 1998). For our purposes, we used a second-generation self-inactivating gene delivery vector: pSIN _hPGK_rtTA2SM21(Barde et al. 2006).

A new area in cancer research started when a subpopulation of cancer stem cells that are able to induce tumors and are responsible for relapse after therapy, were discovered within brain tumors (Singh et al. 2003; Singh et al. 2004; Chen et al. 2010). As they appeared to resist to therapy, targeting these cells became a major goal in the development of new therapeutic approaches (Chen et al. 2012; Schonberg et al. 2013). Since then, research aimed at characterizing the origin of brain cancer stem cells, their role in tumor homeostasis and their genetic profile in order to overcome their resistance to treatments (Tabatabai & Weller 2011; Schonberg et al. 2013; Stiles & Rowitch 2008). Investigating their abilities to form and sustain tumors involved challenging cancer stem cells in an *in vivo* system and implied the use of xenograft models: to investigate how human cancer stem cells react to therapies, studies took advantage of well-established mammalian transplantation systems, mainly using rodents lacking an immune system (Flanagan 1966; Greiner et al. 1995; Christianson et al. 1997; Mecklenburg et al. 2001; Siolas & Hannon 2013).

In this chapter, we will describe and discuss how the tools and experimental setup for assessing the effects of mutant E proteins overexpression in glioma-initiating cells were developed *in vitro* and *in vivo*. Finally, possible methodological approaches for advanced histological analyses, e.g. for assessing the distribution of grafted tumor-initiating cells, will be presented and described for future follow-up *in vivo* studies.

1. Building the tools

1.1 Vector cloning

In order to express our genes of interest in a controlled manner, we selected an inducible lentivirus approach. For this, we received from Dr. Isabelle Barde (Transgenic Core Facility, EPFL) the following second-generation transfer vector: pSIN_mSEAP_hPGK_rtTA2SM21. This vector permits a tight and dose-dependent control of its expression upon application of a Tetracycline analogue: Doxycycline (Barde et al. 2006). First, the mSEAP gene was cut out with the sticky end restriction enzyme MluI and Pfx. Next, polymerase-amplified PCR fragments of RFP or dnE47RFP were inserted. Correct insertion of the fragments was verified by control digestion of the whole vector as well as by sequencing. Cloning procedures for both genes generated two inducible vectors: pSIN_RFP_hPGK_rtTA2SM21 and pSIN_dnE47RFP_hPGK_rtTA2SM21 (**Fig1**).

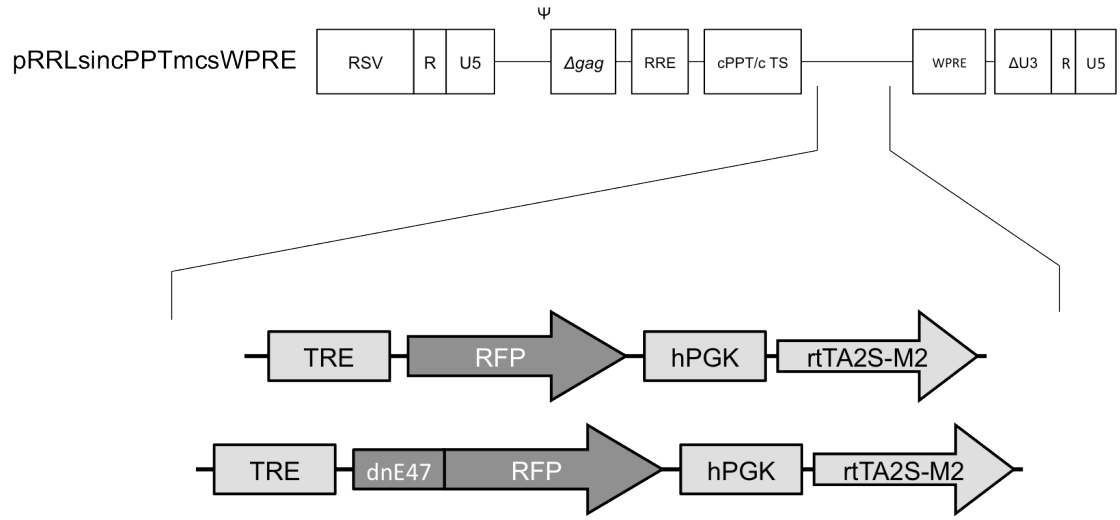

Figure 1 Explanatory scheme of the lentiviral vectors pSIN_RFP_hPGK_rtTA2SM21 and pSIN_dnE47RFP_hPGK_rtTA2SM21engineered for this study.

1.2 Lentivirus production

For lentivirus production, human 293T Hek cells were transfected with three plamids: one encoding for the VSV G envelope protein, one for the HIV-1 Gag, Pol, Tat and Rev proteins as well as the third-generation transfer vector. All three constructs were transfected with Calcium Phosphate and the supernatant containing the virus particles was collected three times before being concentrated by ultracentrifugation (120min, 50'000 x g, 16^{o}C, Beckman). The titer was determined by both flow cytometry and qRT-PCR on HCT116 cells (human colorectal carcinoma). For this, the cells were infected with serially diluted IFU/cell concentrations and harvested after 3 days. The percentage of fluorescent transfected cells upon Doxycycline induction were measured by flow cytometry and the number of copies of the lentivirus integrated in the genome of infected cells by qRT-PCR (Barde 2010). An approximate final volume of 150 µl was collected. The following titers were obtained: $5*10^8$ IU/ml for the pSIN_RFP vector and $5*10^9$ IU/ml for the pSIN_dnE47 vector.

1.3 Optimizing transduction and induction

Next, the optimal settings for the highest transduction and induction efficiency were established. For this, we plated 50'000 T269 cells on Poly-Ornithin/Laminin coated glass coverslips in a 24-well culture plate and infected them with 10, 50, 100 and 200 IFU/cell. In parallel, we tested different concentrations of Doxycycline in the culture medium, ranging from 1 to 10 µg/ml (1/1000 to 1/100 on **Fig2A**). Optimal and efficient transduction and induction were obtained when cells were infected with 100 IFU/cell and exposed to 2 µg/ml (500x) Doxycycline (**Fig2A**).

1.4 Establishment of sphere cultures and assays

Culture conditions vary between different types of cell lines and one has to adapt the frequency of passaging, the density of seeded cells, the need for supplementation of conditioned medium, the optimal CO_2/O_2 concentrations and the temperature. Already at the morphological level, S24 and T269 cells differed significantly. S24 showed a more rounded shape whereas T269 were more elongated when grown as a monolayer (**Fig2 B** and **C**, respectively). The difference in sphere formation capacity of S24 and T269 tumor-initiating cells was noticeable since in our culture conditions S24 cells were more proliferative. In order to test the difference in proliferation and sphere

formation capacity, different cell densities were plated and the formation of spheres bigger than 50µm was analyzed after four days. T269 cells formed 15.78 ± 3.31 spheres at a minimal density of 10 cell/µl whereas S24 cells were faster and only needed 1 cell/µl in order to generate 14.50 ± 1.83 spheres (**Fig2 D** and **E**, respectively). We concluded that T269 cells needed a higher cell density for proliferation and sphere formation. Therefore, for all sphere formation assays, we set the optimal cell density at 7 cells/µl for S24 cells and 10 cells/µl for T269.

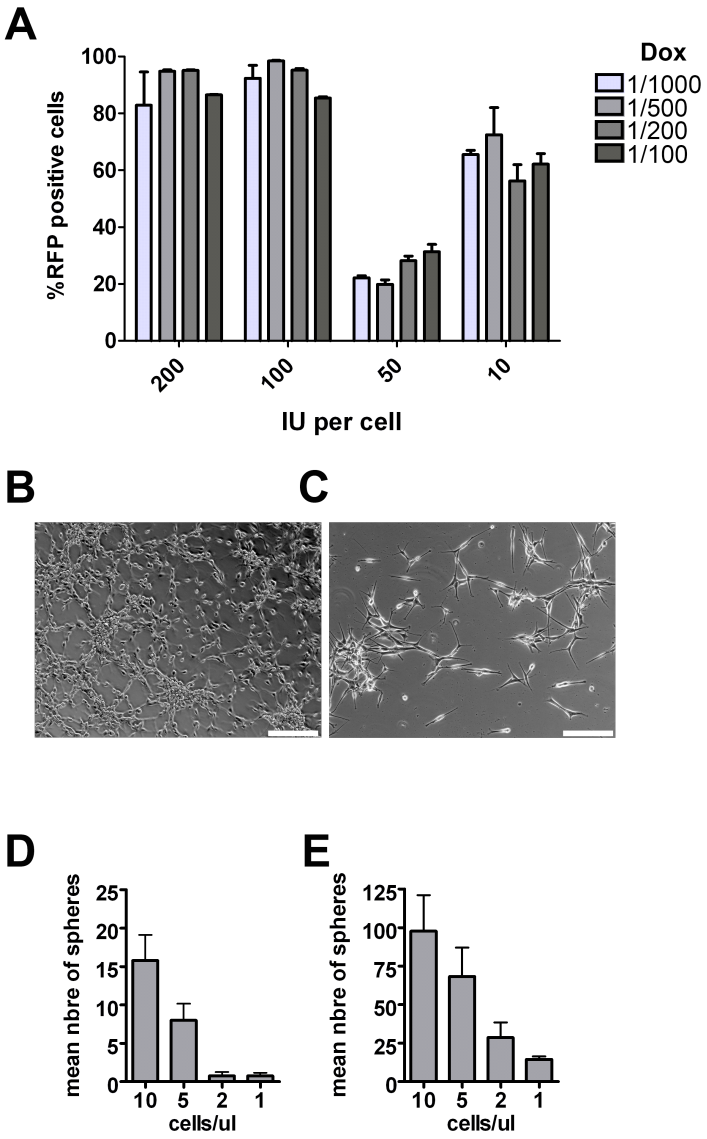

Figure 2 Establishing optimal settings for lentiviral transfection and induction in a sphere formation assay. **A** T269 showed high transduction efficiency with 200 and 100 IU/cell as observed following Doxycycline administration at 2 µg/ml (1/500). S24 cells show a less elongated morphology (**B**) compared with T269 cells (**C**). **D** Four days after seeding 10 cells/µl, T269 generated 15 spheres whereas S24 formed the same number of spheres after seeding 1 cell/µl (**E**) Scale bar = 200µm

2. Translation to in vivo

2.1 Choice of the cells

Glioblastoma multiforme is a highly aggressive type of brain tumor and is known to grow diffusely throughout the brain (Claes et al. 2007, CBTRUS statistical report 2006). To choose one of the cell lines for the *in vivo* assay we compared the migratory capacities of both T269 and S24 cells with a 3D matrigel invasion assay at 24, 48 and 72h and found that T269 were more invasive compared with S24 cells (**Fig3 A-C**). In parallel, we tested whether overexpression of dnE47 influenced invasion using the same assay, but no significant effect was detected except at 72h post-induction for T269 cells (**Fig3 C-E**). We chose T269 tumor-initiating cells for further *in vivo* experiments.

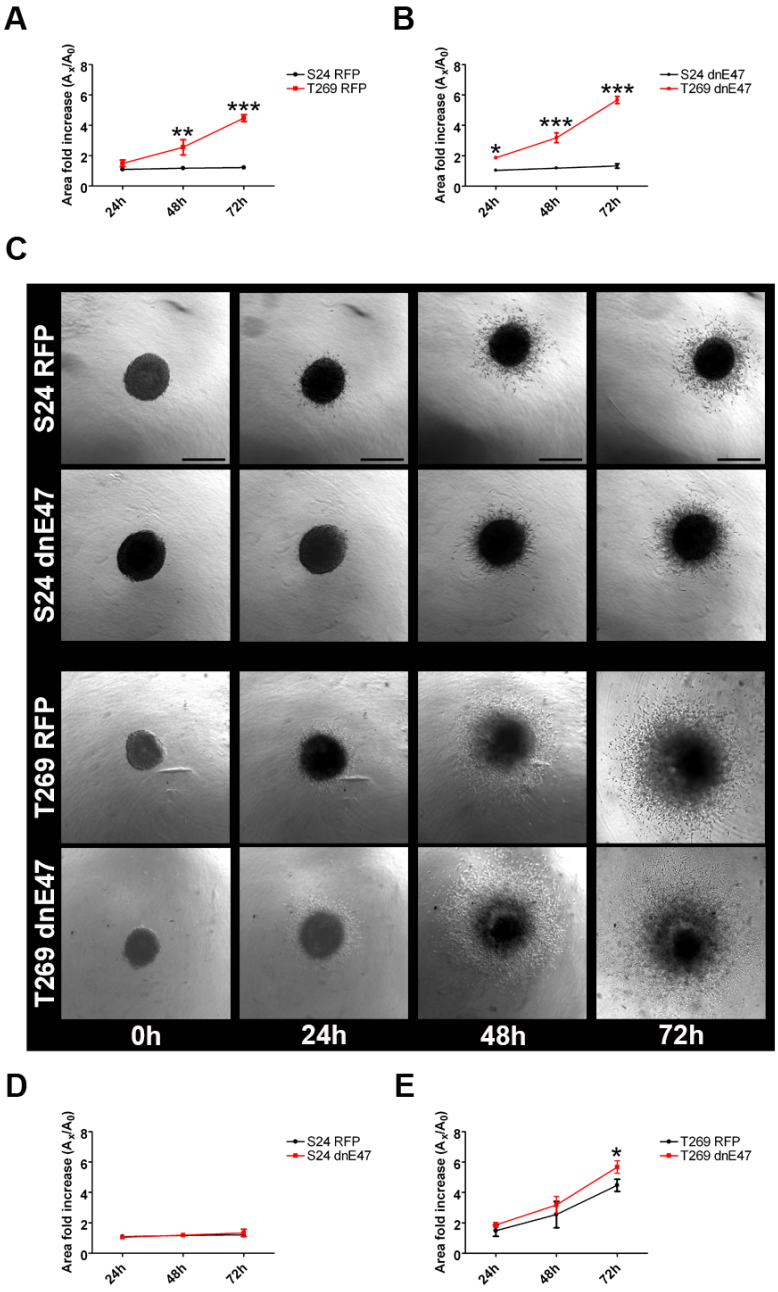

Figure 3 T269 tumor-initiating cells show a more invasive behavior than S24 cells in control RFP conditions and when comparing dnE47 overexpression. Upon Doxycycline induction, no significant difference in the invaded area was detected between T269 and S24 cells neither when RFP (**A**) nor dnE47 (**B**) were overexpressed. The representative close-up pictures show invading tumor-initiating cells migrating out of spheres upon RFP or dnE47 induction (**C**). DnE47 overexpression does not influence invasion of S24 cells (**D**) and has little influence on the invasive properties of T269 cells (**E**). Scale bar = 250 µm

2.2 Tumor evolution and tracking

For visualization of the transplanted cells, T269 cells were transduced with a lentivirus that constitutively expresses GFP. Following transduction, cells were FAC-sorted in order to reach a pure GFP positive culture. After co-transduction with either the RFP or the dnE47 lentivirus, cells were transplanted into the right striatum of immunedeficient mice (2 mm lateral, 1 mm anterior from Bregma, -3 mm dorsoventral). Doxycycline was administered at 30d post-transplantation; 3 animals per group were sacrificed two weeks upon induction and 7 animals were kept alive until the onset of clinical symptoms (such as motor impairments, lack of grooming and explorative behavior and pain symptoms) in order to evaluate the effects of dnE47 overexpression onto tumor formation and to generate a Kaplan-Meier survival curve (**Fig4A**, experimental design and **Chapter 2 Fig6D**). On histological sections collected at 30d and 44d after transplantation, we saw that the tumors had grown diffusely within all brain regions. GFP-positive cells appeared to migrate extensively along white matter tracts (**Fig4B-C**). At the time of onset of clinical symptoms (i.e. when the animals were sacrificed), the tumor was clearly visible in most brain areas (**Fig4D**). We then analyzed the percentage of GFP-human nuclear antigen (hNA) double positive cells by immunohistochemistry to confirm accurate detection of human grafted cells within murine tissue (**Fig4E**). Co-localization between hNA and GFP positive cells reached almost 100% in all the quantified regions: the subventricular zone (SVZ), the corpus callosum (CC) and the Fimbrae hippocampi (HFi) (**Fig4F**).

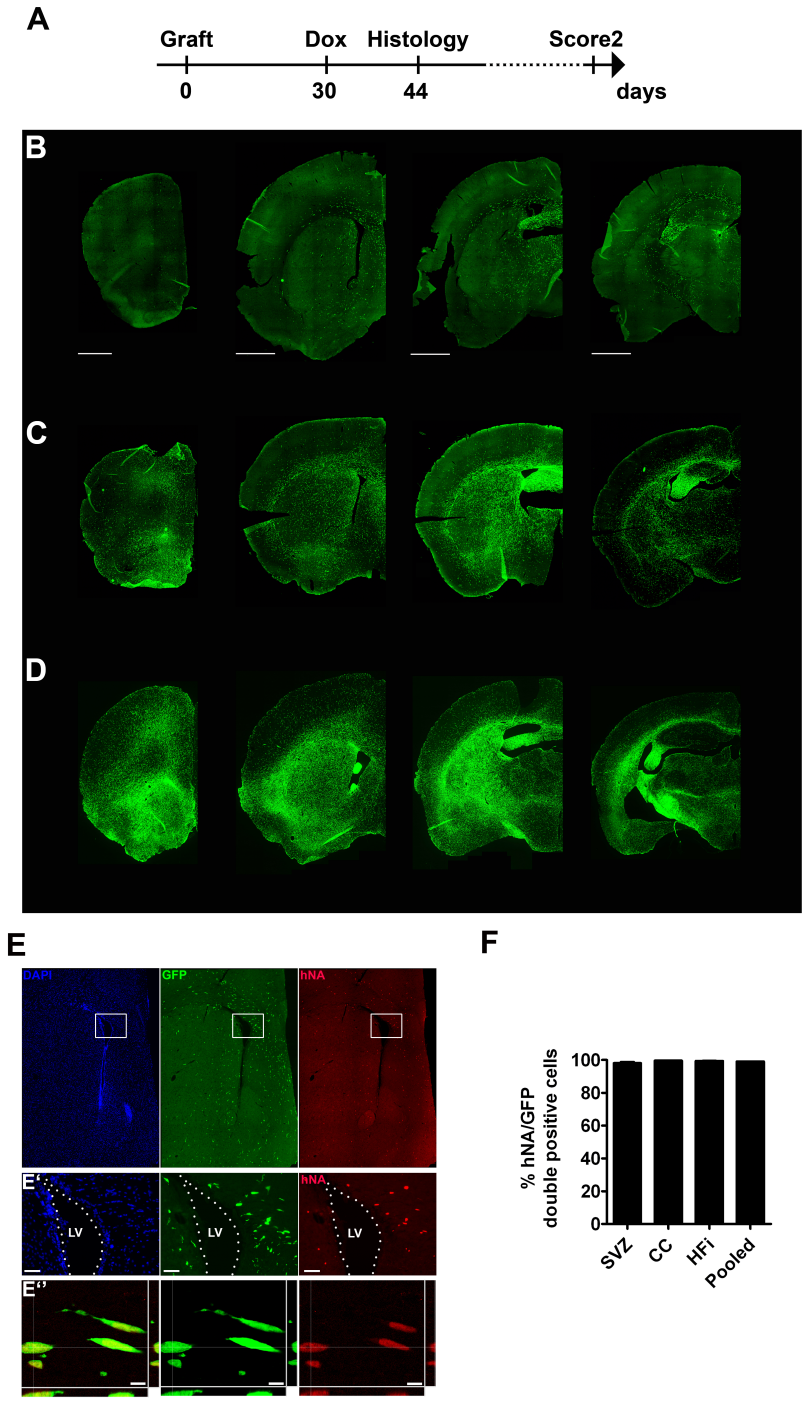

Figure 4 Evolution of T269-induced tumors in athymic mice. **A** Experimental design of the study in which expression of the transgene (i.e. RFP or dnE47-RFP) lentiviruses were induced 30 days after grafting and animals sacrificed either 14 days upon Doxycycline administration for histological analyses or when tumor-bearing mice showed clinical symptoms (i.e. Score 2). Grafted GFP positive cells were clearly visible 30 days after transplantation (**B**), and continued expanding at 44 days (**C**) and 75 days (**D**). **E** Human nuclear antigen and GFP positive cells were detected in all regions of the brain and showed an almost 100% co-localization (**F**). B-D Scale bar = 1000µm, E' Scale bar = 50µm, E'' Scale bar = 10µm

2.3 Induction efficiency *in vivo*

Next, the induction efficiency for both RFP and dnE47 vectors was characterized by analyzing the percentage of GFP-RFP double positive cells in periventricular or parenchymal brain regions. In general, the RFP signal from both induced vectors was strong in regions close to the ventricles (SVZ, Corpus callosum, Fimbrae Hippocampi) whereas RFP expression was weaker and more heterogeneous in regions further away from ventricles such as the striatum and in the forebrain (**Fig5A**). The RFP control vector was induced in 98% ± 0.2 of the GFP positive cells near the ventricles and 92% ± 5.8 in regions further away. Regarding the dnE47 vector, close to the ventricles, 91% ± 0.4 of GFP^+ cells were positive for RFP whereas 71% ± 6.6 were positive further away (**Fig5B**). Overall, the induction efficiency in GFP^+ cells was higher for the RFP control vector (95% ± 2.8) than for dnE47RFP (81% ± 5.2) (**Fig5C**).

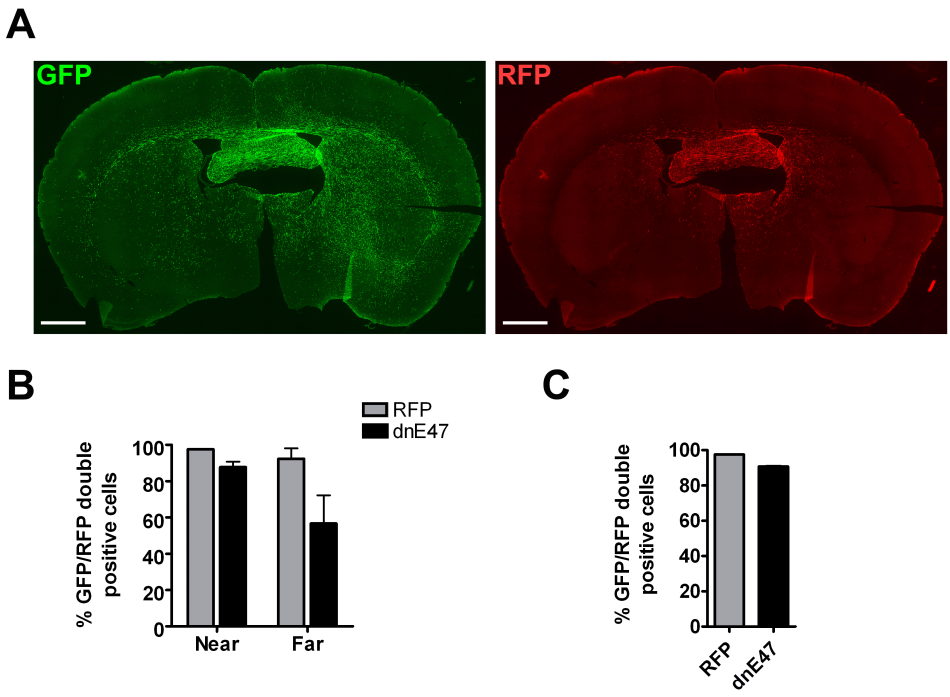

Figure 5 Induction of RFP and dnE47RFP upon Doxycycline treatment is highly efficient *in vivo*. **A** Representative pictures of GFP positive transplanted cells (left) and Doxycycline induced RFP signal. **B** Highest induction efficiency was quantified near the ventricular system whereas it was lower and more heterogeneous away from the ventricles. **C** pSIN_RFP showed higher and more stable induction overall. Scale bar = 1000µm

2.4 Fluorescence intensity-based cell distribution analysis on histological sections

Tumor cells migrated over long distances following engraftment, rendering their quantification particularly challenging. In order to characterize the growth of the tumors in future studies, we tested three different methods in order to analyze the distribution and migratory capacities of transplanted cells.

The first approach consisted in detecting the distribution of GFP^+ cells on a "heatmap" representing their localization in a color-coded manner. This approach includes generating a plot profile of the total grey value distribution over the whole section. To start with, mosaic scans of each section were acquired on a fluorescence microscope equipped with a motorized stage at 10x magnification. The images were converted to a 16bit picture with the software ImageJ. Using the plug-in "heatmap histogram" (created by Dr. Samuel Péan), a heatmap view of the section is created showing the density distribution of the GFP signal which reflects the distribution/location of the tumor cells throughout the section (**Fig6 A-E**). For a more quantitative approach, one can create a plot profile showing the distribution of the signal detected as grey values from the left to the right side of the section (**Fig6 F**). To allow the comparison of different sections, the mosaic scans must be generated using the same settings (exposure time, gain). For example, one could focus on 3-4 sections of a specific anatomical region and the differences in the plot profiles between groups tested. For future follow-up studies, sections from the Fimbriae Hippocampi could be analyzed and the plot profile differences between the RFP control group and the dnE47 overexpression group compared.

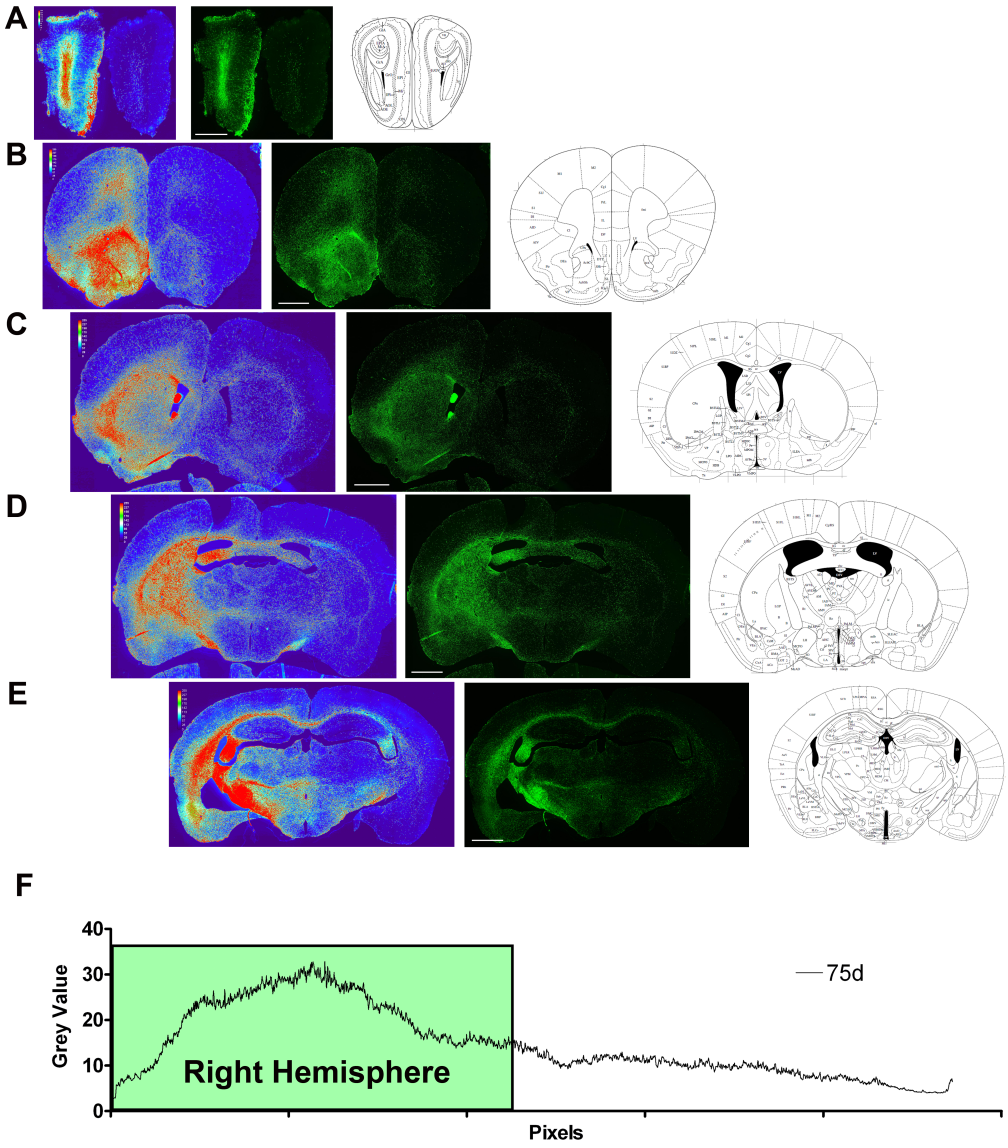

Figure 6 Section heatmaps showing the density distribution of GFP positive cells. **A-E** Heatmaps (left picture) created from mosaic sections (center picture). The sections from the Mouse Brain Atlas (right picture) help illustrating the anatomical location of the transplanted cells. **F** Example of a plot profile of section D showing that the cells are mainly located in the right hemisphere, i.e. the side of the injection. Scale bar = 1000µm

2.5 A stereological approach for Fluorescent Euclidean Vector Analysis (FEVA)

We developed a quantitative approach based on stereology for precise and unbiased counting of spatially distributed cells. 30µm-thick sections were cut, and every 12th serial section was collected. To determine the total area to be analyzed, we used the Cavalieri estimator to generate estimates of sectional surface and volume. A point-grid (x- and y-point distances: 500 micrometers) was placed on each section, and each point falling on the tissue was counted. A total of 27 sections was analyzed, resulting in a point count of 4135. Based on the point count, the area to be sampled was estimated to be 1'033'750'000 µm^2 (**Table1**). The coefficient of error (CE) of this estimate was calculated based on the Gundersen-Jensen estimator (G-J) (Gundersen et al. 1999). Part of the G-J CE estimator is the *smoothnes*s factor *m*, *m*=1 representing a smooth and *m*=0 a jagged distribution (Slomianka & West 2005). In our case, the counts were distributed evenly and therefore a smoothness factor of 1 was considered (**Fig7A**). Analysis of every section resulted in a G-J CE of 0.006, i.e. the standard deviation of repeated measurement would amount to only 0.6% of the mean of the repeated measurement. To determine how the section-sampling interval influenced our G-J CE estimates, we compared the CE for all sections (i.e. 0.006) with that of every second section. Noticeably, analysis of every second section also gave a precision of 0.006.

Next, to determine the distribution of our sampling sites on the sections, we calculated the size of the sampling grid for the optical fractionator considering a number of 400 sampling sites in the total area to be analyzed: square root of (total area/400). This would give us a spacing of 1.6mm, but we decided to use systematically random sampled sites every 1mm providing a total of 1112 sampling sites. The counting frame size was set to 90x110 µm (**Table1**). Both hemispheres were considered separately and the number of GFP$^+$ cells co-localizing with DAPI$^+$ nuclei were counted at 63x magnification. In total, 331 cells were counted and the total number of cells within the brain was calculated using the optical fractionator method:

$$N = \frac{1}{ssf} * \frac{1}{asf} * \frac{1}{hsf} * Q$$

In our example, the section sampling fraction (ssf) is defined by every 12th section being analyzed, i.e ssf = 1/12. The area sampling fraction (asf) is the counting frame area divided by the sampling grid area, i.e asf = (90*110)/(1000*1000) = 0.0099. We counted cells through the whole section thickness, which gives us a height sampling fraction (hsf) of 1 since hsf is the height of each fractionator sample divided by the average section thickness, i.e. hsf = 30/30 = 1. Q stands for the total number of counted cells, i.e. 331 for the entire brain, 183 for the ipsilateral hemisphere and 143 for the contralateral hemisphere. Thus, 30 days after injection of 100'000 cells in the right striatum, the cells proliferated to reach a total number of 401'212 cells; 221'818 cells remained in the ipsilateral hemisphere whereas 173'333 cells migrated contralaterally (see also Table1):

$$N_{tot} = \frac{1}{\frac{1}{12}} * \frac{1}{0.0099} * 1 * 331 = 401'212$$

$$N_{ipsi} = \frac{1}{\frac{1}{12}} * \frac{1}{0.0099} * 1 * 183 = 221'818$$

$$N_{contra} = \frac{1}{\frac{1}{12}} * \frac{1}{0.0099} * 1 * 143 = 173'333$$

Since we used the Stereo Investigator software coupled to an x-y-z motorized stage, each counted cell is located in a Euclidean space and has its own x-y-z coordinates (**Fig7B**). Based on them, and knowing the coordinates of the injection site, it is therefore possible to calculate the minimal migration distance of grafted cells as the norm $\|a\|$ of a Euclidean vector:

$$\|a\| = \sqrt{(x^2 + y^2 + z^2)}$$

Based on bins of 500um, the frequency distribution of our fluorescent vectors showed a bimodal distribution when considering vectors within the whole brain as well as for the ipsilateral hemisphere (**Fig7C-E**).

Table1

	Mean cells	Total count area (μm^2)	Mean CE (m=1)	Sampling grid size (µm)	Counting frame size (µm)	Sections assessed	Cells counted
Whole brain	401‘212	1033750000	0.06	1000 x 1000	90x110	27	331
Ipsilateral	221‘818		0.07				183
Contralateral	173‘333		0.08				143

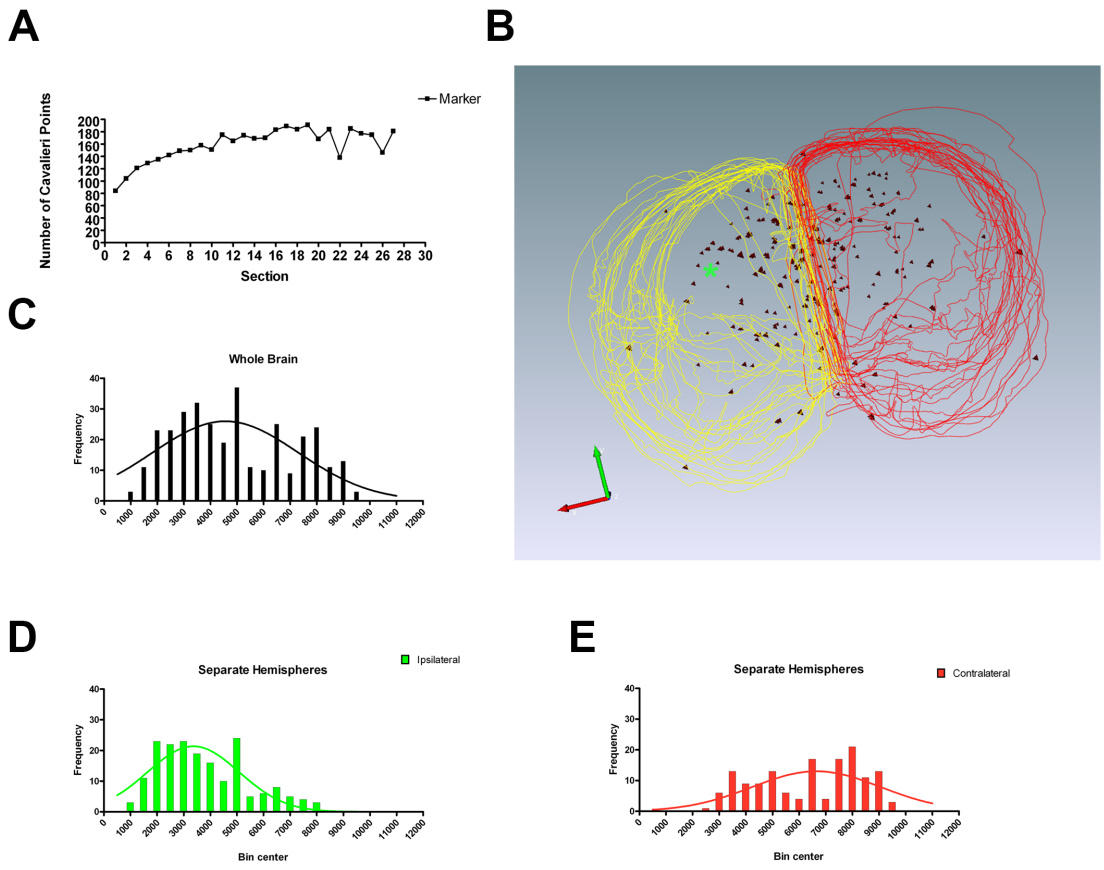

Figure 7 Stereological Fluorescent Euclidean Vector Analysis. The distribution of Cavalieri points over analyzed section shows a smoothness factor of 1 (m=1) (**A**). 3D representation of analyzed sections. Contours from the ipsilateral hemisphere are in yellow, contours from the contralateral hemisphere in red. Black triangles represent counted GFP^+ cells and the green asterisk the injection site (**B**). The distribution of vector frequency within the entire brain (**C**), the ipsilateral (**D**) as well as the contralateral hemisphere (**E**) shows a bimodal distribution. Distances are given in µm from the injection site.

2.6 Automated software-based number and distribution analysis

The third approach for analyzing the number and distribution of GFP^+ glioma-initiating cells in the brain was based on an automated acquisition of the sections and analyses of the cells. Here, images of 25 30µm-thick brain sections were acquired on a Zeiss Mirax Midi Slide Scanner with the same exposure and stitching settings for each slide. Then, the number of GFP^+ cells was counted automatically with the Software HistoQuant Module (3DHISTECH, Budapest, Hungary), adapting the settings for each slide and including cells having a perimeter ranging between 35 and 1000 μm^2. A total of 21'354 cells were counted, which gives an approximation of 256'248 cells in total, considering that every 12^{th} section was serially collected. Then, we analyzed the distribution of grafted cells with the software Imaris 7.5 (Bitplane AG, Zurich, Switzerland). First, a stack containing each section was created with the free software ImageJ and the sections aligned using the StackReg plugin (**Fig8A**) (Thévenaz et al. 1998; Schneider et al. 2012). As a reference for spatial positions, the injection site was labeled in red on the relevant section (**Fig8B**). The injection site was quantified as a surface and GFP^+ cells as spots in a 3D space in order to calculate their xyz position (**Fig8B**). A total number of 12'073 cells were detected in the ipsilateral hemisphere whereas 6'407 cells were positioned in the contralateral side, which gave a total of 18'480 cells in the whole brain. Since we analyzed every 12^{th} section, 221'760 cells were detected 30 days after transplantation. Next, we calculated the migration distance of each grafted cell from the injection site using the same vector norm approach as mentioned above (see Stereological FEVA). Here again, based on bins of 500µm, the frequency distribution of vector norms showed a slight bi-modal shape (**Fig9C-D**).

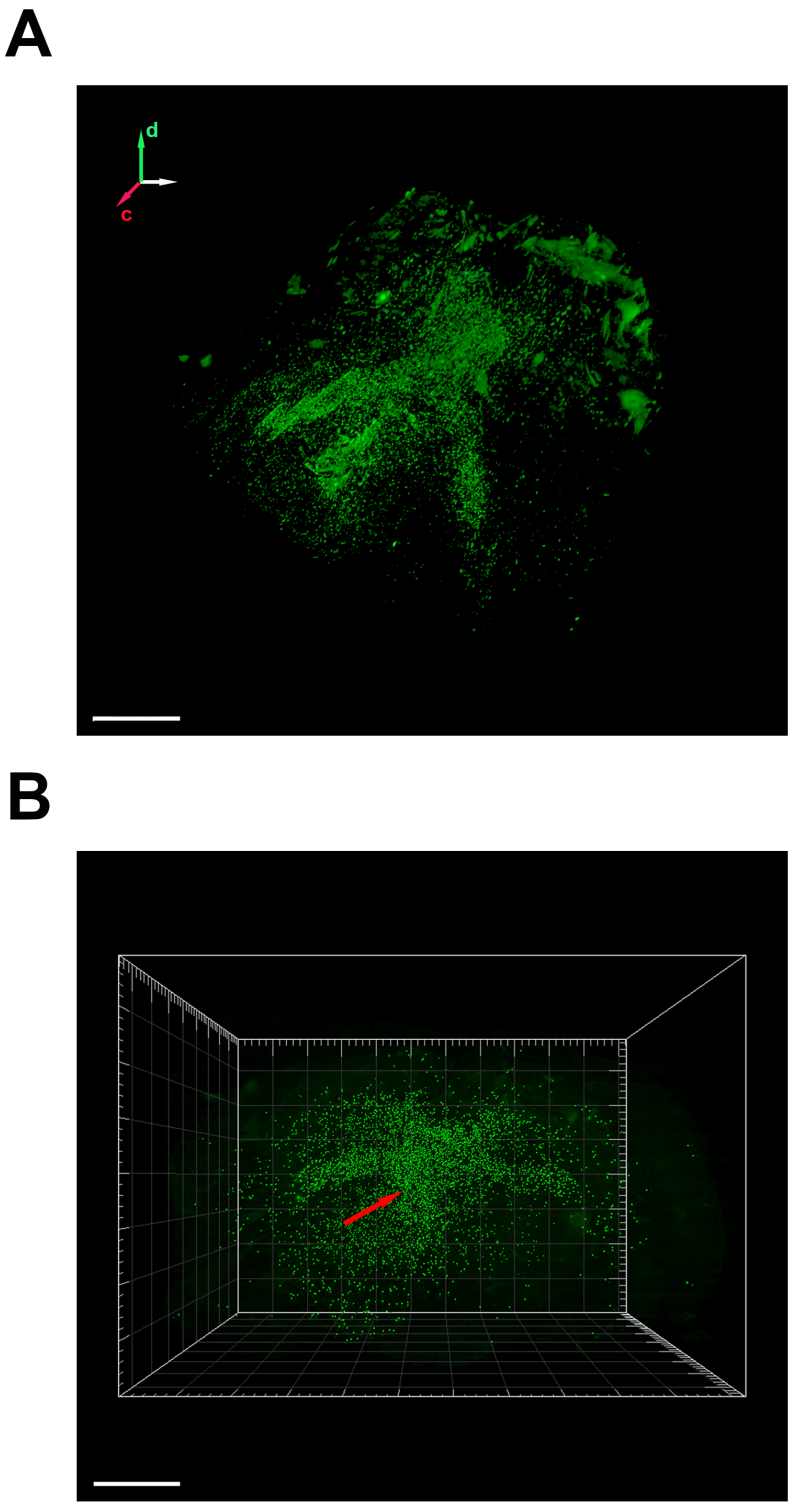

Figure 8 3D views generated with the software Bitplane Imaris. The 3D reconstruction of a stack shows the spatial positioning of transplanted cells 30d after injection (**A**). The green spots detect GFP^+ cells and the red arrow points at the injection site (**B**). Scale bar = 2000 µm.

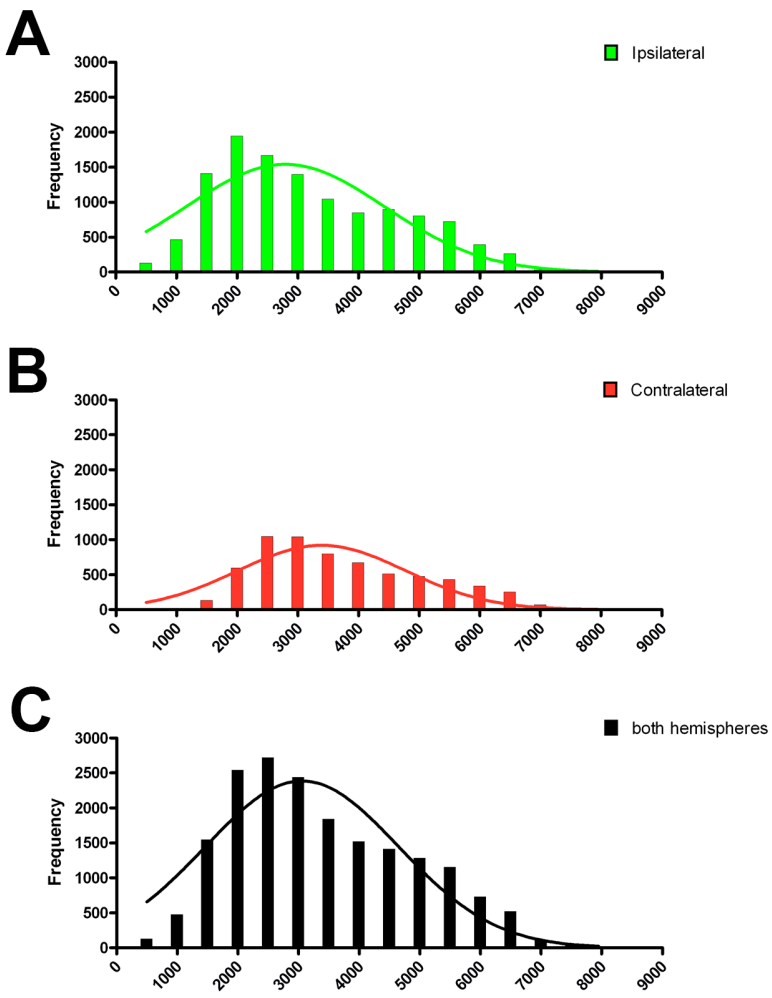

Figure 9 An automated software-based quantification of grafted GFP positive cells shows a bi-modal distribution. The vector norms of transplanted cells located in the ipsilateral (**A**), contralateral (**B**) and whole brain (**C**) show a bi-modal distribution.

Discussion and outlook

In this chapter, we presented the development and establishment of all necessary tools and experimental methods for assessing the effects of (b)HLH transcriptional network disruption in tumors both *in vitro* and *in vivo*. We first cloned and generated high-titer batches of inducible lentiviruses. We then established the optimal conditions for culturing tumor-initiating cell sphere and finally, we translated our findings *in vivo* by inducing tumors in immunosuppressed mice and developed methods to characterize the growth of tumors on serial histological sections.

Tumor-initiating cells isolated from patient biopsies provide new tools to test the efficiency of potential drugs or other therapeutic approaches (Tentler et al. 2012; Schonberg et al. 2013). However, human brain tumors show high heterogeneity in terms of molecular profile and physiology and this is also the case for patient-derived tumor initiating cells (Tang 2012; Schonberg et al. 2013). It is therefore not surprising that S24 and T269 tumor-initiating cells show differences in their gene expression levels, their proliferative behavior and their invasion capacity although they both were derived from glioblastoma multiforme biopsies. For our purposes, we selected the T269 cell line as they showed higher expression levels of (b)HLH transcription factors and mirrored more closely the highly invasive behavior of glioblastoma multiforme tumors (Claes et al. 2007). Their different molecular profiles, proliferation rates and invasive behavior support the concept that cancer stem cells are highly heterogeneous, can lead to different prognoses for patients and therefore should be targeted in a multimodal approach (Tang 2012; Schonberg et al. 2013).

Glioblastoma multiforme grow diffusely throughout the brain and grafting of T269 tumor-initiating cells phenocopied this behavior. Since the tumors were not compact and local, we established new methods for analyzing their number and distribution. The generation of heatmaps appeared to be particularly suited for evaluating whether tumor cells migrate to the hemi-brain contralateral to the injection site. This method is an innovative way of presenting section pictures as a heatmap and gives a fast overview on the cell distribution within sections. However, heatmap histograms cannot be used for exact quantitative analyses but merely for illustrative purposes as they only show in which anatomical regions the cells are mostly located.

A quantitatively more accurate method is an automated quantification using imaging software such as Histoquant, ImageJ and Imaris. Here, it is necessary to set all acquisition and quantification parameters and settings as precisely and reliably as possible in order to avoid false-positive or false-negative results. Nevertheless, the most exact approach, relying on statistic-based methods, is a stereological quantification as both automated software-based methods underestimated the total number of GFP^+ cells. In order to analyze a heterogeneous distribution of cell population, a methodological approach that does not imply counting each cell on each section is required. Stereology fulfills these conditions as it provides a quick, non-costly statistically relevant tool for a large heterogeneously distributed cell population. To conclude, heatmaps can be useful for illustration and the number and distribution of grafted cells can be quantified in an automated way if no stereology software is available. Otherwise, stereology-based analyses provide the most accurate results that reflect the actual number and distribution of grafted cells within the brain.

As an outlook for future studies, these histological and morphological methods will lead to more detailed investigations of the effects of dnE47 overexpression *in vivo*. For instance, alterations in proliferation and apoptosis will be analyzed on histological sections upon two weeks of Doxycycline administration with Ki67, Casp3a, TdT-mediated dUTP-biotin nick end labeling (TUNEL) or intravenously injected fluorescent Annexin V (Bahmani et al. 2011; Pernet et al. 2012). For *in vivo* proliferation analysis, a possibility will also be to give the animals pulses of the thymidine analog 5-ethynyl-2'-deoxyuridine (EdU) in order to label proliferating cells. As a non-invasive approach in order to assess tumor growth, it would be possible to monitor tumor evolution with bioluminescence imaging (BLI), a technique based on luciferase emitting grafts, or with far-red luminescence imaging (Szentirmai et al. 2006; Wu et al. 2009; Sun et al. 2010; Deliolanis et al. 2011). Alternatively, in order to assess the invasive behavior of tumor-initiating cells, an additional approach might be to seed cells or spheres onto organotypic slice cultures and characterize their invasive properties in an *ex vivo* system (Ohnishi et al. 1998; Jenei et al. 2011). The combination of *ex vivo* histological and *in vivo* non-invasive imaging analyses will enable a detailed assessment of tumor growth and histology upon dnE47 overexpression. Furthermore, these tools and methods could also be translated to

other types of cancers and their tumor-initiating stem cells, giving deeper insights about the similarities in regulatory pathways between different cancer types.

Chapter IV

Human tumor-initiating cell transplantation in *Drosophila Melanogaster*

Human tumor-initiating cell transplantation in *Drosophila Melanogaster*

Abstract

In order to confirm results from our *in vitro* experiments, we sought for an innovative approach as an alternative to classical murine xenograft models. *Drosophila melanogaster* is well-established genetic tool and model for cancer research. We transplanted human tumor-initiating cells into the abdomen of fruit flies and monitored the evolution of grafted cells over two weeks. GFP positive human cells were detected up to 4 days after transplantation with a clear loss of grafted cells after 48h. We concluded that this approach was not feasible and chose to use athymic mice instead.

Introduction

The primary goal of life science research is to understand the basic physiological, metabolic and structural mechanisms and functions in the context of healthy and diseased organisms. However, ultimately, research aims at applying this knowledge to the development of diagnostic and therapeutic tools for humans. Since decades, scientists have been seeking the answer to how does a disease arise, how does it develop and how can it be counteracted. In cancer as in any other field of disease research, one has to start with simple tools such as lower model organisms, immortalized cell lines or primary cells or computational models. As a next step, promising *in vitro* results need to be confirmed in a less artificial and more complex system in order to first, confirm and assess the relevance of the findings and second, to take a step closer to the development of novel therapeutic tools for humans in clinical trials.

At this transition point between *in vitro* and *in vivo*, classical procedures consist of combining human orthotopic or heterotopic grafts, with a murine host, which presupposes working with an immunodeficient animal. Two models are widely used: the athymic so-called nude mice that lack T cells and severe combined immundeficient (SCID) mice that lack both T and B cells. Nude mice lack their thymus and cannot produce any T cells because of a mutation in the *FOXN1* gene whereas SCID mice genome harbors a recessive mutation in the gene *prkdc* that impairs the maturation of their humoral and cellular immune system (Flanagan 1966; Bosma et al. 1983; Mecklenburg et al. 2001). More receptive host animals were then developed by combining the SCID mutation with the non-obese diabetic (NOD) model, resulting in a more receptive host for transplantations (Greiner et al. 1995; Christianson et al. 1997). Absence of immunity enables to transplant human grafts and characterize the formation and evolution of human tumors within a murine host.

However, when one needs to translate their findings from *in vitro* to *in vivo*, the ethical question of balance of interest arises where scientists have to consider whether the outcome or the significance of the experiment is worth the life or the pain of an animal. In Switzerland, animal experimentations are tightly regulated by the Confederation and the cantons that allow researchers to work with animals based on a license system (http://www.bvet.admin.ch/themen/tierschutz). For each license, a scientist needs to think about the necessity of the experiment, the wellbeing of the animals and how to minimize the number of animals. This concept is also known as the 3 Rs that are: refine, reduce and replace (http://www.forschung3r.ch). And so in this study, in an attempt to respect the 3Rs and to develop a novel tool, we challenged the fruit fly *Drosophila Melanogaster* with a human tumor-initiating cells xenograft.
Fruit flies are established genetic models in which the homology to human genes enables to conduct basic research with the goal to extrapolate findings to the mammalian system (Gont et al. 2013). They have been used for genetical analyses for a century and their genome has been fully sequenced (Adams et al. 2000). Furthermore, their short generation time, easy handling, low-cost maintenance as well as the inexistence of restrictions in the number of flies used in experimentations, permits to conduct efficient large-scale studies. In the context of cancer research, Drosophila flies have recently been established as GBM and tumor models in which overexpression of EGFR, PI3K, PDGFR or RAS homologs lead to tumor formation (Witte et al. 2009; R. D. Read et al. 2009; Read 2011; Gonzalez 2013). Similarly to mammalian models, tumor generation and characterization via transplantation have also been developed and used in flies (Caussinus & Gonzalez 2005; Berger et al. 2012). Here, overexpression or knockdown of genes prior engraftment influenced the ability of the graft to form tumors within the host. Furthermore, after abdominal transplantation, the migration of tumor cells to ovaries or the eyes gives an insight on their ability to form metastases. One can not only manipulate the cells prior grafting but also the host itself, giving rise to infinite possibilities of experimentations.

In this study, the goal of our approach was to first, test the possibility to transplant human cells into *Drosophila Melanogaster* and second, to overexpress dnE47 in the grafted cells and assess its effects onto tumor formation.

Material and Methods

Cell lines and culture

Both S24 and T269 human tumor-initiating cells were used in this experiment. Results and figures are described and shown for T269 cells only. Similar results were obtained with S24 cells. Cells were cultured in DMEM:F12 (Gibco) supplemented with 2% B-27 minus Vitamin A (Gibco), 1% antibiotic-antimycotic 100x (Gibco), human leukemia inhibitory factor 20ng/ml (Millipore, Merck, Billerica, MA), Heparin 5ug/ml (STEMCELL Technologies, France), recombinant human fibroblast growth factor 20ng/ml (Peprotech, Germany) and epidermal growth factor 20ng/ml. Cells were maintained at clonal densities (10 cells/µl) in T75 culture flasks (TPP) at 37°C/5% CO_2 and passaged once a week using Accutase (Chemie Brunschwig AG, Switzerland) for dissociation.

Drosophila line

Female w^{1118} flies were maintained on standard cornmeal-yeast agar medium at 25^0C. 3-4 days-old host flies were used for all transplantation procedures. Groups of 60 flies per condition were made.

Abdominal transplantation

Transplantations were performed as previously described (Caussinus & Gonzalez 2005). Briefly, injection needles were manufactured by pulling them to a diameter of around 90µm, cut and sharpened. About 1mm away from the needle tip, a constriction was inserted with a microforge. Then, the needle was inserted through a holder into a piece of silicon tubing with a mouthpiece on the other end. The cells or spheres were washed, resuspended in sterile PBS 1X and placed in small drops of PBS on a microscope slide. Before starting transplantations, host flies were anesthetized with CO_2 and stuck on an ice-cold plate, ventral side up, with double-sided sticky tape. Cells or spheres were aspirated within the tip of the needle and injected tangentially in the mid-ventral abdomen. Post-recovery from anesthesia, flies were let to recover and kept under standard conditions at 25^0C and 29^0C.

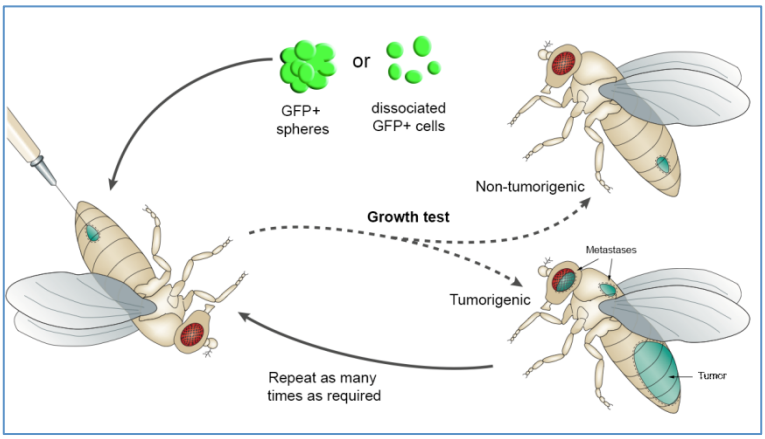

Figure 1 Schematic overview of abdominal transplantation procedure (adapted from Gonzalez et al. 2007)

Microscopy

Pictures were taken with a Leica MZFLIII fluorescence microscope (Leica Microsystems, Mannheim, Germany) at 2.5x and 3.5x fold magnification.

Results

As an alternative to the use of nude mice, we attempted to develop a novel tumor xenograft model in flies. We transplanted T269GFP$^+$ and S24GFP$^+$ tumor-initiating cells in the abdomen of female wild-type *Drosophila* flies. Either dissociated cells or entire spheres were grafted and the GFP signal was monitored on the day of the transplantation, at 24h, 48h, 4d, 7d and 14d after injection. After transplantation, one group of flies per condition was maintained at 25^{0}C and one at 29^{0}C. At 24h after injection, tumor cells were seen to spread in the whole body of the flies, with GFP$^+$ cells detected in the thorax as well as the eyes. Their presence could be detected up to 4d (**Fig2**). However, a net loss was evidenced after 48h and no cells (neither dissociated nor entire spheres) could be detected 7 days and 14 days after the transplantation suggesting that the flies had rejected the human graft. Both T269 and S24 cells showed similar results regarding the loss of cells as well as the death of animals being quicker when the flies were kept at 29^{0}C. The failure of grafted cells to develop into tumors lead us to the conclusions that the immune system of *Drosophila Melanogaster* must have reacted to the xenograft and get rid of it. Therefore, we concluded that a more common approach with immunodeficient mice was the appropriate way to translate our findings *in vivo*.

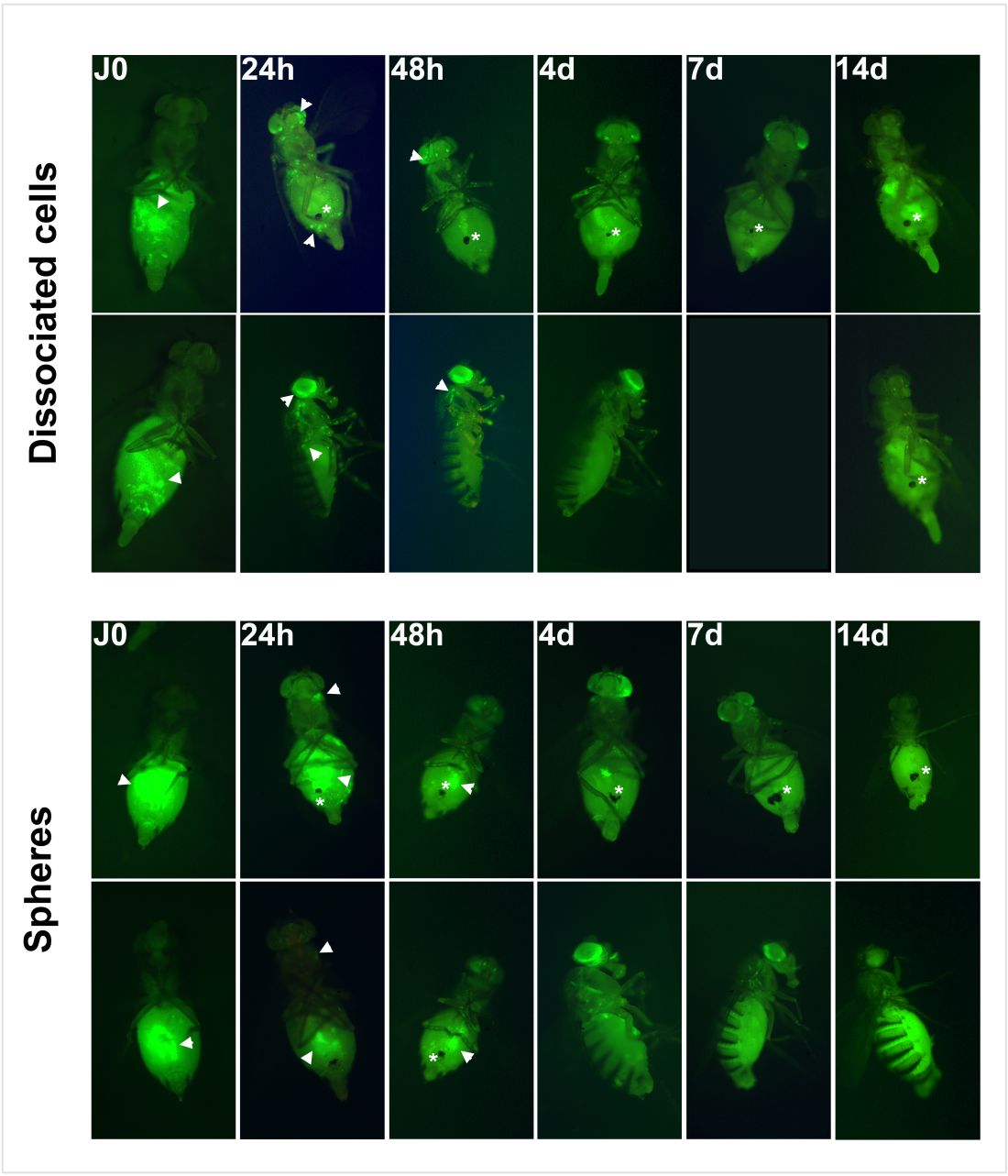

Figure 2 T269 tumor-initiating cells transplanted in the abdomen of *Drosophila Melanogaster* flies. Transplanted cells transduced with a constitutive GFP lentivirus can be detected in the abdomen from the day of injection and up to 4 days. 1 week and 2 weeks later, only the injection scar is seen (white star).

Discussion

In this study, human tumor-initiating cells were transplanted into the abdomen of *Drosophila Melanogaster.* The cells migrated up to thoracic levels and to the eyes but could only be detected until 4d after injection. The fact that the invertebrate environment seems deleterious to a human graft stands in sharp contrast with the high homology between the fruit fly and the human genomes (Reiter et al. 2001; Pandey & Nichols 2011). More interestingly, the bHLH transcriptional network this whole project is focusing on is also present in *D. Melanogaster*. For example, the fly gene *Daughterless* is the homolog of the human E2A gene that codes for E47 (Quong et al. 1993). Homologs of ID proteins have also been characterized: the gene *extramacrochaetae* (emc) codes for a protein lacking its DNA binding domain and involved in development and the formation of the midgut (Ellis et al. 1990; Ellis 1994). This high homology between the genomes of *D. Melanogaster* and *Homo sapiens* would have presupposed better survival chances for a human xenograft in fruit flies. It would however be interesting to test whether a similar dominant-negative approach as shown with dnE47 could be translated to *Daughterless* since this gene is know to be involved in the regulation of cell cycle in *Drosophila* and its *C. elegans* homolog *HLH-2* in cell invasion (Sukhanova et al. 2007; Sukhanova & Du 2008; Schindler & Sherwood 2011).

Our attempt to develop an alternative approach to classical immunodeficient models had to face the fact that transplanted GFP positive cells could not be detected one week after engraftment anymore. This argues for the presence of an immune system in Drosophila flies. Indeed, fruit flies can resist to different pathogens, such as *C.Albicans*, thanks to an innate immune system, present in the systemic circulation (Boman et al. 1972; Lemaitre et al. 1996). In order to circumvent this system and give the chance to a human xenograft to survive in this organism, one possibility would be to use genetically modified Drosophila, similar to immunodeficient mice. Immunosuppressed mutants have already been described such as flies that lack a functional Toll receptor or such as near *Black cell* mutants (Corbo & Levine 1996; Alarco et al. 2004). The Toll-receptor pathway controls the production of an antifungal peptide, drosomycin in response to infections whereas a mutation near the *Black cell* gene impairs the response of immunity genes such as cecropins and

diphterins (Kylsten et al. 1990; Wicker et al. 1990). Mutations in these genes impair therefore a response from the immune system after infection and might also avoid a rejection of a xenograft.

Next to immunodeficient *D. melanogaster*, an alternative method would be to use another well-established genetic model such as *Danio rerio* (zebrafish). First, this organism has the similar advantages to *Drosophila Melanogaster* regarding the maintenance and care: low costs, short breeding time, established genetic tools. Second, being a vertebrate makes it therefore phylogenetically closer to humans. In fact, zebrafishes have been widely used as models to genetically dissect diverse human diseases, including cancer (Goldsmith & Jobin 2012). In the context of colon cancer, the RAS-MAPK pathway has been shown to promote tumor formation in zebrafish similar to humans (Hruban et al. 1993; Park et al. 2008). Furthermore, as in murine and fruit fly models, xenograft transplantation assays have been developed and established complemented with imaging methods to follow the expansion of the disease (Taylor & Zon 2009; Ignatius & Langenau 2011; Cao et al. 2013).

As a conclusion, both immunosuppressed Drosophila flies and xenograft transplantations in zebrafish underline the potential of alternative methods to canonical mammalian tumor models and should be considered as valid models for cancer research as well. Not only will they reveal new hits for the development of new therapeutic approaches but will also give the possibility to screen for drugs and treatments.

Chapter V

Discussion

Discussion

Glioma cells are characterized by their highly proliferative behavior, their invasive properties and their angiogenic capacities (Furnari et al. 2007; Westphal & Lamszus 2011). The transcription factor family of helix-loop-helix (HLH) and basic HLH (bHLH) proteins was shown to be involved in all of these features (Perk et al. 2005; Aguirre-Cruz et al. 2004; Somasundaram et al. 2005). Originally, this study was designed to use E proteins as an anti-glioma tool to 1) counteract pro-proliferative effects of ID proteins and 2) transactivate proneural proteins in order to promote terminal differentiation. However, this strategy appeared to be efficient in a subpopulation of glioma cells that expressed low level of proneural proteins only, suggesting instead that proneural proteins transactivation participate to tumorogenesis. Indeed, engineering a dominant-negative E protein that concomitantly sequestered both ID and bHLH proteins in the cytoplasm, hence impairing their transcriptional activity, proved to be effective more consistently. It should however be noted that although overexpression of dnE47 consistently led to proliferation impairments and induced apoptosis in both immortalized cell lines and patient-derived tumor-initiating cell lines, eradication of the tumor cells was neither reached *in vitro* nor *in vivo*. This observation suggests the presence and/or development of resistance or escape mechanisms in the targeted cells and raises several issues, which will be discussed here.

Class I bHLH proteins consists of four E proteins (E47, E12, E2-2 and HEB) which have been shown to be interchangeable regarding their ability to bind ID proteins (Massari & Murre 2000; Teachenor et al. 2012). This suggests that overexpression of dnE47 alone might not be sufficient enough to disrupt the whole transcriptional network, as it needs to "compete" with all endogenous E-proteins that are expressed at a given time in glioma cells. It is also possible that different E proteins may have slightly different targets. Supporting this idea, E47 and E12 have different functions in the maturation of B cells, suggesting differential transcriptional functions for each E protein (Beck et al. 2009).

It should also be mentioned that in addition to their partner roles for bHLH proteins in promoting their transcriptional activity, E proteins might also directly participate to tumor homeostasis. Some of these functions might be mediated by the formation of E-proteins homodimers. For example, it has been shown that E47 is involved in promoting proliferation, epithelial to mesenchymal transition (EMT) and apoptosis in cancer cells (Engel & Murre 1999a; Peverali et al. 1994; Trabosh et al. 2009; Perez-Moreno et al. 2001). Besides E47, E2-2 was also shown to regulate epithelial-mesenchymal transition (EMT) via *E-cadherin* repression *in vitro* (Sobrado et al. 2009). Dominant negative E proteins overexpression is likely to disrupt formation of functional homo and/or heterodimers, by sequestering other Class I proteins in the cell cytoplasm as well, disrupting thereby their oncogenic role (Massari & Murre 2000; Murre 2005). In conclusion, the incomplete anti-glioma effects of dnE47 overexpression might be due to a compensatory mechanism from the other E proteins or to the pro-tumor properties of E47.

Post-translational modifications such as phosphorylation greatly influence protein functions and could affect the anti-glioma effects after dnE47 overexpression. In neural stem cells of the embryonic spinal cord for example, Olig2 has a pro-proliferative function when phosphorylated whereas in its unphosphorylated state, it supports oligodendrocytes differentiation (Li et al. 2011). Similarly, E47 is subjected to post-translational phosphorylation, which influences its stability and transcriptional activity in skeletal myoblasts and B-lymphocytes (Sloan et al. 1996; Page et al. 2004). The question remains whether phosphorylation of E proteins occurs in cancer cells and thereby alters their binding properties and functions, for example in apoptosis and/or E-cadherin mediated EMT. Post-translational modifications of both HLH and bHLH proteins could influence the interplay between E and ID proteins which regulates proliferation and differentiation during development as well as in the diseased brain (Massari & Murre 2000; Jones 2004). Supporting this idea, phosphorylation by cyclin-dependent kinase 2 (cdk2) of ID proteins modulates their function in cell cycle progression as well as their binding abilities (Deed et al. 1997; Hara et al. 1997). In general, aberrant tyrosine phosphorylation through deregulated protein-tyrosine kinase and phosphatase signaling is a hallmark of many cancers (Hunter 1998; Blume-Jensen & Hunter 2001). Hence, it would be interesting to

investigate whether phosphorylation of dnE47 would perturb or enhance its anti-glioma effects.

Besides phosphorylation, epigenetic mechanisms modify proteins expression and/or activity at the post-translational level and are known to interplay with the HLH/bHLH network. E proteins were shown to interplay with epigenetic modulators such as microRNAs. For example, E47 up-regulates mir-495 in breast cancer stem cells and induces hypoxia resistance and oncogenesis (Hwang-Verslues et al. 2011). Furthermore, E2A proteins are able to recruit a histone acetyltransferase in nonlymphoid cells in vitro (Sakamoto et al. 2012). Using the protein-interaction software STRING (STRING 9.05, http://www.string-db.org/), E2A was shown to interact with the histone deacetylase 2 (HDAC2) suggesting that E proteins are involved in the initiation of epigenetic modifications of the genome. Regarding ID proteins, epigenetic silencing of ID4 has been reported in liver cancer and in glioblastoma patients (Sharma et al. 2012; Martini et al. 2013). Since both E and ID proteins interact with epigenetic mechanisms, dnE47 overexpression might impair these post-translational modifications. This still needs to be further investigated in order to better understand the relations between the HLH/bHLH network and epigenetic modulations.

ID proteins lack a DNA binding domain and act as negative regulators of E proteins (Ruzinova & Benezra 2003). ID proteins are highly expressed in tumor cells and mainly sustain their proliferative behavior as well as neo-angiogenesis within the tumor (Benezra et al. 2001; Perk et al. 2005). However, so far it is not clear whether each ID protein has unique functions and how their properties are regulated (Perk et al. 2005). ID proteins interact directly with many proteins involved in cell cycle regulation such as p16 or the retinoblastoma protein (Rb) for example (Ruzinova & Benezra 2003). E protein overexpression therefore is likely to impair interactions between ID proteins and their dimerization partners, thereby inhibiting the inhibitors (in other words ID proteins). What is known about ID functions and properties is mainly based on *in vitro* experiments and knockout studies and very few data about their endogenous *in vivo* properties is available. ID1 and ID3 were shown to interact with E26 transformation-specific (ETS) proteins and to be regulated by TGFbeta, VEGF and bone morphogenic protein 4 (BMP4) (Ying et al. 2003; Kang et al. 2003;

Kowanetz et al. 2004; Lyden et al. 2001; Ohtani et al. 2001). ID2 can interact with ETS proteins as well and is regulated by Rb and the MYC pathway (Nishimori et al. 2002; Lasorella et al. 2000). There is less data on ID4 and its functions. In breast cancer cells, ID4 forms a feedback loop with the tumor suppressor breast cancer type 1 susceptibility protein (BRCA1) and methylation of the ID promoter correlates with poor prognosis in the case of colorectal carcinomas (Welcsh et al. 2002; Umetani et al. 2004). These data therefore suggest a tumor suppressive role for ID4. However, which effects the deregulation of ID proteins has depends also on the cell type and it would not be surprising if different ID proteins had different functions depending on the type of cancer they are involved in (Perk et al. 2005). This high interplaying complexity between the (b)HLH network and other physiological pathways justifies a therapeutic approach aiming at targeting a network in its ensemble. Nevertheless, a possible drawback of this approach that needs to be further tested, is the possibility that network disruption may also hinder tumor suppressor pathways and may therefore lead to more aggressive tumors.

Going along this line, numerous canonical cancer pathways were modulated after dnE47 overexpression, as illustrated by the qRT-PCR array results presented in **Chapter 2**. For instance, genes involved in proliferation, apoptosis, angiogenesis and metastasis were significantly up- or down-regulated following dnE47 overexpression. It will be interesting to investigate these changes in more details, e.g. to study their consequences for the cells behavior. Considering the broad spectrum of transcriptional modulations, it is reasonable to think that other canonical pathways such as Wnt or Notch signaling which play a role in tumor formation and maintenance, are also influenced by dnE47 overexpression. The Wnt pathway is implicated in both glioma and cancer stem cells homeostasis whereas Notch and its downstream targets are involved in the formation of medulloblastomas (Hatten & Roussel 2011; Gong & Huang 2012; Zhang et al. 2012). Further whole-genome transcriptional investigations will enable to understand to which extent (b)HLH network disruption affects tumor homeostasis. It will also give insights on the identity of which pathways (b)HLH proteins have the ability to interact with.

Despite numerous common pathways regulating their physiology, brain tumors are extremely various in their genomic and molecular profiles (Furnari et al. 2007; Westphal & Lamszus 2011; Verhaak et al. 2010; Phillips et al. 2006). This might be explained by two main reasons. First, studies revealed different cell types as possible cell-of-origin for tumor formation. Tumors can arise from diverse cycling cell populations such as neural progenitor and neural stem cells (Persson et al. 2010; Liu et al. 2011; Holland et al. 2000; Alcantara Llaguno et al. 2009; Cheng et al. 2009). Second, cells within a tumor are highly heterogeneous and show extremely dynamic abilities to adapt to changes of their microenvironment (Beier et al. 2011; Charles et al. 2011; Sottoriva et al. 2013). Consequently, inter- and intra-tumor heterogeneity challenges the development of therapeutic approaches specific for each tumor type and highlights the necessity to develop personalized treatments (Furnari et al. 2007; Schonberg et al. 2013; Chaudhry et al. 2013; Verhaak et al. 2010). A significant step in the direction of personalized therapy was the discovery that patients with *MGMT* methylation respond better to radiotherapy combined with TMZ treatment (Stupp et al. 2009). However, this is true only for glioblastoma but not for other types of brain tumors such as medulloblastoma or oligodendroglioma, which underlines again the need for development of tumor type-specific treatments (van den Bent et al. 2009; Faoro et al. 2011).

Although we focused on the most aggressive type of brain tumors: glioblastoma multiforme, it should be noted that HLH and bHLH networks are also involved in numerous other cancer types. E, ID and bHLH transcription factors are also implicated in breast cancer, prostate cancer or leukemia (Perk et al. 2005; Ligon et al. 2006; Desprez et al. 2003; Baer 1993; Perez-Moreno et al. 2001; Lee et al. 2011). Similarly to their functions in brain tumors, ID proteins are upregulated and sustain the proliferative behavior of cancer cells in a wide range of tumors (Ruzinova & Benezra 2003; Perk et al. 2005). As similar pathways regulate tumor stem cells from different cancer types, it would be interesting to investigate the effects of dnE47 overexpression in a wide range of cancers. Providing that dnE47 overexpression shows consistent effects in different cancer types, this would validate the manipulation of E proteins and (b)HLH network disruption as a therapeutic approach against global networks and would strengthen the possibility to consider transcription factors as potential therapeutic targets.

Targeting transcription factors as a therapeutic approach has been investigated recently with the aim to find central interactions on which formation, transformation and evolution of cancer cells and tumors rely (Ivanov et al. 2013; Yan & Higgins 2013). The discovery of vital transcriptional pathway nodes relies on structure-based design studies and advanced screening methods (Ivanov et al. 2013). These approaches can be used to reveal effective protein-interaction modulators that proved to be efficient for cancer treatment. For example, small molecules inhibiting Signal Transducers and Activators of Transcription 3 (STAT3) impair its transcriptional activity and induce antitumor effects in breast cancer xenografts (Turkson et al. 2001; Siddiquee et al. 2007). Targeting the p53 tumor suppressor pathway with a Mouse double minute 2 homolog (MDM2) antagonist is in clinical trials for leukemia and lymphoma (Vassilev et al. 2004; Andreeff et al. 2003). In this project, we overexpressed a mutant E protein missing its nuclear localization signal as a protein-protein inhibitor. Previous studies already took a similar approach using peptides for ID protein targeting. There, small peptides and aptamers were designed for binding ID proteins and impaired their dimerization interactions (Ciarapica et al. 2009; D S Mern et al. 2010b; Demissew S Mern et al. 2010). These studies showed that by narrowing down the peptides to their HLH domain, ID proteins are counteracted but the binding sites of these peptides for other bHLH dimerization partners are lost (Ciarapica et al. 2003). Hence, these approaches targeted only ID proteins without aiming at the whole HLH/bHLH network. Since we used a full-length protein in our approach, an interesting follow-up project could consist of trying to narrow down dnE47 to an inhibiting peptide that still has its binding functions and anti-glioma properties.

Considering the vast heterogeneity of brain tumors and numerous pathways involved in tumor homeostasis, several aspects will need to be investigated in more details. It will be crucial in the future to decipher the possibl multiple origins of tumors, to understand their regulatory pathways as well as to correlate their histology or molecular profiles with responses to therapy. These findings will be decisive in order to develop new multimodal and global therapeutic approaches as well as individualized therapies. For this, it will be necessary to bridge both bench work in neurobiology and bedside clinical trials with constant exchanges between both sides.

Acknowledgments

First, I would like to thank Dr. Olivier Raineteau for his supervision as well as Prof. Esther Stöckli and Prof. Martin Schwab for their guidance and inputs during this PhD thesis.

For creating a nice atmosphere in the lab, I would like to say thank you to all current and past members of the Hifo Raineteau lab: Kazum Azim, Anahi Hurtado, Roberto Fiorelli, Bruno Fischer, Clara Orlando, Nidhi Koppole and my master student Michel Fries.

I am very grateful to Ghazaleh Tabatabai for her collaboration, her input from the cancer field and support. I would also like to thank Matthias Scholl, Felice Burn, Hans-Georg Wirsching, Isabelle Barde, Sonia Verp, Sandra Offner, Anne-Sophie Laurenson and Lutz Slomianka for all the suggestions and technical help I received for this project.

I would like to thank the technical staff of the Brain Research Institute for being so helpful: Hansjörg Kasper, Stefan Giger, Martin Wieckhorst, Marco Tedaldi, Frank David and Pietro Morciano as well as Gisep Bazzell for taking care of the mice with such a great sense of humor.

For all their scientific, technical and emotional support inside and outside of the institute, I would like to thank Sandrine Joly, Katharina Gapp, Michael Arzt, Vincent Pernet, Miriam Gullo, Regula Schneider and the chicks' office J12.

A special thank you to Michaela Thallmair for being more than a supervisor and a mentor since the beginning of the Hifo adventure, I owe her a lot.

For being the safe keepers of a healthy work-life balance in Zürich, I would like to thank Michelle Starkey, my ASVZ basketball friends and my BC Flying Divac team.

And thank you to the safe keepers in Fribourg: Audrey Saumon, Delphine Page, Amélie Pasquier, Emilie Gachet and Matthieu Raemy.

My warmest and deepest thank you goes to Peter Horner for his precious support and love.

Finally, there are no words strong enough to express my gratitude and love towards my parents, Hermann and Marie-Claire, and my brothers, Stefan and Florian. They are my safety net and the roots on which my whole life is based on.

References

Aboody, K.S. et al., 2000. Neural stem cells display extensive tropism for pathology in adult brain: evidence from intracranial gliomas. *Proceedings of the National Academy of Sciences of the United States of America*, 97(23), pp.12846–51.

Aboody, K.S., Najbauer, J. & Danks, M.K., 2008. Stem and progenitor cell-mediated tumor selective gene therapy. *Gene therapy*, 15(10), pp.739–52.

Aboud, O.A. & Weiss, R.H., 2013. New opportunities from the cancer metabolome. *Clinical chemistry*, 59(1), pp.138–46.

Adams, M.D. et al., 2000. The genome sequence of Drosophila melanogaster. *Science (New York, N.Y.)*, 287(5461), pp.2185–95.

Aguirre-Cruz, L. et al., 2004. Analysis of the bHLH transcription factors Olig1 and Olig2 in brain tumors. *Journal of neuro-oncology*, 67(3), pp.265–71.

Alarco, A.-M. et al., 2004. Immune-deficient Drosophila melanogaster: a model for the innate immune response to human fungal pathogens. *Journal of immunology (Baltimore, Md. : 1950)*, 172(9), pp.5622–8.

Alberici, L. et al., 2012. De Novo Design of a Tumor-Penetrating Peptide. *Cancer research*.

Alcantara Llaguno, S. et al., 2009. Malignant Astrocytomas Originate from Neural Stem/Progenitor Cells in a Somatic Tumor Suppressor Mouse Model. *Cancer Cell*, 15(1), pp.45–56.

Alvarez-Buylla, A. & Lim, D.A., 2004. For the long run: maintaining germinal niches in the adult brain. *Neuron*, 41(5), pp.683–6.

Andreeff, M., Kojima, K. & Padmanabhan, S., 2003. *A multi-center, open-label, phase I study of single agent RG7112, a first in class p53-MDM2 antagonist, in patients with relapsed/refractory acute myeloid and lymphoid leukemias (AML/ALL) and refractory chronic lymphocytic leukemia/small cell lymphocytic*,

Anido, J. et al., 2010. TGF-β Receptor Inhibitors Target the CD44(high)/Id1(high) Glioma-Initiating Cell Population in Human Glioblastoma. *Cancer cell*, 18(6), pp.655–68.

Bach, P. et al., 2013. Specific elimination of CD133+ tumor cells with targeted oncolytic measles virus. *Cancer research*, 73(2), pp.865–74.

Bachoo, R.M. et al., 2002. Epidermal growth factor receptor and Ink4a/Arf: convergent mechanisms governing terminal differentiation and transformation along the neural stem cell to astrocyte axis. *Cancer cell*, 1(3), pp.269–77.

Baer, R., 1993. TAL1, TAL2 and LYL1: a family of basic helix-loop-helix proteins implicated in T cell acute leukaemia. *Seminars in cancer biology*, 4(6), pp.341–7.

Bahmani, P. et al., 2011. Visualization of cell death in mice with focal cerebral ischemia using fluorescent annexin A5, propidium iodide, and TUNEL staining. *Journal of cerebral blood flow and metabolism : official journal of the International Society of Cerebral Blood Flow and Metabolism*, 31(5), pp.1311–20.

Bao, S. et al., 2006. Glioma stem cells promote radioresistance by preferential activation of the DNA damage response. *Nature*, 444(7120), pp.756–60.

Barde, I. et al., 2006. Efficient control of gene expression in the hematopoietic system using a single Tet-on inducible lentiviral vector. *Molecular therapy : the journal of the American Society of Gene Therapy*, 13(2), pp.382–90.

Barde, I., Salmon, P. & Trono, D., 2010. Production and titration of lentiviral vectors. *Current protocols in neuroscience / editorial board, Jacqueline N. Crawley ... [et al.]*, Chapter 4, p.Unit 4.21.

Barnabé-Heider, F. et al., 2010. Origin of new glial cells in intact and injured adult spinal cord. *Cell stem cell*, 7(4), pp.470–82.

Beck, K. et al., 2009. Distinct roles for E12 and E47 in B cell specification and the sequential rearrangement of immunoglobulin light chain loci. *The Journal of experimental medicine*, 206(10), pp.2271–84.

Beckervordersandforth, R. et al., 2010. In Vivo Fate Mapping and Expression Analysis Reveals Molecular Hallmarks of Prospectively Isolated Adult Neural Stem Cells. *Cell Stem Cell*, 7(6), pp.744–758.

Beier, D. et al., 2008. Temozolomide preferentially depletes cancer stem cells in glioblastoma. *Cancer research*, 68(14), pp.5706–15.

Beier, D., Schulz, J.B. & Beier, C.P., 2011. Chemoresistance of glioblastoma cancer stem cells--much more complex than expected. *Molecular cancer*, 10(1), p.128.

Belachew, S. et al., 2003. Postnatal NG2 proteoglycan-expressing progenitor cells are intrinsically multipotent and generate functional neurons. *The Journal of cell biology*, 161(1), pp.169–86.

Benedetti, S. et al., 2000. Gene therapy of experimental brain tumors using neural progenitor cells. *Nature medicine*, 6(4), pp.447–50.

Benezra, R. et al., 1990. The protein Id: a negative regulator of helix-loop-helix DNA binding proteins. *Cell*, 61(1), pp.49–59.

Benezra, R., Rafii, S. & Lyden, D., 2001. The Id proteins and angiogenesis. *Oncogene*, 20(58), pp.8334–41.

Van den Bent, M.J. et al., 2009. MGMT promoter methylation is prognostic but not predictive for outcome to adjuvant PCV chemotherapy in anaplastic oligodendroglial tumors: a report from EORTC Brain Tumor Group Study 26951. *Journal of clinical oncology : official journal of the American Society of Clinical Oncology*, 27(35), pp.5881–6.

Berger, C. et al., 2012. FACS Purification and Transcriptome Analysis of Drosophila Neural Stem Cells Reveals a Role for Klumpfuss in Self-Renewal. *Cell Reports*, 2(2), pp.407–418.

Berninger, B. et al., 2007. Functional properties of neurons derived from in vitro reprogrammed postnatal astroglia. *The Journal of neuroscience : the official journal of the Society for Neuroscience*, 27(32), pp.8654–64.

Blume-Jensen, P. & Hunter, T., 2001. Oncogenic kinase signalling. *Nature*, 411(6835), pp.355–65.

Boman, H.G., Nilsson, I. & Rasmuson, B., 1972. Inducible Antibacterial Defence System in Drosophila. *Nature*, 237(5352), pp.232–235.

Bosma, G.C., Custer, R.P. & Bosma, M.J., 1983. A severe combined immunodeficiency mutation in the mouse. *Nature*, 301(5900), pp.527–30.

Brada, M. et al., 2001. Multicenter phase II trial of temozolomide in patients with glioblastoma multiforme at first relapse. *Annals of oncology : official journal of the European Society for Medical Oncology / ESMO*, 12(2), pp.259–66.

Del Burgo, L.S. et al., 2013. Nanotherapeutic approaches for brain cancer management. *Nanomedicine: Nanotechnology, Biology, and Medicine*, pp.1–15.

Cao, Y. et al., 2013. Neuropilin-2 promotes extravasation and metastasis by interacting with endothelial α5 integrin. *Cancer research*, 73(14), pp.4579–90.

Castro, D.S. et al., 2011. A novel function of the proneural factor Ascl1 in progenitor proliferation identified by genome-wide characterization of its targets. *Genes & development*, 25(9), pp.930–45.

Caussinus, E. & Gonzalez, C., 2005. Induction of tumor growth by altered stem-cell asymmetric division in Drosophila melanogaster. *Nature genetics*, 37(10), pp.1125–9.

Cayre, M., Canoll, P. & Goldman, J.E., 2009. Cell migration in the normal and pathological postnatal mammalian brain. *Progress in neurobiology*, 88(1), pp.41–63.

Charles, N. a et al., 2011. The brain tumor microenvironment. *Glia*, 1180(March), pp.1169–1180.

Chaudhry, N.S. et al., 2013. Predictors of long-term survival in patients with glioblastoma multiforme: advancements from the last quarter century. *Cancer investigation*, 31(5), pp.287–308.

Chen, J. et al., 2012. A restricted cell population propagates glioblastoma growth after chemotherapy. *Nature*, pp.1–6.

Chen, R. et al., 2010. A hierarchy of self-renewing tumor-initiating cell types in glioblastoma. *Cancer cell*, 17(4), pp.362–75.

Cheng, C.K., Fan, Q.-W. & Weiss, W.A., 2009. PI3K signaling in glioma--animal models and therapeutic challenges. *Brain pathology (Zurich, Switzerland)*, 19(1), pp.112–20.

Christianson, S.W. et al., 1997. Enhanced human CD4+ T cell engraftment in beta2-microglobulin-deficient NOD-scid mice. *Journal of immunology (Baltimore, Md. : 1950)*, 158(8), pp.3578–86.

Christy, B. & Nathans, D., 1989. DNA binding site of the growth factor-inducible protein Zif268. *Proceedings of the National Academy of Sciences of the United States of America*, 86(22), pp.8737–41.

Ciarapica, R. et al., 2003. Molecular recognition in helix-loop-helix and helix-loop-helix-leucine zipper domains. Design of repertoires and selection of high affinity ligands for natural proteins. *The Journal of biological chemistry*, 278(14), pp.12182–90.

Ciarapica, R. et al., 2009. Targeting Id protein interactions by an engineered HLH domain induces human neuroblastoma cell differentiation. *Oncogene*, 28(17), pp.1881–91.

Claes, A., Idema, A.J. & Wesseling, P., 2007. Diffuse glioma growth: a guerilla war. *Acta neuropathologica*, 114(5), pp.443–58.

Clément, V. et al., 2009. Limits of CD133 as a marker of glioma self-renewing cells. *International journal of cancer. Journal international du cancer*, 125(1), pp.244–8.

Clément, V. et al., 2010. Marker-independent identification of glioma-initiating cells. *Nature methods*, 7(3), pp.224–8.

Coma, S. et al., 2010. Id2 promotes tumor cell migration and invasion through transcriptional repression of semaphorin 3F. *Cancer research*, 70(9), pp.3823–32.

Corbo, J.C. & Levine, M., 1996. Characterization of an immunodeficiency mutant in Drosophila. *Mechanisms of development*, 55(2), pp.211–20.

Dawson, M.R., Levine, J.M. & Reynolds, R., 2000. NG2-expressing cells in the central nervous system: are they oligodendroglial progenitors? *Journal of neuroscience research*, 61(5), pp.471–9.

Deed, R.W. et al., 1997. Regulation of Id3 cell cycle function by Cdk-2-dependent phosphorylation. *Molecular and cellular biology*, 17(12), pp.6815–21.

Deed, R.W., Armitage, S. & Norton, J.D., 1996. Nuclear Localization and Regulation of Id Protein through an E Protein-mediated Chaperone Mechanism *. *Biochemistry*, pp.23603–23606.

Deliolanis, N.C. et al., 2011. In vivo tomographic imaging of red-shifted fluorescent proteins. *Biomedical optics express*, 2(4), pp.887–900.

Desprez, P.-Y., Sumida, T. & Coppé, J.-P., 2003. Helix-loop-helix proteins in mammary gland development and breast cancer. *Journal of mammary gland biology and neoplasia*, 8(2), pp.225–39.

Dorshkind, K., 1994. Transcriptional control points during lymphopoiesis. *Cell*, 79(5), pp.751–3.

Dull, T. et al., 1998. A third-generation lentivirus vector with a conditional packaging system. *Journal of virology*, 72(11), pp.8463–71.

Ellis, H.M., 1994. Embryonic expression and function of the Drosophila helix-loop-helix gene, extramacrochaetae. *Mechanisms of development*, 47(1), pp.65–72.

Ellis, H.M., Spann, D.R. & Posakony, J.W., 1990. extramacrochaetae, a negative regulator of sensory organ development in Drosophila, defines a new class of helix-loop-helix proteins. *Cell*, 61(1), pp.27–38.

Engel, I. & Murre, C., 1999a. Ectopic expression of E47 or E12 promotes the death of E2A-deficient lymphomas. *Proc. Natl. Acad. Sci. U.SA.*, 96, pp.996–1001.

Engel, I. & Murre, C., 1999b. Ectopic expression of E47 or E12 promotes the death of E2A-deficient lymphomas. *Proceedings of the National Academy of Sciences of the United States of America*, 96(3), pp.996–1001.

Eramo, A. et al., 2006. Chemotherapy resistance of glioblastoma stem cells. *Cell death and differentiation*, 13(7), pp.1238–41.

Eriksson, P.S. et al., 1998. Neurogenesis in the adult human hippocampus. *Nature medicine*, 4(11), pp.1313–7.

Fan, X. et al., 2006. Notch pathway inhibition depletes stem-like cells and blocks engraftment in embryonal brain tumors. *Cancer research*, 66(15), pp.7445–52.

Faoro, D. et al., 2011. Expression of O^6-methylguanine-DNA methyltransferase in childhood medulloblastoma. *Journal of neuro-oncology*, 103(1), pp.59–69.

Feldkamp, M.M., Lau, N. & Guha, A., 1997. Signal transduction pathways and their relevance in human astrocytomas. *Journal of neuro-oncology*, 35(3), pp.223–48.

Flanagan, S.P., 1966. “Nude”, a new hairless gene with pleiotropic effects in the mouse. *Genetical research*, 8(3), pp.295–309.

Follenzi, A. et al., 2000. Gene transfer by lentiviral vectors is limited by nuclear translocation and rescued by HIV-1 pol sequences. *Nature genetics*, 25(2), pp.217–22.

Fong, S., Debs, R.J. & Desprez, P.-Y., 2004. Id genes and proteins as promising targets in cancer therapy. *Trends in molecular medicine*, 10(8), pp.387–92.

Friedmann-Morvinski, D. et al., 2012. Dedifferentiation of Neurons and Astrocytes by Oncogenes Can Induce Gliomas in Mice. *Science (New York, N.Y.)*, (October), pp.1–6.

Furnari, F.B. et al., 2007. Malignant astrocytic glioma: genetics, biology, and paths to treatment. *Genes & development*, 21(21), pp.2683–710.

Geoffroy, C.G. et al., 2009. Engineering of dominant active basic helix-loop-helix proteins that are resistant to negative regulation by postnatal central nervous system antineurogenic cues. *Stem cells (Dayton, Ohio)*, 27(4), pp.847–56.

Germano, I., Swiss, V. & Casaccia, P., 2010. Primary brain tumors, neural stem cell, and brain tumor cancer cells: where is the link? *Neuropharmacology*, 58(6), pp.903–10.

Gilbert, M.R. et al., 2011. RTOG 0525: A randomized phase III trial comparing standard adjuvant temozolomide (TMZ) with a dose-dense (dd) schedule in newly diagnosed

glioblastoma (GBM). | 2011 ASCO Annual Meeting | Abstracts | Meeting Library. *Journal of clinical oncology : official journal of the American Society of Clinical Oncology*. Available at: http://meetinglibrary.asco.org/content/79659-102.

Goldsmith, J.R. & Jobin, C., 2012. Think small: zebrafish as a model system of human pathology. *Journal of biomedicine & biotechnology*, 2012, p.817341.

Gong, A. & Huang, S., 2012. FoxM1 and Wnt/β-catenin signaling in glioma stem cells. *Cancer research*, 72(22), pp.5658–62.

Gont, A. et al., 2013. PTEN loss represses glioblastoma tumor initiating cell differentiation via inactivation of Lgl1. *Oncotarget*, 4(8), pp.1266–79.

Gonzalez, C., 2013. Drosophila melanogaster: a model and a tool to investigate malignancy and identify new therapeutics. *Nature reviews. Cancer*, 13(3), pp.172–83.

Greiner, D.L. et al., 1995. Improved engraftment of human spleen cells in NOD/LtSz-scid/scid mice as compared with C.B-17-scid/scid mice. *The American journal of pathology*, 146(4), pp.888–902.

Griguer, C.E. et al., 2008. CD133 is a marker of bioenergetic stress in human glioma. *PloS one*, 3(11), p.e3655.

Guichet, P.-O. et al., 2012. Cell death and neuronal differentiation of glioblastoma stem-like cells induced by neurogenic transcription factors. *Glia*, 000, pp.1–15.

Gundersen, H.J. et al., 1999. The efficiency of systematic sampling in stereology--reconsidered. *Journal of microscopy*, 193(Pt 3), pp.199–211.

Gupta, S. & Chawla, K., 2013. Oncometabolomics in cancer research. *Expert review of proteomics*, 10(4), pp.325–36.

Hara, E., Hall, M. & Peters, G., 1997. Cdk2-dependent phosphorylation of Id2 modulates activity of E2A-related transcription factors. *The EMBO journal*, 16(2), pp.332–42.

Hasskarl, J. & Munger, K., 2002. Id Proteins - Tumor Markers or Oncogenes? *Cancer Biology & Therapy*, 1(2), pp.89–94.

Hatten, M.E. & Roussel, M.F., 2011. Development and cancer of the cerebellum. *Trends in neurosciences*, 34(3), pp.134–42.

Heins, N. et al., 2002. Glial cells generate neurons: the role of the transcription factor Pax6. *Nature neuroscience*, 5(4), pp.308–15.

Henke, E. et al., 2008. Peptide-conjugated antisense oligonucleotides for targeted inhibition of a transcriptional regulator in vivo. *Nature biotechnology*, 26(1), pp.91–100.

Holland, E.C. et al., 2000. Combined activation of Ras and Akt in neural progenitors induces glioblastoma formation in mice. *Nature genetics*, 25(1), pp.55–7.

Horner, P.J. et al., 2000. Proliferation and Differentiation of Progenitor Cells Throughout the Intact Adult Rat Spinal Cord. *Journal of Neuroscience*, 20(6), pp.2218–2228.

Hruban, R.H. et al., 1993. K-ras oncogene activation in adenocarcinoma of the human pancreas. A study of 82 carcinomas using a combination of mutant-enriched polymerase chain reaction analysis and allele-specific oligonucleotide hybridization. *The American journal of pathology*, 143(2), pp.545–54.

Hunter, T., 1998. The Croonian Lecture 1997. The phosphorylation of proteins on tyrosine: its role in cell growth and disease. *Philosophical transactions of the Royal Society of London. Series B, Biological sciences*, 353(1368), pp.583–605.

Hwang-Verslues, W.W. et al., 2011. miR-495 is upregulated by E12/E47 in breast cancer stem cells, and promotes oncogenesis and hypoxia resistance via downregulation of E-cadherin and REDD1. *Oncogene*, 30(21), pp.2463–74.

Iavarone, A. et al., 1994. The helix-loop-helix protein Id-2 enhances cell proliferation and binds to the retinoblastoma protein. *Genes & development*, 8(11), pp.1270–84.

Iavarone, A. & Lasorella, A., 2006. ID proteins as targets in cancer and tools in neurobiology. *Trends in molecular medicine*, 12(12), pp.588–94.

Ignatius, M.S. & Langenau, D.M., 2011. Fluorescent imaging of cancer in zebrafish. *Methods in cell biology*, 105, pp.437–59.

Ivanov, A.A., Khuri, F.R. & Fu, H., 2013. Targeting protein-protein interactions as an anticancer strategy. *Trends in pharmacological sciences*.

Jackson, E.L. et al., 2006. PDGFR alpha-positive B cells are neural stem cells in the adult SVZ that form glioma-like growths in response to increased PDGF signaling. *Neuron*, 51(2), pp.187–99.

Jenei, V., Nystrom, M.L. & Thomas, G.J., 2011. Measuring invasion in an organotypic model. *Methods in molecular biology (Clifton, N.J.)*, 769, pp.223–32.

Jones, S., 2004. An overview of the basic helix-loop-helix proteins. *Genome biology*, 5(6), p.226.

Kang, Y., Chen, C.-R. & Massagué, J., 2003. A self-enabling TGFbeta response coupled to stress signaling: Smad engages stress response factor ATF3 for Id1 repression in epithelial cells. *Molecular cell*, 11(4), pp.915–26.

Kemper, K. et al., 2010. The AC133 epitope, but not the CD133 protein, is lost upon cancer stem cell differentiation. *Cancer research*, 70(2), pp.719–29.

Knight, Z. a, Lin, H. & Shokat, K.M., 2010. Targeting the cancer kinome through polypharmacology. *Nature reviews. Cancer*, 10(2), pp.130–7.

Komitova, M. & Eriksson, P.S., 2004. Sox-2 is expressed by neural progenitors and astroglia in the adult rat brain. *Neuroscience letters*, 369(1), pp.24–7.

Kondo, T., 2000. Oligodendrocyte Precursor Cells Reprogrammed to Become Multipotential CNS Stem Cells. *Science*, 289(5485), pp.1754–1757.

Kowanetz, M. et al., 2004. Id2 and Id3 define the potency of cell proliferation and differentiation responses to transforming growth factor beta and bone morphogenetic protein. *Molecular and cellular biology*, 24(10), pp.4241–54.

Kylsten, P., Samakovlis, C. & Hultmark, D., 1990. The cecropin locus in Drosophila; a compact gene cluster involved in the response to infection. *The EMBO journal*, 9(1), pp.217–24.

Laperriere, N., Zuraw, L. & Cairncross, G., 2002. Radiotherapy for newly diagnosed malignant glioma in adults: a systematic review. *Radiotherapy and oncology : journal of the European Society for Therapeutic Radiology and Oncology*, 64(3), pp.259–73.

Lasorella, a, Iavarone, a & Israel, M. a, 1996. Id2 specifically alters regulation of the cell cycle by tumor suppressor proteins. *Molecular and cellular biology*, 16(6), pp.2570–8.

Lasorella, A. et al., 2000. Id2 is a retinoblastoma protein target and mediates signalling by Myc oncoproteins. *Nature*, 407, pp.592–598.

Lasorella, A., Uo, T. & Iavarone, A., 2001. Id proteins at the cross-road of development and cancer. *Oncogene*, 20(58), pp.8326–33.

Lee, J. et al., 2006. Tumor stem cells derived from glioblastomas cultured in bFGF and EGF more closely mirror the phenotype and genotype of primary tumors than do serum-cultured cell lines. *Cancer cell*, 9(5), pp.391–403.

Lee, J.E., 1997. Basic helix-loop-helix genes in neural development. *Current opinion in neurobiology*, 7(1), pp.13–20.

Lee, S.-H. et al., 2011. The Id3/E47 axis mediates cell-cycle control in human pancreatic ducts and adenocarcinoma. *Molecular cancer research : MCR*, 9(6), pp.782–90.

Lemaitre, B. et al., 1996. The Dorsoventral Regulatory Gene Cassette spätzle/Toll/cactus Controls the Potent Antifungal Response in Drosophila Adults. *Cell*, 86(6), pp.973–983.

Lendahl, U., Zimmerman, L.B. & McKay, R.D., 1990. CNS stem cells express a new class of intermediate filament protein. *Cell*, 60(4), pp.585–95.

Levine, J.M., Reynolds, R. & Fawcett, J.W., 2001. The oligodendrocyte precursor cell in health and disease. *Trends in Neurosciences*, 24(1), pp.39–47.

Levine, J.M., Stincone, F. & Lee, Y.S., 1993. Development and differentiation of glial precursor cells in the rat cerebellum. *Glia*, 7(4), pp.307–21.

Li, H. et al., 2011. Phosphorylation Regulates OLIG2 Cofactor Choice and the Motor Neuron-Oligodendrocyte Fate Switch. *Neuron*, 69(5), pp.918–29.

Liang, Y. et al., 2005. Gene expression profiling reveals molecularly and clinically distinct subtypes of glioblastoma multiforme. *Proceedings of the National Academy of Sciences of the United States of America*, 102(16), pp.5814–9.

Ligon, K.L. et al., 2006. Olig gene function in CNS development and disease. *Glia*, 54(1), pp.1–10.

Ligon, K.L. et al., 2007. Olig2-regulated lineage-restricted pathway controls replication competence in neural stem cells and malignant glioma. *Neuron*, 53(4), pp.503–17.

Ligon, K.L. et al., 2004. The oligodendroglial lineage marker OLIG2 is universally expressed in diffuse gliomas. *Journal of neuropathology and experimental neurology*, 63(5), pp.499–509.

Liu, C. et al., 2011. Mosaic Analysis with Double Markers Reveals Tumor Cell of Origin in Glioma. *Cell*, 146(2), pp.209–221.

Liu, Y., Miyoshi, H. & Nakamura, M., 2007. Nanomedicine for drug delivery and imaging: a promising avenue for cancer therapy and diagnosis using targeted functional nanoparticles. *International journal of cancer. Journal international du cancer*, 120(12), pp.2527–37.

Louis, D.N., 2006. Molecular pathology of malignant gliomas. *Annual review of pathology*, 1, pp.97–117.

Louis, D.N. et al., 2007. The 2007 WHO classification of tumours of the central nervous system. *Acta neuropathologica*, 114(2), pp.97–109.

Lu, Q.R. et al., 2001. Oligodendrocyte lineage genes (OLIG) as molecular markers for human glial brain tumors. *Proceedings of the National Academy of Sciences of the United States of America*, 98(19), pp.10851–6.

Lyden, D. et al., 1999. Id1 and Id3 are required for neurogenesis, angiogenesis and vascularization of tumour xenografts. *Nature*, 401(6754), pp.670–7.

Lyden, D. et al., 2001. Impaired recruitment of bone-marrow-derived endothelial and hematopoietic precursor cells blocks tumor angiogenesis and growth. *Nature medicine*, 7(11), pp.1194–201.

Maher, E.A. et al., 2006. Marked genomic differences characterize primary and secondary glioblastoma subtypes and identify two distinct molecular and clinical secondary glioblastoma entities. *Cancer research*, 66(23), pp.11502–13.

Mapara, K.Y. et al., 2007. Stem cells as vehicles for the treatment of brain cancer. *Neurosurgery clinics of North America*, 18(1), pp.71–80, ix.

Martini, M. et al., 2013. Epigenetic silencing of Id4 identifies a glioblastoma subgroup with a better prognosis as a consequence of an inhibition of angiogenesis. *Cancer*, 119(5), pp.1004–12.

Massari, M.E. & Murre, C., 2000. Helix-loop-helix proteins: regulators of transcription in eucaryotic organisms. *Molecular and cellular biology*, 20(2), pp.429–40.

Mecklenburg, L. et al., 2001. The nude mouse skin phenotype: the role of Foxn1 in hair follicle development and cycling. *Experimental and molecular pathology*, 71(2), pp.171–8.

Mehmood, R. et al., 2009. Synergistic nuclear import of NeuroD1 and its partner transcription factor, E47, via heterodimerization. *Experimental cell research*, 315(10), pp.1639–52.

Mehta, S. et al., 2011. The central nervous system-restricted transcription factor Olig2 opposes p53 responses to genotoxic damage in neural progenitors and malignant glioma. *Cancer cell*, 19(3), pp.359–71.

Mellick, A.S. et al., 2010. Using the transcription factor inhibitor of DNA binding 1 to selectively target endothelial progenitor cells offers novel strategies to inhibit tumor angiogenesis and growth. *Cancer research*, 70(18), pp.7273–82.

Mern, Demissew S et al., 2010. Targeting Id1 and Id3 by a specific peptide aptamer induces E-box promoter activity, cell cycle arrest, and apoptosis in breast cancer cells. *Breast cancer research and treatment*, 124(3), pp.623–633–633.

Mern, D S, Hasskarl, J. & Burwinkel, B., 2010a. Inhibition of Id proteins by a peptide aptamer induces cell-cycle arrest and apoptosis in ovarian cancer cells. *British journal of cancer*, 103(8), pp.1237–44.

Mern, D S, Hasskarl, J. & Burwinkel, B., 2010b. Inhibition of Id proteins by a peptide aptamer induces cell-cycle arrest and apoptosis in ovarian cancer cells. *British journal of cancer*, 103(8), pp.1237–44.

Miller, C.R. & Perry, A., 2007. Glioblastoma. *Archives of pathology & laboratory medicine*, 131(3), pp.397–406.

Moon, J.-H. et al., 2011. Nanog-induced dedifferentiation of p53-deficient mouse astrocytes into brain cancer stem-like cells. *Biochemical and biophysical research communications*, 412(1), pp.175–81.

Murphy, J.J. & Norton, J.D., 1990. Cell-type-specific early response gene expression during plasmacytoid differentiation of human B lymphocytic leukemia cells. *Biochimica et biophysica acta*, 1049(3), pp.261–71.

Murre, C., 2005. Helix-loop-helix proteins and lymphocyte development. *Nature immunology*, 6(11), pp.1079–86.

Murre, C., McCaw, P.S., Vaessin, H., et al., 1989. Interactions between heterologous helix-loop-helix proteins generate complexes that bind specifically to a common DNA sequence. *Cell*, 58(3), pp.537–44.

Murre, C. et al., 1994. Structure and function of helix-loop-helix proteins. *Biochimica et biophysica acta*, 1218(2), pp.129–35.

Murre, C., McCaw, P.S. & Baltimore, D., 1989. A new DNA binding and dimerization motif in immunoglobulin enhancer binding, daughterless, MyoD, and myc proteins. *Cell*, 56(5), pp.777–83.

Naldini, L. et al., 1996. In vivo gene delivery and stable transduction of nondividing cells by a lentiviral vector. *Science (New York, N.Y.)*, 272(5259), pp.263–7.

Niola, F. et al., 2012. Id proteins synchronize stemness and anchorage to the niche of neural stem cells. *Nature cell biology*, 14(5), pp.477–87.

Nishide, K. et al., 2009. Glioblastoma formation from cell population depleted of Prominin1-expressing cells. *PloS one*, 4(8), p.e6869.

Nishimori, H. et al., 2002. The Id2 gene is a novel target of transcriptional activation by EWS-ETS fusion proteins in Ewing family tumors. *Oncogene*, 21(54), pp.8302–9.

Norton, J.D. & Atherton, G.T., 1998. Coupling of cell growth control and apoptosis functions of Id proteins. *Molecular and cellular biology*, 18(4), pp.2371–81.

Nunes, M.C. et al., 2003. Identification and isolation of multipotential neural progenitor cells from the subcortical white matter of the adult human brain. *Nature medicine*, 9(4), pp.439–47.

O'Brien, C. a et al., 2012. ID1 and ID3 regulate the self-renewal capacity of human colon cancer-initiating cells through p21. *Cancer cell*, 21(6), pp.777–92.

O'Connor, T.P. & Crystal, R.G., 2006. Genetic medicines: treatment strategies for hereditary disorders. *Nature reviews. Genetics*, 7(4), pp.261–76.

Obermair, F.-J. et al., 2010. A novel classification of quiescent and transit amplifying adult neural stem cells by surface and metabolic markers permits a defined simultaneous isolation. *Stem cell research*, 5(2), pp.131–43.

Ohgaki, H. & Kleihues, P., 2005. Epidemiology and etiology of gliomas. *Acta neuropathologica*, 109(1), pp.93–108.

Ohnishi, T. et al., 1998. A novel model of glioma cell invasion using organotypic brain slice culture. *Cancer research*, 58(14), pp.2935–40.

Ohtani, N. et al., 2001. Opposing effects of Ets and Id proteins on p16INK4a expression during cellular senescence. *Nature*, 409(6823), pp.1067–70.

Ouyang, X.S. et al., 2002. Id-1 stimulates serum independent prostate cancer cell proliferation through inactivation of p16 INK4a / pRB pathway It has been suggested that the helix – loop – helix protein Id-1 of human cancer . Previously , we reported that Id-1 was expression vecto. , 23(5), pp.721–725.

Page, J.L. et al., 2004. MEKK1 signaling through p38 leads to transcriptional inactivation of E47 and repression of skeletal myogenesis. *The Journal of biological chemistry*, 279(30), pp.30966–72.

Pagliuca, a et al., 2000. Class A helix-loop-helix proteins are positive regulators of several cyclin-dependent kinase inhibitors' promoter activity and negatively affect cell growth. *Cancer research*, 60(5), pp.1376–82.

Pandey, U.B. & Nichols, C.D., 2011. Human disease models in Drosophila melanogaster and the role of the fly in therapeutic drug discovery. *Pharmacological reviews*, 63(2), pp.411–36.

Paolella, B.R. et al., 2011. p53 directly represses Id2 to inhibit the proliferation of neural progenitor cells. *Stem cells (Dayton, Ohio)*, 29(7), pp.1090–101.

Pardridge, W.M., 2005. The blood-brain barrier: bottleneck in brain drug development. *NeuroRx : the journal of the American Society for Experimental NeuroTherapeutics*, 2(1), pp.3–14.

Park, S.T., Nolan, G.P. & Sun, X.H., 1999. Growth inhibition and apoptosis due to restoration of E2A activity in T cell acute lymphoblastic leukemia cells. *The Journal of experimental medicine*, 189(3), pp.501–8.

Park, S.W. et al., 2008. Oncogenic KRAS induces progenitor cell expansion and malignant transformation in zebrafish exocrine pancreas. *Gastroenterology*, 134(7), pp.2080–90.

Parkin, D.M. & Muir, C.S., 1992. Cancer Incidence in Five Continents. Comparability and quality of data. *IARC scientific publications*, (120), pp.45–173.

Perez-Moreno, M.A. et al., 2001. A new role for E12/E47 in the repression of E-cadherin expression and epithelial-mesenchymal transitions. *The Journal of biological chemistry*, 276(29), pp.27424–31.

Perk, J., Iavarone, A. & Benezra, R., 2005. Id family of helix-loop-helix proteins in cancer. *Nature reviews. Cancer*, 5(8), pp.603–14.

Pernet, V. et al., 2012. Neuronal Nogo-A upregulation does not contribute to ER stress-associated apoptosis but participates in the regenerative response in the axotomized adult retina. *Cell death and differentiation*, 19(7), pp.1096–108.

Persson, A.I. et al., 2010. Non-Stem Cell Origin for Oligodendroglioma. *Cancer Cell*, 18(6), pp.669–682.

Peverali, F.A. et al., 1994. Regulation of G1 progression by E2A and Id helix-loop-helix proteins. *The EMBO journal*, 13(18), pp.4291–301.

Phillips, H.S. et al., 2006. Molecular subclasses of high-grade glioma predict prognosis, delineate a pattern of disease progression, and resemble stages in neurogenesis. *Cancer cell*, 9(3), pp.157–73.

Pierfelice, T.J. et al., 2008. Notch, neural stem cells, and brain tumors. *Cold Spring Harbor symposia on quantitative biology*, 73, pp.367–75.

Quong, M.W. et al., 1993. A new transcriptional-activation motif restricted to a class of helix-loop-helix proteins is functionally conserved in both yeast and mammalian cells. *Molecular and cellular biology*, 13(2), pp.792–800.

Rampazzo, E. et al., 2013. Wnt activation promotes neuronal differentiation of glioblastoma. *Cell death & disease*, 4(2), p.e500.

Read, R.D. et al., 2009. A drosophila model for EGFR-Ras and PI3K-dependent human glioma. *PLoS genetics*, 5(2), p.e1000374.

Read, R.D., 2011. Drosophila melanogaster as a model system for human brain cancers. *Glia*, 59(9), pp.1364–76.

Read, T.-A. et al., 2009. Identification of CD15 as a Marker for Tumor-Propagating Cells in a Mouse Model of Medulloblastoma. *Cancer Cell*, 15(2), pp.135–147.

Rehemtulla, A., 2012. Overcoming Intratumor Heterogeneity of Polygenic Cancer Drug Resistance with. , 14(12), pp.1278–1289.

Reiter, L.T. et al., 2001. A systematic analysis of human disease-associated gene sequences in Drosophila melanogaster. *Genome research*, 11(6), pp.1114–25.

Riemenschneider, M.J. & Reifenberger, G., 2009. Molecular neuropathology of gliomas. *International journal of molecular sciences*, 10(1), pp.184–212.

Roth, W. et al., 2000. Bag-1 and Bcl-2 gene transfer in malignant glioma: modulation of cell cycle regulation and apoptosis. *Brain pathology (Zurich, Switzerland)*, 10(2), pp.223–34.

Ruzinova, M.B. & Benezra, R., 2003. Id proteins in development, cell cycle and cancer. *Trends Cell Biol*, 13, pp.410–418.

Sakamoto, S. et al., 2012. E2A and CBP/p300 act in synergy to promote chromatin accessibility of the immunoglobulin κ locus. *Journal of immunology (Baltimore, Md. : 1950)*, 188(11), pp.5547–60.

Samanta, J. & Kessler, J. a, 2004. Interactions between ID and OLIG proteins mediate the inhibitory effects of BMP4 on oligodendroglial differentiation. *Development (Cambridge, England)*, 131(17), pp.4131–42.

Sandberg, C.J. et al., 2013. Comparison of glioma stem cells to neural stem cells from the adult human brain identi fi es dysregulated Wnt- signaling and a fi ngerprint associated with clinical outcome $. *Experimental Cell Research*, pp.1–14.

Schindler, A.J. & Sherwood, D.R., 2011. The transcription factor HLH-2/E/Daughterless regulates anchor cell invasion across basement membrane in C. elegans. *Developmental biology*, 357(2), pp.380–91.

Schneider, C.A., Rasband, W.S. & Eliceiri, K.W., 2012. NIH Image to ImageJ: 25 years of image analysis. *Nature Methods*, 9(7), pp.671–675.

Schonberg, D.L. et al., 2013. Brain tumor stem cells: Molecular characteristics and their impact on therapy. *Molecular aspects of medicine*, pp.1–20.

Sharma, M.K. et al., 2007. Distinct genetic signatures among pilocytic astrocytomas relate to their brain region origin. *Cancer research*, 67(3), pp.890–900.

Sharma, P. et al., 2012. Epigenetic inactivation of inhibitor of differentiation 4 (Id4) correlates with prostate cancer. *Cancer medicine*, 1(2), pp.176–86.

Sherr, C.J., 1996. Cancer cell cycles. *Science (New York, N.Y.)*, 274(5293), pp.1672–7.

Shih, H.A. et al., 2005. Genetic analyses for predictors of radiation response in glioblastoma. *International journal of radiation oncology, biology, physics*, 63(3), pp.704–10.

Siddiquee, K.A.Z. et al., 2007. An oxazole-based small-molecule Stat3 inhibitor modulates Stat3 stability and processing and induces antitumor cell effects. *ACS chemical biology*, 2(12), pp.787–98.

Singh, S.K. et al., 2003. Identification of a Cancer Stem Cell in Human Brain Tumors. *Cancer Research*, pp.5821–5828.

Singh, S.K. et al., 2004. Identification of human brain tumour initiating cells. *Nature*, 432(7015), pp.396–401.

Siolas, D. & Hannon, G.J., 2013. Patient-derived tumor xenografts: transforming clinical samples into mouse models. *Cancer research*, 73(17), pp.5315–9.

Sloan, S.R. et al., 1996. Phosphorylation of E47 as a Potential Determinant of B-Cell-Specific Activity. *Microbiology*, 16(12), pp.6900–6908.

Slomianka, L. & West, M.J., 2005. Estimators of the precision of stereological estimates: an example based on the CA1 pyramidal cell layer of rats. *Neuroscience*, 136(3), pp.757–67.

Sobrado, V.R. et al., 2009. The class I bHLH factors E2-2A and E2-2B regulate EMT. *Journal of cell science*, 122(Pt 7), pp.1014–24.

Soeda, A. et al., 2009. Hypoxia promotes expansion of the CD133-positive glioma stem cells through activation of HIF-1alpha. *Oncogene*, 28(45), pp.3949–59.

Somasundaram, K. et al., 2005. Upregulation of ASCL1 and inhibition of Notch signaling pathway characterize progressive astrocytoma. *Oncogene*, 24(47), pp.7073–83.

Son, M.J. et al., 2009. SSEA-1 is an enrichment marker for tumor-initiating cells in human glioblastoma. *Cell stem cell*, 4(5), pp.440–52.

Sottoriva, A. et al., 2013. Intratumor heterogeneity in human glioblastoma reflects cancer evolutionary dynamics. *Proceedings of the National Academy of Sciences of the United States of America*, 110(10), pp.4009–14.

Stewart, L. a, 2002. Chemotherapy in adult high-grade glioma: a systematic review and meta-analysis of individual patient data from 12 randomised trials. *Lancet*, 359(9311), pp.1011–8.

Stiles, C.D. & Rowitch, D.H., 2008. Glioma stem cells: a midterm exam. *Neuron*, 58(6), pp.832–46.

Stupp, R. et al., 2009. Effects of radiotherapy with concomitant and adjuvant temozolomide versus radiotherapy alone on survival in glioblastoma in a randomised phase III study: 5-year analysis of the EORTC-NCIC trial. *The lancet oncology*, 10(5), pp.459–66.

Stupp, R. et al., 2005. Radiotherapy plus concomitant and adjuvant temozolomide for glioblastoma. *The New England journal of medicine*, 352(10), pp.987–96.

Sukhanova, M.J. et al., 2007. Proneural basic helix-loop-helix proteins and epidermal growth factor receptor signaling coordinately regulate cell type specification and cdk inhibitor expression during development. *Molecular and cellular biology*, 27(8), pp.2987–96.

Sukhanova, M.J. & Du, W., 2008. Control of cell cycle entry and exiting from the second mitotic wave in the Drosophila developing eye. *BMC developmental biology*, 8, p.7.

Sun, A. et al., 2010. Firefly luciferase-based dynamic bioluminescence imaging: a noninvasive technique to assess tumor angiogenesis. *Neurosurgery*, 66(4), pp.751–7; discussion 757.

Sun, Y. et al., 2011. Phosphorylation state of olig2 regulates proliferation of neural progenitors. *Neuron*, 69(5), pp.906–17.

Swanton, C., 2012. Intratumor heterogeneity: evolution through space and time. *Cancer research*, 72(19), pp.4875–82.

Szentirmai, O. et al., 2006. Noninvasive bioluminescence imaging of luciferase expressing intracranial U87 xenografts: correlation with magnetic resonance imaging determined tumor volume and longitudinal use in assessing tumor growth and antiangiogenic treatment effect. *Neurosurgery*, 58(2), pp.365–72; discussion 365–72.

Tabatabai, G. & Weller, M., 2011. Glioblastoma stem cells. *Cell and tissue research*.

Tabu, K. et al., 2006. A novel function of OLIG2 to suppress human glial tumor cell growth via p27 Kip1 transactivation. *Journal of Cell Science*.

Tang, D.G., 2012. Understanding cancer stem cell heterogeneity and plasticity. *Cell research*, 22(3), pp.457–72.

Tang, J. et al., 2013. Target inhibition networks: predicting selective combinations of druggable targets to block cancer survival pathways. *PLoS computational biology*, 9(9), p.e1003226.

Tang, J. & Aittokallio, T., 2013. Network pharmacology strategies toward multi-target anticancer therapies: from computational models to experimental design principles. *Current pharmaceutical design*.

Taylor, A.M. & Zon, L.I., 2009. Zebrafish tumor assays: the state of transplantation. *Zebrafish*, 6(4), pp.339–46.

Taylor, M.D. et al., 2005. Radial glia cells are candidate stem cells of ependymoma. *Cancer cell*, 8(4), pp.323–35.

Teachenor, R. et al., 2012. Biochemical and phosphoproteomic analysis of the helix-loop-helix protein E47. *Molecular and cellular biology*, 32(9), pp.1671–82.

Teesalu, T. et al., 2009. C-end rule peptides mediate neuropilin-1-dependent cell, vascular, and tissue penetration. *Proceedings of the National Academy of Sciences of the United States of America*, 106(38), pp.16157–62.

Tentler, J.J. et al., 2012. Patient-derived tumour xenografts as models for oncology drug development. *Nature reviews. Clinical oncology*, 9(6), pp.338–50.

Thévenaz, P., Ruttimann, U.E. & Unser, M., 1998. A pyramid approach to subpixel registration based on intensity. *IEEE transactions on image processing : a publication of the IEEE Signal Processing Society*, 7(1), pp.27–41.

Trabosh, V. a et al., 2009. Sequestration of E12/E47 and suppression of p27KIP1 play a role in Id2-induced proliferation and tumorigenesis. *Carcinogenesis*, 30(7), pp.1252–9.

Turkson, J. et al., 2001. Phosphotyrosyl peptides block Stat3-mediated DNA binding activity, gene regulation, and cell transformation. *The Journal of biological chemistry*, 276(48), pp.45443–55.

Uhl, M. et al., 2005. Migratory neural stem cells for improved thymidine kinase-based gene therapy of malignant gliomas. *Biochemical and biophysical research communications*, 328(1), pp.125–9.

Umetani, N. et al., 2004. Epigenetic inactivation of ID4 in colorectal carcinomas correlates with poor differentiation and unfavorable prognosis. *Clinical cancer research : an official journal of the American Association for Cancer Research*, 10(22), pp.7475–83.

Valent, P., Bonnet, D. & ..., 2012. Cancer stem cell definitions and terminology: the devil is in the details. *Nature Reviews Cancer*. Available at: http://www.nature.com/nrc/journal/v12/n11/pdf/nrc3368.pdf [Accessed November 12, 2012].

Vassilev, L.T. et al., 2004. In vivo activation of the p53 pathway by small-molecule antagonists of MDM2. *Science (New York, N.Y.)*, 303(5659), pp.844–8.

Verhaak, R.G.W. et al., 2010. Integrated genomic analysis identifies clinically relevant subtypes of glioblastoma characterized by abnormalities in PDGFRA, IDH1, EGFR, and NF1. *Cancer cell*, 17(1), pp.98–110.

De Vries, N.A. et al., 2006. Blood-brain barrier and chemotherapeutic treatment of brain tumors. *Expert review of neurotherapeutics*, 6(8), pp.1199–209.

Walker, M.D. et al., 1980. Randomized comparisons of radiotherapy and nitrosoureas for the treatment of malignant glioma after surgery. *The New England journal of medicine*, 303(23), pp.1323–9.

Weiler, M. et al., 2006. BCL-xL: time-dependent dissociation between modulation of apoptosis and invasiveness in human malignant glioma cells. *Cell death and differentiation*, 13(7), pp.1156–69.

Weiss, W.A. et al., 2003. Genetic determinants of malignancy in a mouse model for oligodendroglioma. *Cancer research*, 63(7), pp.1589–95.

Welcsh, P.L. et al., 2002. BRCA1 transcriptionally regulates genes involved in breast tumorigenesis. *Proceedings of the National Academy of Sciences of the United States of America*, 99(11), pp.7560–5.

Westphal, M. & Lamszus, K., 2011. The neurobiology of gliomas: from cell biology to the development of therapeutic approaches. *Nature reviews. Neuroscience*, 12(9), pp.495–508.

Wick, W. et al., 2012. Temozolomide chemotherapy alone versus radiotherapy alone for malignant astrocytoma in the elderly: the NOA-08 randomised, phase 3 trial. *The lancet oncology*, 13(7), pp.707–15.

Wicker, C. et al., 1990. Insect immunity. Characterization of a Drosophila cDNA encoding a novel member of the diptericin family of immune peptides. *The Journal of biological chemistry*, 265(36), pp.22493–8.

Wischhusen, J. et al., 2003. CP-31398, a novel p53-stabilizing agent, induces p53-dependent and p53-independent glioma cell death. *Oncogene*, 22(51), pp.8233–45.

Witte, H.T. et al., 2009. Modeling glioma growth and invasion in Drosophila melanogaster. *Neoplasia (New York, N.Y.)*, 11(9), pp.882–8.

Wojton, J. et al., 2013. Systemic delivery of SapC-DOPS has antiangiogenic and antitumor effects against glioblastoma. *Molecular therapy : the journal of the American Society of Gene Therapy*, 21(8), pp.1517–25.

Wu, C. et al., 2009. In vivo far-red luminescence imaging of a biomarker based on BRET from Cypridina bioluminescence to an organic dye. *Proceedings of the National Academy of Sciences of the United States of America*, 106(37), pp.15599–603.

Yan, C. & Higgins, P.J., 2013. Drugging the undruggable: transcription therapy for cancer. *Biochimica et biophysica acta*, 1835(1), pp.76–85.

Ying, Q.L. et al., 2003. BMP induction of Id proteins suppresses differentiation and sustains embryonic stem cell self-renewal in collaboration with STAT3. *Cell*, 115(3), pp.281–92.

Yuan, X. et al., 2004. Isolation of cancer stem cells from adult glioblastoma multiforme. *Oncogene*, 23(58), pp.9392–400.

Zennou, V. et al., 2000. HIV-1 genome nuclear import is mediated by a central DNA flap. *Cell*, 101(2), pp.173–85.

Zhang, K. et al., 2012. Wnt/beta-catenin signaling in glioma. *Journal of neuroimmune pharmacology : the official journal of the Society on NeuroImmune Pharmacology*, 7(4), pp.740–9.

Zhou, B.-B.S. et al., 2009. Tumour-initiating cells: challenges and opportunities for anticancer drug discovery. *Nature reviews. Drug discovery*, 8(10), pp.806–23.

Zufferey, R. et al., 1997. Multiply attenuated lentiviral vector achieves efficient gene delivery in vivo. *Nature biotechnology*, 15(9), pp.871–5.

Zufferey, R. et al., 1998. Self-inactivating lentivirus vector for safe and efficient in vivo gene delivery. *Journal of virology*, 72(12), pp.9873–80.

Zufferey, R. et al., 1999. Woodchuck hepatitis virus posttranscriptional regulatory element enhances expression of transgenes delivered by retroviral vectors. *Journal of virology*, 73(4), pp.2886–92.

Curriculum Vitae

BEYELER Sarah

Date of Birth: 11.02.1984

Citizenship: Avry FR

Education

08/09 – 02/14: **PhD student**
- University of Zürich (CH),
- Thesis in Neurosciences "bHLH Transcription Factor Manipulation in Human Glioma".
- A mutated form of E proteins is investigated as a potential approach to induce apoptosis and a reduction in proliferation in human glioblastoma multiforme.

09/07 –01/09: **Master of Science in Neurosciences**
- University of Zürich (CH)
- "Differentiation and Survival Potential of Adult Mouse Neural Progenitor Cell Populations after Grafting in the Adult Hippocampus".
- Final grade 5.5

09/04 – 06/07 : **Bachelor of Science in Biology**
- University of Fribourg (CH)
- Options Neurosciences and Special Biology (Anatomy, Physiology, Biochemistry)
- Bachelor Thesis " Analysis of FEM-3 expression in *Caenorhabditis elegans* by Western Blotting and Immunochemical Staining. "

09/99 – 06/03: **Swiss Federal Maturity**
- College Sainte-Croix, Fribourg (CH)
- Options Latin, English and Biology
- Final average grade 5.25

Tutoring

09/12-09/13:	Supervision of an ETHZ master thesis "Over-expression of mutant E47 in human glioblastoma stem cells as an anti-glioma approach"
03/10-12:	Supervision of 2 students during the ETHZ block course Cellular Neurobiology 551-0332-00
02/11-05/11:	Supervision of a 3 month ETHZ semester project

Funding

2009	Forschungskredit der Universität Zürich 2009

Courses attended

2013:	Stress Management
	Project Management for Research
2011:	Crash course in statistics
	Supervising students – dealing with roles and relationships
2008:	Scientific writing

Publications

2010	F.J. Obermair, R. Fiorelli, A. Schroeter, S. Beyeler, C. Blatti, B. Zoerner, M. Thallmair. A novel classification of quiescent and transit amplifying adult neural stem cells by surface and metabolic markers permits a defined simultaneous isolation. Stem Cell Res., 5(2): 131-143, 2010.

Personal interests

Play basketball in a team, listen to a wide-range of music styles and read novels.